Poxvirus K3 Orthologs Differentially Modulate NF-kB Activity through Targeting the PKR-eIF2a Phosphorylation Pathway

By

HUIBIN YU
DISSERTATION

Submitted in partial satisfaction of the requirements for the degree of

DOCTOR OF PHILOSOPHY

in

Medical Microbiology and Immunology

in the

OFFICE OF GRADUATE STUDIES

of the

UNIVERSITY OF CALIFORNIA

DAVIS

Approved:

Stefan Rothenburg, Chair

Barbara Shacklett

Jeroen Saeij

Committee in Charge

2021

Abstract

Myxoma virus (MYXV) is a rabbit-specific poxvirus. It causes an innocuous localized cutaneous fibroma in brush rabbits, its nature host. In contrast, the same virus exhibits up to 99.8 % fatality rates in European rabbits, causing the lethal disease myxomatosis. MYXV was deliberately released as a biocontrol agent against European rabbits in Australia and European. The subsequent results of coevolution are both attenuation of MYXV and increased resistance in rabbits. This provided us with one of the best documented examples of host-pathogen evolution and the opportunity to investigate the molecular mechanism underlying virulence changes after encountering with new hosts. In response to virus infection, host protein kinase R (PKR) can sense double-stranded RNA, which is generated during virus replication. Activated PKR phosphorylates the translation initiation factor eIF2α, resulting in the globally inhibition of protein synthesis. PKR has also been reported to involve in the regulation of other signaling pathways, including eIF2α/ATF4 responses and NF-κB activities. Poxviruses encodes two inhibitors, E3 and K3, to inhibit PKR mediated eIF2α phosphorylation and repress the inhibition of protein synthesis, facilitating virus replication. The molecular mechanisms behind PKR associated NF-κB activation and regulation of PKR associated NF-κB transcriptional activities by K3 orthologs are still largely unknown. The main goal of this study is to elucidate molecular mechanisms for the crosstalk between PKR-eIF2α antiviral pathway and NF-κB dependent pro-inflammatory response during MYXV infection. We examined the antiviral function of PKRs from diverse mammalian species during MYXV infection. Activation of PKR induced ATF4 responses and NF-κB transcriptional activities. Of note, rabbit PKRs from nature host and new host of MYXV showed different sensitivity to M156 inhibition. Higher inhibition of PKR inhibition exerted by M156 or other K3 orthologs from different poxviruses resulted in low level

of NF-κB activation. In conclusion, our research reveals the interaction between PKR and K3 orthologs affect the outcome of NF-κB dependent pro-inflammatory response, possibly contributing to viral replication and pathogenesis in vivo.

Table of Contents

List of Figures

List of Abbreviations

ADAR1: adenosine deaminase acting on RNA 1; ADP: adenosine diphosphate; AIM2: absent in melanoma 2; AMP: adenosine monophosphate; AP1: activator protein 1; ASC: apoptosis-associated speck-like protein containing a CARD; ATP: adenosine triphosphate; Bcl-2: B-cell CLL/lymphoma 2; CARD: caspase activation and recruitment domains; CCL5: chemokine (C-C motif) ligand 5; cGAS: cyclic GMP-AMP synthase; CNPV: canarypox virus; COP: Copenhagen; CPXV: cowpox virus; CPXV: cowpox viruses; CREP: constitutive repressor of eIF2α phosphorylation; CrmA: cytokine response modifier A; CTD: carboxy-terminal domain; CXCL2: chemokine (C-X-C Motif) ligand 2; DAMPs: damage-associated molecular patterns; DDX3: Asp-Glu-Ala-Asp (DEAD) box polypeptide 3; DDX41: Asp-Glu-Ala-Asp (DEAD) box polypeptide 41; DHX9: DExH-Box helicase 9; DNA-PK: DNA-dependent protein kinase; DNA-PKcs: DNA-dependent protein kinase catalytic subunit; dsDNA: double-stranded DNA; dsRBD: dsRNA-binding domain; dsRNA: double-stranded RNA; ECTV: ectromelia virus; eIF2: eukaryotic translation initiation factor 2; eIF2B: eukaryotic translation initiation factor 2B; eIF2α: alpha-subunit of the eukaryotic translation initiation factor 2; ER: endoplasmic reticulum; GADD34: growth arrest and DNA damage-inducible protein 34; GDP: guanosine diphosphate; GMP: guanosine monophosphate; GTP: guanosine-5'-triphosphate; HSV-1: herpes simplex virus 1 HIN-200: hematopoietic interferon-inducible nuclear proteins with a 200 amino acid repeat; HMGB1: high mobility group box protein 1; IFI16: interferon-γ inducible protein 16; IFNAR: type I interferon receptor; IFNs: interferons; IKKα: IκBα kinase α; IKKβ: IκBα kinase β; IKKε: IκBα kinase ε; IKKγ: IκBα kinase γ; IL-18: interleukin-18; IL-1β: interleukin-1β; IL-6: interleukin-6; IRAK1/2/4: interleukin-1 receptor-associated kinase 1/2/4; IRF1/3/7: interferon regulatory factor 1/3/7; ISGs: IFN-stimulated genes; IκBα: inhibitor κBα; KD: kinase domain;

LPS: lipopolysaccharide; LRRFIP1: leucine-rich repeat flightless- interacting protein 1; Mal: myD88-adapter-like; Malp2: macrophage-activating lipopeptide 2; MAVS: mitochondrial antiviral-signaling protein; MCP1: monocyte chemoattractant protein 1; MD-2: myeloid differentiation factor 2; MDA5: melanoma differentiation-associated protein 5; MIP2: macrophage inflammatory protein 2; MLKL: mixed lineage kinase-like; MRE11: meiotic recombination 11; mTORC1/2: mammalian target of rapamycin complex 1/2; MVA: modified vaccinia virus Ankara; MyD88: myeloid differentiation primary response gene 88; MYXV: myxoma virus; NF-κB: nuclear factor kappa B; NLRP3: NOD-, LRR- and pyrin domain-containing protein 3; NOD; nucleotide-binding and oligomerization domain; OAS: 2′-5′-oligoadenylate synthetases; OASL: OAS like; p65/p50: NF-κB heterodimer p50/p65 subunit; PAMPs: pathogen-associated molecular patterns; PKR: protein kinase R; PRRs: pattern recognition receptors; PYD: pyrin domain; LRR: leucine-rich repeats; PYHIN: pyrin and HIN domain; RFV: rabbit fibroma virus; RHIM: RIP homotypic interaction motif; RIG-I: retinoic acid-inducible gene I; RIP1: receptor-interacting protein 1; RIPK: receptor interacting protein kinase; RLRs: RIG-I-like receptors; RNA pol III: DNA-dependent RNA polymerase III; RNase L: ribonuclease L; ROS: reactive oxygen species; SPI-2: serine proteinase inhibitor 2; ssDNA: single-stranded DNA; ssRNA: single-stranded RNA; STING: stimulator of interferon genes; TAK1: TGF-β activated kinase 1; TBK1: TRAF family member-associated NF-κB activator (TANK)-binding kinase 1; TIR: toll/Interleukin-1 receptor; TIRAP: toll/interleukin 1 receptor (TIR) domain-containing adapter protein; TLRs: toll-like receptors; TNFα: tumor necrosis factor-alpha; TRAF3/6: tumor necrosis factor receptor-associated factor 3/6; TRIF: toll/interleukin-1 receptor domain-containing adapter-inducing interferon-β; TRAM: TRIF-related adapter molecule; VACV: vaccinia virus; VARV: variola virus; vIL-18BPs: viral IL-18

binding proteins; vIL-1βR: viral IL-1β receptor; VIPER: viral inhibitory peptide of TLR4; vPOP: viral pyrin-only proteins; vSlfn: viral Schlafen; WR: Western Reserve; ZBP1: Z-DNA binding protein 1; Zα: Z-nucleic acid-binding domain; 2-5As: 2′-5′-oligoadenylates; 2′3′ cGAMP: 2′3′ cyclic guanosine monophosphate–adenosine monophosphate; 5'ppp-dsRNA: 5' triphosphate double-stranded RNA.

Acknowledgements

I would like to thank all people who have helped me and supported me to accomplish this dissertation.

First of all, I would like to express my sincere gratitude to my respectful mentor Dr. Stefan Rothenburg for all of his patient mentorship, gracious support and endless inspiration. Specifically, my mentor Stefan provided me with a high level of research platform to do interesting scientific researches, his excellent academic guidance and critical scientific vision greatly helped in establishing my research interests and developing my own scientific and critical thinking. I would never have been able to achieve anything without your encouragement. Thank you so much for the support in my professional development.

I would like to extend my gratitude to my dear committee members, Dr. Barbara Shacklett and Dr. Jeroen Saeij, who generously spent their valuable time on evaluating my research progress, providing valuable advice on my thesis, and kindly provided support for my academic career plans.

I would also like to thank Dr. Greg Brennan for helping review and edit manuscripts and providing good suggestions. Thanks to every current Rothenburg lab members: Ryan C. Bruneau, Jeannine Nicole Stroup, Anak Agung Dewi Megawati, Dr. Ana Stoian, previous lab members: Dr. Chen Peng, Dr. Julhasur Rahman, Dr. Chorong Park for their valuable inputs on my manuscripts and for the discussions and suggestions.

Last but not least, I would like to thank my parents for their everlasting love, reassuring encouragements and endless support.

Chapter-1: Introduction

Battle Royale: Innate Recognition of Poxviruses and Viral Immune Evasion

Huibin Yu[1], Ryan C. Bruneau[1], Greg Brennan[1], Stefan Rothenburg[1*]

[1]Department of Medical Microbiology and Immunology, School of Medicine, University of California, Davis 95618, USA

*To whom correspondence should be addressed

Stefan Rothenburg

Email: rothenburg@ucdavis.edu. ORCID iD:0000-0002-2525-8230

1. Poxviruses

Members of the family Poxviridae can infect a diverse range of vertebrates and invertebrates, although some poxviruses have narrow host ranges and others have very broad host ranges [1]. Poxvirus infections have posed serious threats for both humans and animals worldwide [2]. Poxviridae is a large family of DNA viruses comprised of two subfamilies: Chordopoxvirinae and Entomopoxvirinae. There are currently 18 recognized genera of Chordopoxvirinae, which infect vertebrates, and 4 genera of Entomopoxvirinae which infect invertebrates [1]. Poxviruses possess a single, linear double-stranded DNA (dsDNA) genome, which ranges in size from 127 kb to 456 kb and encodes several hundred gene products. Unlike most other DNA viruses, poxviruses replicate exclusively within the cytoplasm of permissive cells [3].

One of the best-known poxviruses is variola virus (VARV), a member of the orthopoxvirus genus. VARV is the causative agent of human smallpox, which was one of the most devastating human diseases in history [4]. Despite the success of global smallpox eradication through a vaccination campaign led by the World Health Organization (WHO), other pathogenic poxviruses, such as monkeypox virus, cowpox viruses (CPXV), camelpox virus, tanapox virus, and capripoxviruses remain threats to human and animal health [1,2,5,6]. The most intensively studied poxviruses, such as vaccinia virus (VACV) and myxoma virus (MYXV), have proven to be excellent research models to study host innate recognition and virus-host protein interactions and have provided important insights into the fields of virology and immunology [7,8]. In turn, these fundamental insights have direct translational applications to improve the development of safer and more effective attenuated viral vectors for vaccines, cancer therapeutics, and other treatment modalities [9]. For example, in VACV inactivation of either IL-1β-binding protein or IL-18-binding protein, encoded by B15R and C12L respectively, enhanced $CD8^+$ T-cell memory

responses after immunization and improved the protection against virulent VACV WR challenge [10,11]. In addition, VACV has the genomic capacity to incorporate >25 kb of foreign DNA without noticeable impacts on viral replication. This capacity has been employed to genetically engineer VACV chimeras carrying multiple heterologous genes, as both polyvalent vaccines and treatment of various genetic diseases [12–15]. Multiple poxviruses are being investigated for use in oncolytic virotherapy. Myxoma virus (MYXV) is one such preclinical candidate oncolytic virus, and recombinant MYXV lacking various viral death modulator genes, such as M-T5 [16], M11 [17], M13 [18], and Serp2 [19], have enhanced anti-tumor activity that appears to be mediated through viral induction of programmed cell death rather than through viral replication (Reviewed in [20]).

The recognition of viral pathogens and the host defense against them are provided by the innate and the adaptive immune system. The adaptive immune system is broadly comprised of antigen-specific $CD8^+$ T cells, $CD4^+$ helper T-cells, and B-cell antibody responses for specific, anamnestic protection against distinct pathogens [21–23]. Prior to the initiation of the adaptive immune response, pathogen-associated molecular patterns (PAMPs) derived from poxviruses, such as DNA and RNA, as well as envelope or core proteins, can be sensed by a diverse set of pattern recognition receptors (PRRs) to initiate the faster but less specific innate immune responses [24–31]. The innate immune response provides the first line of host defense and includes antiviral proteins that can lead to the direct elimination of viruses or induce expression of type I interferons (IFNs), proinflammatory cytokines, chemokines, and other antiviral proteins [32,33]. These effector molecules mediate direct antiviral effects or orchestrate the adaptive immune response to contain poxvirus infections at various stages. In particular, type I IFNs, the hallmark effector of antiviral responses, are essential to initiate innate immunity and also to

mediate the subsequent development of adaptive immunity against invading poxviruses [34]. In addition, type I IFNs upregulate the expression of hundreds of IFN-stimulated genes (ISGs) that directly influence protein synthesis, cell growth, and survival to establish an antiviral state [35,36]. Furthermore, multiple cytokines, such as interleukin-6 (IL-6), IL-12, and tumor necrosis factor-alpha (TNFα), can be induced during poxvirus infections which then act systemically to induce immune responses [37,38].

Over the past few decades, substantial progress has been made defining the roles of PRRs and the subsequent signaling pathways that are involved in the sensing of and response to poxviruses. IFN expression is transcriptionally regulated through activation of IFN regulatory factor (IRF) family members or coordinated activation of IRFs and nuclear factor kappa B (NF-κB) [39]. The stimulation of pro-inflammatory genes depends on activation of the transcription factors NF-κB and activator protein 1 (AP1) [40]. Despite the diversity of PRR ligands, many PRR-regulated signaling pathways share common downstream molecules, such as adaptor like myeloid differentiation primary response gene 88 (MyD88) and toll/interleukin-1 receptor domain-containing adapter-inducing interferon-β (TRIF). As such, there is substantial crosstalk and overlap between the signaling cascades stimulated by different PRRs, which lead to IFN activation and also drive the production of other cytokines [41–43].

A broad spectrum of PRRs has been implicated in poxviruses recognition, including RNA sensors, cytosolic DNA sensors, multiple toll-like receptors (TLRs), and components of the inflammasome. In order to establish successful infections in the face of this multi-pronged immune response, poxviruses evade host antiviral responses by expressing a variety of viral proteins. Those viral proteins interact with and antagonize the key components of these intracellular signal transduction pathways.

2. Double-stranded RNA-activated Sensors and Poxvirus Antagonists

The lifecycle of most virus families generates double-stranded RNA (dsRNA). In Poxviridae, dsRNA is the result of overlapping transcripts, which form duplexes, primarily at intermediate and late time points in the viral replication cycle [44–46]. Because of the ubiquity of this PAMP, it is perhaps not surprising that the first PRRs to be described were the dsRNA-activated molecules PKR and OAS/RNase L [35,47–51]. Since these initial discoveries, other broadly-acting antiviral dsRNA sensors have been identified, and we have developed a better understanding of the plethora of mechanisms that viruses employ to evade these host proteins (Fig. 1.1). In this section, we describe the mechanisms that these host proteins use to sense dsRNA, the antiviral pathways that they initiate, and the strategies poxviruses employ to inhibit them.

2.1. Protein kinase R

Protein kinase R (PKR) was first discovered as an IFN stimulated, dsRNA-dependent protein kinase [35,47,48]. PKR is comprised of two N-terminal dsRNA-binding domains (dsRBDs) and a C-terminal catalytic kinase domain [52]. These functional domains allow PKR to serve as both an intracellular sensor for double-stranded RNA (dsRNA) and an effector serine/threonine protein kinase. PKR is expressed in most cell types as an inactive monomer at intermediate levels. PKR recognizes dsRNA via its dsRBDs, and this binding event leads to PKR dimerization and autophosphorylation [53,54]. Activated PKR phosphorylates the alpha subunit of the eukaryotic translation initiation factor 2 (eIF2), which forms the ternary complex together with initiator methionyl-tRNA and GTP. Concomitant with translation initiation, GTP is hydrolyzed to GDP, which must subsequently be exchanged with GTP by the guanine nucleotide exchange factor eIF2B (reviewed in [55]). However, phosphorylated eIF2α has increased binding affinity

between eIF2 and eIF2B. This increased affinity effectively turns eIF2α into an inhibitor of eIF2B, thus impairing the generation of active GTP-bound eIF2 and inhibiting the initiation of cap-dependent translation, ultimately leading to cell death and inhibition of viral replication (Fig. 1.1) [56–59].

In addition to its canonical function as an eIF2α kinase, PKR has also been implicated in different stress-induced signaling pathways including IFN responses and NF-κB-dependent inflammatory responses [60–62]. It has been reported that PKR activation decreases the protein levels of IκBα, the NF-κB inhibitor, thus activating this pathway. The molecular mechanism underlying this activation appears to rely on the kinase activity of PKR which has been shown to be essential for NF-κB activation [61,63]. Additionally, during infection with VVΔE3L, a VACV lacking the PKR antagonist protein E3, PKR was shown to regulate melanoma differentiation-associated protein 5 (MDA5)-mediated IFNβ production through a mechanism that does not require eIF2α phosphorylation. Interestingly, PKR activation also upregulated IFN induction by MAVS (mitochondrial antiviral-signaling protein) in an MDA5-independent manner [64]. Similarly, in human and murine cells infected with a modified vaccinia virus Ankara (MVA) strain engineered to produce more dsRNA, the expression of IFNβ increased. Furthermore, mice infected with this MVA strain showed increased expression of IFNα, IFNγ, and other cytokines, which were enhanced in a PKR-dependent manner [27].

2.1.1. Poxvirus evasion of PKR

Poxviruses encode diverse PKR antagonists that either directly or indirectly inhibit the PKR pathway. In VACV, these proteins are encoded by E3L, K3L, D9R, and D10R. In addition, avipoxviruses possess homologs of cellular protein phosphatase 1 (PP1) targeting growth arrest and growth arrest and DNA damage-inducible protein 34 (GADD34) (PPP1R15A) and

constitutive repressor of eIF2α phosphorylation (CREP) (PPP1R15B), which promote the dephosphorylation of eIF2α (Fig. 1.1) [65].

E3 was initially characterized as a dsRNA binding protein responsible for IFN resistance. This phenotype was dependent on the C-terminal domain of E3, which contains a dsRBD [66]. E3 can bind dsRNA via this dsRBD to prevent PKR dimerization and activation [67,68]. In human-derived HeLa cells, an E3L-deleted VACV displayed a replication defect [69]. Moreover, this E3L-deleted VACV was able to replicate in PKR-deficient HeLa cells as efficiently as wildtype VACV, which demonstrated that PKR was the major target of E3 in these cells [70]. However, VACVΔE3L replication in Syrian hamster-derived BHK cells was not affected, suggesting that, like most other host range genes, there is a species-specific component to E3 activity. Additionally, E3 orthologs from myxoma virus and swinepox virus were shown to inhibit PKR activity and impair the induction of IFNβ and proinflammatory cytokines, like TNFα and IL-6, during viral infection [68,71]. Interestingly, E3L orthologs from myxoma virus and swinepox, but not from sheeppox virus, were able to rescue virus replication when expressed by a VACVΔE3L chimera. These PKR-inhibitory activities correlated with PKR inhibition in vitro studies as well, further supporting the hypothesis that there are ortholog-specific differences in E3 activity [68,72].

VACV K3 and its orthologs in other poxviruses are structural mimics of eIF2α. They act as pseudosubstrate inhibitors and compete with eIF2α to bind PKR, thus preventing eIF2α phosphorylation and allowing protein synthesis to continue [73–75]. Like E3L, K3L was also identified as a VACV host range gene when a K3L-deleted VACV was able to replicate in HeLa cells but not in BHK cells [69]. Further evidence for this host range function is provided by the

observation that K3 orthologs from multiple poxvirus genera exhibited both virus-and host-specific inhibition of PKR in both reporter and infection-based assays [72,76–79].

VACV encodes two decapping enzymes D9 and D10, which share approximately 25% amino acid sequence identity [80,81]. D9 and D10 are expressed either early or late in infection, respectively. They cleave m^7GDP from capped RNA substrates through nudix hydrolase motifs. This decapping activity reduced mRNA stability and prevented dsRNA accumulation, thereby indirectly preventing PKR activation. Inactivation of D9 and D10 catalytic activities increased PKR-induced eIF2α phosphorylation and enhanced PKR and OAS/RNase L-mediated anti-viral responses during VACV infection [81–84].

E3 and K3 orthologs evolved in mammalian poxviruses after the split from avipoxviruses [85]. In order to inhibit PKR, avipoxviruses evolved inhibitors that act later in the PKR pathway, facilitating the dephosphorylation of eIF2α. These proteins are homologous to the PP1 adaptor proteins GADD34 and CREP. In a yeast-based system, the canarypox virus protein 231 reversed the cytotoxic effects of ectopically expressed human PKR and reduced the level of PKR-induced eIF2α phosphorylation [65]. The roles of avipoxviral GADD34 homologs in poxvirus infection still need to be elucidated.

2.2. 2′-5′-. oligoadenylate synthetase (OAS)/RNase L

The 2′-5′-oligoadenylate synthetase (OAS)/RNase L-mediated antiviral pathway was discovered as one of the first interferon-induced systems in response to diverse viral infections [36]. The OAS family includes OAS1, OAS2, and OAS3 and their expression can be upregulated by type I and type III IFNs [86]. These molecules detect accumulated dsRNA species from diverse sources, which are usually viral but may sometimes have cellular origins [87,88]. Upon binding dsRNA, enzymatically active OAS1, OAS2, and OAS3 use ATP to synthesize linear 2′-5′-linked

second messenger molecules called 2′-5′-oligoadenylates (2-5As) [36,89]. 2-5As, in turn, bind and activate latent RNase L monomers in the cytoplasm, inducing RNase L dimerization and activation. Activated RNase L suppresses viral replication by cleaving viral and cellular RNAs, limiting mRNA translation and promoting apoptosis (Fig. 1.1). The resulting RNA cleavage products can be recognized by other RNA sensors, such as PKR, retinoic acid-inducible gene I (RIG-I), and MDA5 (Fig. 1.1). Thus, RNase L acts to both inhibit viral replication itself and amplify the response of other innate immune proteins [90–93]. For example, RNase L activation has been shown to amplify IRF3-dependent IFN production by inducing the formation of antiviral stress granules, for which PKR and RIG-I are essential mediators [93].

Multiple studies have demonstrated that the antiviral activity of OAS/RNase L limits poxvirus infections. In response to VACV infection, RNase L knock out (KO) C57BL/6 mice were more susceptible to viral infection than wild type mice, indicating that RNase L plays an antiviral role in vivo [28]. Recombinant VACV expressing OAS or RNase L showed impaired viral replication relative to wild type VACV. This replication defect was accompanied by increased rRNA degradation and inhibition of virus protein synthesis [94]. In A549 cells, OAS3, but not OAS1 or OAS2, played the dominant role in RNase L activation and subsequent antiviral effects in response to VACV infection [89].

2.2.1. Poxvirus evasion of OAS/RNase L

VACV E3 has been shown to inhibit the activation of the OAS/RNase L system [95]. Compared to MVA infection, HeLa cells infected with MVA-ΔE3L inhibited viral replication at multiple steps including viral late transcription, late mRNA translation, and viral DNA replication. These replication blocks were associated with activation of OAS/RNase L, rRNA degradation, and up-regulation of host transcripts, such as IL-6 [96]. Furthermore, VACVΔE3L replicated

approximately 20-fold higher in RNase L^{ko} MEF cells than in cells with intact RNase L, suggesting that E3 is involved in suppression of the OAS/RNase L system [97]. As described above, the VACV decapping enzymes D9 and D10 reduce dsRNA accumulation, and thus also inhibit OAS/RNase L mediated antiviral responses [81,83,98]. In A549 cells, knocking out both RNase L and PKR was necessary to allow replication of VACVΔE3L, whereas in HAP1 cells PKR knockout alone was sufficient to allow VACVΔE3L replication. These data highlight the cell type-specific activities of the OAS/RNase L pathway [99].

2.3. RIG-I and MDA5

Retinoic acid-inducible gene I (RIG-I) and melanoma differentiation-associated protein 5 (MDA5) are intracellular pathogen sensors and type I IFN inducers, which belong to the RIG-I-like receptors (RLRs) family [100,101]. RIG-I and MDA5 are localized in the cytosol of most cell types, where they recognize dsRNA derived from a variety of viral infections [64,102–108]. Both RIG-I and MDA5 contain a carboxy-terminal domain (CTD), two central helicase domains (Hel1 and Hel2), and two N-terminal caspase activation and recruitment domains (CARDs) [109]. Despite these similarities, RIG-I and MDA5 show different RNA binding preferences. RIG-I primarily senses and recognizes short RNA ligands containing 5′ triphosphate groups, while MDA5 mainly recognizes long dsRNA and replication intermediates [110–113]. Once activated, RIG-I and MDA5 both initiate signaling cascades through the adaptor protein MAVS. MAVS forms a multilayered complex to mediate downstream signal transduction, inducing type I interferons (IFNs) through IRF3 and IRF7 phosphorylation, and activating NF-κB through the tumor necrosis factor receptor (TNFR)-associated factor 6 (TRAF6) mediated signal cascade (Fig. 1.1) [112,114,115].

During poxvirus infections, RIG-I has been shown to play an essential role in sensing MYXV and triggering the induction of TNFα and type I IFN in primary human macrophages in an IRF3- and IRF7-dependent manner [107]. Furthermore, in the presence of VACV DNA, RNA polymerase III exerts its antiviral effect by generating 5'ppp RNA, which acts as a RIG-I substrate [106]. Additionally, VACV late RNA transcripts can be sensed by either RIG-I or MDA5 in a cell type-specific manner, triggering IFNβ gene transcription [116]. However, during MVA infection, MDA-5, but not RIG-I, was essential for the induction of IFNβ mRNA responses in THP-1 cells [29]. Although this activation specifically by late transcripts is intriguing, it remains unclear which poxviral RNA structures or motifs activate RIG-I and/or MDA5.

2.3.1. Poxvirus evasion of RIG-I and MDA5

When infected with VACVΔE3L, mouse primary keratinocytes produced IFNβ, IL-6, and other cytokines in a MAVS- and IRF-3-dependent manner. MAVS and IRF3 are essential components of the RIG-I- and MDA5-pathway. Production of these cytokines was completely prevented by infection with wild type VACV, or by VACV expressing only the E3 dsRNA-binding domain [108]. Similarly, a second mechanism of E3 inhibition of RIG-I has been proposed that is mediated by inhibiting RIG-I recognition of RNA generated by RNA polymerase III [117].

3. Dual RNA/DNA sensor

3.1. Z-DNA binding protein 1

Z-DNA binding protein 1 (ZBP1), previously known as DLM-1 or DNA-dependent activator of IFN-regulatory factors (DAI), is a stress granule-associated protein, which contains two functional Z-DNA/RNA binding (Zα) domains in its N-terminus [118–121]. In addition to binding Z-DNA, it can also bind left-handed double-stranded Z-RNA and RNA, which adopts Z-

RNA-like conformations [122]. ZBP1 has been identified as a putative cytosolic DNA sensor and activator for the induction of type I IFNs and other genes involved in innate immunity [123]. Upon binding DNA, ZBP1 dimerizes and recruits TANK-binding kinase 1 (TBK1) and IFN regulatory factor 3 (IRF3) to induce the production of type I IFNs and the NF-κB pathway (Fig. 1.2) [123–125]. Activated ZBP1 can also activate receptor interacting protein kinase 3 (RIPK3) by binding through RIP homotypic interaction motifs (RHIM). This interaction leads to the activation of the mixed lineage kinase-like protein (MLKL), ultimately inducing necroptotic cell death (Fig. 1.2) [126–130]. However, it is still unclear what specific ligand generated during VACV infection is recognized by ZBP1.

3.1.1. Poxvirus evasion of ZBP1

VACV E3 contains an amino-terminal Zα domain that is homologous to the ZBP1 Zα domains. E3 is critical for VACV pathogenicity in vivo and inhibition of the IFN response [97,131,132]. It has been proposed that E3 competes with ZBP1 for Z-nucleic acid-binding in VACV-infected cells. This hypothesis is supported by the observation that E3 overexpression reduced DNA-mediated induction of IFNβ responses [124]. In addition, a VACV E3 mutant that lacks the ability to bind Z-DNA is less pathogenic in a wild type mouse infection model, but not in either ZBP1- or RIPK3-deficient mice. However, this pathogenicity could be restored by an E3 chimera expressing the first Zα domain of ZBP1 or ADAR1 [126,132]. Overexpression of E3 was also described to reduce DNA-mediated induction of IFNβ responses [124]. During VACV infection, only full-length E3 but not a Zα-deleted E3 mutant (Δ83N) prevented ZBP1-mediated RIPK3-dependent necroptosis. Importantly, VACV-E3LΔ83N showed strong attenuation in wild type mice, but not in either ZBP1 or RIPK3- or DAI-deficient [126]. While most mammalian poxviruses contain E3L orthologs, some of these orthologs, including monkeypox virus and

myxoma virus, do not encode functional Zα domains [85]. In the myxoma virus and rabbit fibroma virus, which only productively infect rabbits and hares, the complete Zα domain-encoding DNA of their E3 orthologs are deleted [85] and are therefore not predicted to inhibit RIPK3-dependent necroptosis.

4. DNA-Activated Sensors and Poxvirus Antagonists

Cytosolic DNA sensing mainly induces transcription of type I interferons, but also can initiate NF-κB-dependent proinflammatory cytokines, which constitute an important frontline of antiviral defense against DNA viruses. Initial research demonstrated that multiple ligands such as long poly(dA:dT), and dsDNA oligonucleotides led to the activation of the IRF3 pathway and subsequent type I interferons responses [133,134]. More recently, investigations have focused on defining the upstream DNA receptors, and this effort has advanced considerably over the past decade [135]. Along with TLR9, discussed in a separate section, this effort has led to the identification of multiple DNA receptors, of which cyclic GMP-AMP synthase (cGAS), DNA-dependent RNA polymerase III (Pol-III), interferon-γ inducible protein 16 (IFI16), DNA-dependent protein kinase (DNA-PK), and DEAD box polypeptide 41 (DDX41) have been implicated in detecting poxviruses (Fig. 1.2).

4.1. Cyclic GMP-AMP synthase

Cyclic GMP-AMP synthase (cGAS) belongs to the oligoadenylate synthase (OAS) protein family and recognizes DNA in the cytosol [136]. Upon binding DNA, cGAS dimerizes and catalyzes the synthesis of 2′,3′ cyclic guanosine monophosphate–adenosine monophosphate (2′,3′ cGAMP), a 2′-5′-linked cyclic dinucleotide second messenger [137]. cGAMP binds to and activates the adaptor protein STING (stimulator of interferon genes). In turn, STING activates the protein kinases IκBα kinase (IKK) and TANK-binding kinase 1 (TBK1), leading to the

induction of interferons and cytokines through activation of NF-κB and IRF3, respectively (Fig. 1.2) [136,138–141].

The cGAS-STING axis is an important recognition pathway for multiple DNA viruses, including poxviruses. In ectromelia virus (ECTV) infected inflammatory monocytes, STING played an essential role in inducing interferon production through the activation of IRF7 and NF-κB signaling. Mice deficient for IRF7- and NF-κB were susceptible to ECTV infection [142]. Additional work demonstrated that cGAS is a key sensor for ECTV infection. Knockdown of either cGAS or STING decreased transcription of IFNα and IFNβ in L929 cells infected with ECTV. This phenotype was also observed in cGAS or STING deficient mice [143]. The cGAS-STING axis has also been shown to detect VACV infection. IFNβ induction after VACV infection was largely abolished in cGAS or STING-deficient mouse lung fibroblasts and dendritic cells [144]. In line with this observation, the cGAS-STING axis was necessary for type I IFN production in MVA-infected murine bone marrow-derived cDCs. Furthermore, cGAS and STING deficiency abolished TBK1- and IRF3-phosphorylation in these cells, and mice lacking STING or IRF3 showed decreased type I IFN expression compared to wild-type mice in response to MVA infection [145].

4.1.1. Poxvirus evasion of cGAS

Poxviruses encode several proteins that target cGAS/STING at different steps in the pathway (Fig. 1.2). STING phosphorylation and dimerization were suppressed during VACV-COP and -WR infection, indicating the existence of inhibitors that target this pathway upstream of STING [146]. The poxvirus protein F17, a late structural protein, has been reported to help evade cytosolic cGAS sensing. In response to infection with VACV lacking F17, cGAS mediated IRF activation and interferon-stimulated gene (ISG) responses in both macrophages and lung

fibroblasts [147]. F17 bound and sequestered Raptor and Rictor, which are regulators of mammalian target of rapamycin complexes mTORC1 and mTORC2, respectively. F17-mediated mTOR dysregulation blocked STING-mediated ISG induction and antiviral responses in part through mTOR-dependent cGAS degradation [148]. More recently, VACV B2 was shown to degrade the second messenger 2',3'-cGAMP, and this family of enzymes has been named "poxins". Deleting VACV poxin led to significant attenuation in a skin infection mouse model, although interestingly IFNβ levels were not increased, suggesting that poxins act by preventing cGAMP spread more than they prevent downstream effector production [149].

Poxin-encoding genes are found in many other poxviruses but are notably inactivated in VARV and VACV-MVA. In VACV and the closely related horsepox and rabbitpox viruses, the poxin domain is found by itself. However, in most orthopoxviruses, the poxin domain is found in combination with a Schlafen (Slfn) family-related domain [149]. In ECTV, this protein was called vSlfn. vSlfn deficient-ECTV was strongly attenuated in mouse infection models and unable to block activation of STING, TBK1, and IRF3 in macrophages and correlated with a strong IFN response [150].

4.1.2. Poxvirus evasion of STING

It was found that DNA-induced activation of STING and IRF3 can be inhibited by infection with cowpox virus, ECTV and VACV strains Copenhagen (COP) and Western Reserve (WR), but not by MVA [146]. Both TBK1 and IRF3 are key downstream components of the STING pathway, which mediate the IFN response. These downstream effectors are also targeted by poxviral antagonists such as VACV-C6, N1, N2, and E3 proteins (Fig. 1.2). VACV-C6, N1, and N2 belong to a family of B-cell CLL/lymphoma 2 (Bcl-2)-like proteins. C6 inhibits the IFNβ response induced by poly(dA:dT) DNA by blocking the activation of TBK1 and IKKε while

inhibiting translocation and activation of IRF3 [151]. VACV N1 was shown to directly associate with TBK1 to inhibit IRF3-mediated IFNβ responses. As an example of this effect, repairing the defective N1L gene in MVA abrogated the type I IFN response relative to infection with unaltered MVA. This IFN reduction coincided with reduced levels of TBK1- and IRF3-phosphorylation [145]. The early nuclear protein N2 acts further downstream in this pathway, inhibiting an IRF3-specific reporter (ISG56) response that was induced by overexpression of TBK1 or by poly(dA:dT) DNA stimulation. In addition, N2 also inhibited TBK1 elicited IFNβ promoter responses [152].

4.2. RNA polymerase III

DNA-dependent RNA polymerase III (Pol III) is a ubiquitous enzyme, which mainly resides in the nucleus, where it fulfills most of its cellular functions, including transcription of short untranslated RNAs, including transfer RNAs, 5S rRNA, and U6 spliceosomal RNA, using DNA as a template. However, Pol III may also localize to the cytosol, where it acts as a DNA sensor and engages the RIG-I mediated pathway [106]. In the cytosol, Pol III serves as a DNA sensor of several pathogens, including Legionella pneumophila, herpes simplex virus 1 (HSV-1), Epstein-Barr virus, and VACV [106,117]. It detects cytosolic AT-rich dsDNA through its DNA binding regions. Pol III then transcribes the DNA template into 5′-triphosphate-containing dsRNA, which activates RIG-I and leads to the induction of type I interferons and NF-κB activation (Fig. 1.2) [106,153,154].

4.2.1. Poxvirus evasion of Pol III

To date, the only described inhibitor of Pol III dsDNA-sensing is VACV E3. In 293T cells transfected with full-length E3, poly(dA:dT) DNA induced IFNβ expression and NF-κB activity

was abolished. Furthermore, the dsRBD-containing C-terminus alone was sufficient to inhibit these responses, whereas the Zα domain-containing N terminus was dispensable [117].

4.3. Interferon-γ inducible protein 16

The intracellular DNA sensor interferon-γ inducible protein 16 (IFI16) belongs to the pyrin and HIN200 domain (PYHIN) protein family. Although IFI16 contains a nuclear localization signal and is mainly located in the nucleus it can also be found in the cytosol, where it can recognize single-stranded (ss) DNA and dsDNA [155]. The HIN domain of IFI16 recognizes DNA ligands in a length-dependent manner [156]. Activated IFI16 induced the expression of IFNβ through IRF3 activation and the production of NF-κB-dependent pro-inflammatory genes during infection with several DNA viruses, including HIV, HSV-1, and VACV (Fig. 1.2) [155,157–159]. IFNβ expression induced by transfection with VACV DNA was dependent upon STING, TBK1, and IRF3, but not TLRs, ZBP1, or Pol III. IFI16 physically interacted with STING and BMDMs lacking STING failed to trigger IFNβ secretion in response to viral DNA [159]. IFI16 deficiency inhibited IRF3 activation- and NF-κB-dependent gene production induced by transfected DNA, and during infection with either MVA or HSV-1 [155,159]. During VACV infection, IFI16 shuttled from the nucleus of keratinocytes to viral factories in the cytosol for viral DNA recognition. Infection with the highly attenuated VACV strain MVA, but not with VACV-WR, induced IFI16-dependent CCL5 and ISG56 expression. These data indicate that VACV-WR can inhibit the IFI16 pathway, presumably via one or more of the genes missing in MVA [155]. The precise mechanisms of how VACV modulates IFI16-mediated DNA sensing are unclear, but viral immunomodulators that target downstream signaling of STING likely play a role.

4.4. DNA-dependent protein kinase

DNA-dependent protein kinase (DNA-PK) is best studied for its involvement in DNA repair and V(D)J recombination [160]. However, in addition to this well-documented activity, DNA-PK can also recognize cytosolic DNA [161]. As a heterotrimeric complex, DNA-PK is comprised of the catalytic subunit DNA-PKcs and the Ku heterodimer, consisting of Ku70 and Ku80 subunits. Upon exposure to exogenous DNA, Ku70 translocated from the nucleus to the cytosol and triggered the production of type III IFN (IFNλ1), which involved STING and TBK1 as mediators. This activity was associated with the activation of the transcription factors IRF1, IRF3, and IRF7 (Fig. 1.2) [161,162]. DNA-PK-dependent DNA sensing was shown to contribute to the initiation of the immune response to VACV in fibroblasts. Supporting this contribution, DNA-PK deficiency in either cell lines or mice significantly impaired the induction of IFNβ and IL-6 in response to infection with MVA or HSV-1 [163].

4.4.1. Poxvirus evasion of DNA-PK

VACV expresses two related proteins, called C16 and C4 in the WR strain, that target the DNA-PK mediated DNA sensing pathway (Fig. 1.2). These proteins share about 54% amino acid identity in their C-terminal region [164–166]. The C-terminal region of C16 interacts directly with the Ku heterodimer of the DNA-PK complex to prevent DNA-PK binding to DNA, ultimately reducing the production of cytokines and chemokines. Consistent with this in vitro observation, mice infected with C16-deficient VACV, produced more cytokines and chemokines than mice infected with wild type VACV [164]. Like C16, VACV protein C4 also interacts with Ku and blocks DNA binding through its C-terminal domain, resulting in decreased IRF3 phosphorylation. Additionally, C4 inhibits the recruitment and activation of immune cells and suppresses cytokine production, such as IL-6 both in vitro and in vivo [165]. While C16 and C4

have overlapping functions, viruses with deletions of only one of these proteins were still attenuated in mouse infection models. The two most likely interpretations of this data are that there might be currently unrecognized non-redundant functions between the two proteins, or that C16 and C4 work in tandem by mass action [165].

4.5. DEAD box polypeptide 41

DEAD box polypeptide 41 (DDX41) was identified as a cytosolic sensor that recognizes diverse pathogen-derived nucleic acids, such as viral dsDNA, cyclic di-GMP, and cyclic di-AMP [167,168]. DDX41 is a member of the DEAD-box protein family and is composed of two RecA-like domains (DEADc and HELICc domains) and a zinc finger [169]. Upon binding dsDNA via its DEADc domain, DDX41 associates with STING and initiates the activation of NF-κB and IFN signaling pathways in myeloid dendritic cells (Fig. 1.2) [167].

DDX41 directly recognized a repeating 70 bp motif (VACV 70mer), which is located in the inverted terminal repeat region of the VACV genome [159,167]. Knockdown of DDX41 or STING in THP-1 cells abolished the production of IFNβ and IL-6 in response to either the VACV 70mer or HSV-1 DNA [167]. It is unknown if poxviruses directly target DDX41, but it is possible that poxviral inhibitors that act downstream of STING activation can also interfere with this DDX41-mediated immune response (see Poxvirus evasion of STING).

5. Toll-Like Receptor-Mediated Poxvirus Recognition and Poxvirus Antagonists

Toll-like receptors (TLRs) are a family of PRRs, which derive their name from their homology with the Drosophila toll gene [170]. In Drosophila, activation of the toll pathway by ligands from gram-positive bacteria or fungi triggers cellular immunity and production of antimicrobial peptides [171–173]. Toll-like receptors function as PRRs to initiate signaling cascades important

for host defense against many pathogens. There are 13 currently known TLRs in mammals (TLR1 to TLR13), although humans only possess TLR 1 through 10 [174].

TLRs are type I integral membrane glycoproteins expressed in both immune cells and non-immune cells such as fibroblasts and endothelial cells. These receptors have a common architecture, with an N-terminal extracellular leucine-rich repeat-containing ectodomain, which is responsible for the recognition of PAMPs, a single transmembrane helix, and a C-terminal cytoplasmic toll/interleukin-1 receptor (TIR) homology domain [175]. TLRs localize to the plasma membrane of the cell surface (TLRs 1, 2, 4, 5, 6, and 10) or to various intracellular compartments (TLRs 3, 7, 8, 9, 11, 12, and 13), such as the endoplasmic reticulum (ER), endosome, lysosome and endolysosome [176]. This cellular localization is one determinant of the PAMPs sensed by TLRs [176]. Once activated, TLRs typically activate downstream effectors through either adaptor proteins, typically myeloid differentiation primary response gene 88 (MyD88) or TRIF.

TLR2/6, TLR4, TLR8, and TLR9 recruit myeloid differentiation primary response gene 88 (MyD88) to transduce their signaling cascades [41]. Activation of MyD88 dependent signaling induces proinflammatory cytokines and chemokines (Fig. 1.3). TLR8-MyD88 and TLR9-MyD88 signaling pathways are also engaged in IFN induction through IFN regulatory factor 7 (IRF7) activation in dendritic cell (DC) subsets, such as the plasmacytoid DCs (pDCs) [177]. MyD88 recruits and interacts with interleukin 1 receptor-associated kinase 4 (IRAK4) to form a structure known as the Myddosome along with two other IRAK kinase family members, IRAK1 and IRAK2. This complex activates tumor necrosis factor receptor-associated factor 6 (TRAF6) [178]. TRAF6-induced activation of TGF-β activated kinase 1 (TAK1) subsequently phosphorylates the IKKβ subunit of the canonical IκB kinase (IKK) complex [179] leading to

ubiquitination and proteasomal degradation of IκBα and release of NF-κB [180] leading to the production of proinflammatory cytokines (Fig. 1.3) [181]. Notably, toll/interleukin 1 receptor (TIR) domain-containing adapter protein (TIRAP, also known as Mal) and TRIF-related adaptor molecule (TRAM) are further required for bridging MyD88 to TLR2/6 and TLR4.

The adaptor TRIF-dependent pathways are initiated through TLR3 and endosomal TLR4 and induce both inflammatory responses and type I IFNs through activation of TRAF6 or TRAF3, respectively [42]. TRIF associates with TRAF6 and RIP1 to activate the classical IKK complex through the activation of TAK1 kinase complex, resulting in the production of NF-κB-dependent proinflammatory cytokines and chemokines [181]. In contrast, TRIF interacts with TRAF3 to recruit the noncanonical IKK-related kinases TBK1 and IKKε for phosphorylation and activation of IRF3/IRF7, resulting in the subsequent induction of type I and type III IFNs (Fig. 1.3) [182]. Several TLRs have been implicated to play roles in poxvirus infections, including endosomal TLR3, TLR8 and TLR9, and membrane-bound extracellular TLR2 and TLR4 (Fig. 1.3).

5.1. TLR3

TLR3 localizes to the endosome and was the first characterized TLR to recognize nucleic acid [183]. The primary ligand of TLR3 dsRNA is recognized via the N-terminal ectodomain (ECD) [183–185]. After binding dsRNA, downstream signaling transduction is mediated through the TIR domain-containing adaptor-inducing interferon-β (TRIF) [186]. Activation of the TLR3-TRIF pathway leads to the production of NF-κB-dependent proinflammatory cytokines, and type I and type III IFNs (Fig. 1.3) [183].

Paradoxically, when infected with VACV, TLR3-/- mice showed decreased disease morbidity, accompanied by reduced VACV replication in the respiratory tract and impaired viral dissemination [25]. This TLR3 deficiency did not change the level of IFNβ but did reduce the

levels of inflammatory cytokines, including IL-6, TNFα, and monocyte chemoattractant protein-1 (MCP-1/CCL2). These cytokine increases suggest that the increased morbidity and viral dissemination observed in TLR3 competent mice may be mediated through NF-κB-dependent inflammatory cytokines [25]. However, TLR3 has also been shown to improve post-exposure vaccine efficacy in response to ECTV infection in mice. BALB/c mice infected with ECTV can be cured by post-exposure vaccination with either the VACV-Lister or MVA strains up to three days after infection. However, post-exposure treatment with poly(I:C), an agonist of TLR and other dsRNA-binding proteins, either alone or in combination with traditional vaccination improved the efficacy of this treatment regimen by modulating TLR3 activation and IFNα induction [187]. Thus, the antiviral activity of TLR3 is complex and merits further investigation.

5.1.1. Poxvirus evasion of TLR3

Poxviruses encode multiple Bcl-2-like proteins that target the TLR3 pathway, including A52, A46, N1, B14, K7, N2, and C6 proteins (Fig. 1.3). Intriguingly, the first five of these proteins share homology although as described below they inhibit TLR3 through distinct mechanisms. A52 was shown to block TLR3-mediated activation of NF-κB induced by poly(I:C) stimulation through interaction with both interleukin 1 receptor-associated kinase 2 (IRAK2) and tumor necrosis factor receptor-associated factor 6 (TRAF6), disrupting the Mal-IRAK2 signaling complex or TRAF6-TAB1-containing complex, respectively [188]. In response to poly(I:C), A46 was directly associated with TRIF, which acted as TIR adapter for TLR3 signaling, to inhibit IRF3 activation and gene induction [189]. However, in the presence of poly(I:C), N1 physically interacted with components of the IKK complex and also associated with IKKε and TBK1, thereby inhibiting NF-κB activation and IRF3 mediated IFNβ responses [190]. B14, an immediate-early gene product of VACV, prevented phosphorylation of IKKβ, a component of

the IKK complex, resulting in inhibition of NF-κB signaling induced by poly(I:C) [191,192]. K7 has been shown to interact with DEAD-box RNA helicase (DDX3) to inhibit TRIF-induced IRF3/7 activation, and also prevented IFNβ promoter induction at the level of TBK1/IKKε [193]. VACV N2 localized to the nucleus and functionally inhibited IRF3 activity after translocation of IRF3 into the nucleus. Ultimately, this N2-IRF3 interaction decreased activation of the IFNβ promoter in response to poly(I:C) stimulation [152]. Finally, C6 has been reported to be a multifunctional interferon antagonist during VACV infection. In the context of the TLR3 pathway, C6 prevented TBK1- and IKKε-dependent IRF3 activation, resulting in inhibition of IFNβ-promoter activation induced by poly(I:C) [151,152].

5.2. TLR8

TLR8 is broadly expressed in the endosomes of myeloid cells, such as monocytes, macrophages, and myeloid dendritic cells (DCs) [194,195]. TLR8 is non-functional until it undergoes proteolytic processing to generate a functional receptor in the endosome [195]. Activation of this toll-like receptor is traditionally mediated through recognition of uridine- and guanosine-rich single-stranded RNA (ssRNA) of either bacterial or viral origin [196,197]. However, a recent report has shown that murine TLR8 can be activated by poxviral DNA or by synthetic poly(A) and poly(T) oligodeoxynucleotides both in vitro and in vivo. Either VACV infection or VACV DNA activated an NF-κB reporter expressed by HEK293 cells that expressed murine TLR8, but not in cells expressing murine TLR7. Similarly, siRNA-mediated knockdown of TLR8 reduced the secretion of IFNα in pDCs [198]. However, the underlying mechanism is yet to be determined.

Regardless of the ligand, binding transduces signaling through MyD88, ultimately resulting in the induction of IRF7 activation, IFN production, and NF-κB-dependent proinflammatory

responses (Fig. 1.3). In addition, VACV infection-induced IFNα production by pDCs in vitro and in vivo and TLR8-dependent pDC activation played an important role in the control of VACV infection in vivo [198].

5.2.1. Poxvirus evasion of TLR8

VACV E3 has been reported to target TLR8-dependent pathways. In human monocytes, E3 reduced the expression of TLR8-dependent cytokines and chemokines, including pro-inflammatory cytokines such as TNFα, IL-6, and chemokines such as interferon gamma-induced protein 10 (IP-10), and chemokine (C-C motif) ligand 5 (CCL5, also known as RANTES). In addition, E3 directly interacted with DExH-Box helicase 9 (DHX9) to antagonize IL-6 promoter activation [199].

5.3. TLR9

TLR9 was the first identified DNA sensor. It is localized in endosomes in a variety of cells including plasmacytoid dendritic cells (pDCs), B cells, neutrophils, monocytes, and some non-immune cells [200,201]. TLR9 undergoes proteolytic cleavage of its ectodomain to recognize unmethylated cytosine-guanosine (CpG)-rich DNA derived from bacteria or viral genomic dsDNA [200,202–204].

As the primary DNA-sensing TLR, TLR9 has been implicated in the response to multiple poxvirus infections. For example, TLR9 depletion dramatically decreased mouse survival after ECTV infection, which required TLR9 expression in DCs [26]. TLR9 depletion in these mice abolished ECTV induced DC maturation and IFNα production, highlighting the important role of TLR9 when controlling ECTV infection [26]. In this ECTV model, the TLR9-MyD88-IRF7 pathway was essential for proinflammatory cytokine expression in $CD11c^{+}$cells and for the recruitment of inflammatory monocytes to the draining lymph node [142].

In response to MVA infection, TLR9-deficient or MyD88-deficient murine cDCs showed decreased production of IFNα and IFNβ compared to wild type cDCs [145]. TLR9 has also been implicated in the host response to fowlpox virus and MYXV through the above described MyD88 signal transduction cascade [205,206].

5.3.1. Poxvirus evasion of TLR9

To date, VACV E3 is the only described viral antagonist of the TLR9 pathway [206]. In cells treated with CpG-containing DNA, a TLR9 agonist, wild type VACV significantly inhibited IFNβ, TNF, and IL-12p70 (IL-12) production in murine pDCs. In contrast, infecting these cells with VACV lacking E3L reduced this inhibitory effect, which could be rescued by co-infection with wild type VACV. These results were also phenocopied if only the N-terminal Z-DNA-binding (Zα) domain of E3 was deleted, demonstrating that this domain is important for TLR9 pathway inhibition [206].

5.4. TLR4

TLR4 was identified as a human toll homolog in 1997 [207].TLR4 predominantly recognizes bacterial lipopolysaccharide (LPS), mannuronic acid polymers and teichuronic acid. TLR4 has also been shown to recognize viral glycoproteins, fusion proteins, and damage-associated molecular patterns (DAMPs) [208–212]. Whether TLR4 directly recognizes poxvirus ligands is not yet clear. One possibility is that TLR4 is indirectly activated after poxvirus infections. Previous work has demonstrated that infection with either VACV strains WR or MVA can lead to the extracellular release of high mobility group box protein 1 (HMGB1). Outside the cell, HMGB1 binds to myeloid differentiation factor 2 (MD-2), the extracellular adaptor of TLR4, to activate this pathway [213–215]. There is also some evidence that TLR4 may recognize a viral protein, potentially on the virion surface, rather than ligands released or generated during

infection [216]. It is currently unclear if either or both of these mechanisms are the primary mode of TLR4 activation by poxviruses. After ligand binding, TLR4 dimerizes and initiates a signaling cascade via TLR adapter molecules MyD88 adaptor-like (Mal)/TIRAP, MyD88, TRAM, and TRIF, resulting in the production of inflammatory cytokines and type I IFNs (Fig. 1.3) [217]. In response to VACV infection, TLR4 provided maximal protection against pulmonary VACV infection in a mouse model. Surprisingly, TLR4 dampened the cytokine response of bone marrow macrophages to VACV, and TLR4 deficiency promoted an increase in IFNβ and IL-6 production in the lungs [216].

5.4.1. Poxvirus evasion of TLR4

VACV proteins A46, A52, K7, and N1 have been implicated in TLR4 evasion (Fig. 1.3). A46 and A52 share amino acid sequence similarity with the toll/interleukin-1 receptor (TIR) domain. The VACV A46 protein directly interacts with the TLR4, MyD88, Mal, TRIF, and TRIF-related adaptor molecule (TRAM), disrupting receptor-adaptor interactions and inhibiting downstream signaling [218–222]. A46 deficient VACV showed attenuated virulence in a murine intranasal infection model [189]. A52 targets TLR4 signaling, potently suppressing both IL-1- and TLR4-mediated NF-κB activation by mimicking the dominant-negative effect of a truncated version of MyD88 [223]. VACV K7 blocks both IRAK2 and TRAF6 activation to inhibit the TLR4-NF-κB signaling axis [193]. Finally, N1 has been shown to target the TRAF6-TBK1-IKK complex, interacting with IKKα and IKKβ to block NF-B responses [190].

5.5. TLR2

TLR2, first identified in 1998 [170], is expressed on the surface of immune cells, such as monocytes, macrophages, dendritic cells, and NK cells. On the cell surface, TLR2 forms heterodimers with either TLR1 or TLR6 to recognize a wide array of distinct ligands including

lipopeptides and lipoteichoic acid from bacteria, and fungal polysaccharides [224–227]. TLR2 also recognizes multiple viral ligands, including envelope glycoproteins and core proteins from cytomegalovirus, HIV-1, and hepatitis C virus [228–230]. Upon ligand binding, TLR2 interacts with the adaptor protein MyD88, ultimately inducing NF-κB-dependent inflammatory responses (Fig. 1.3). While TLR2 has been implicated in the innate response to VACV infection [202, 203], defining the poxvirus ligands is still an ongoing area of research. As with TLR4, poxviruses may indirectly initiate TLR2 signaling through HMGB1 and MD-2. This mechanism was proposed for TLR2 activation by a MVA-vectored tuberculosis vaccine candidate (MVA85A), supported by the observation that treating mouse PBMCs with anti-HMGB1 antibodies reduced in vitro production of chemokine (C-X-C Motif) ligand 2 (CXCL2) [214]. However, the more basic question of whether TLR2 can be activated through this HMGB1/MD-2 axis remains controversial [231,232]. Both VACV and UV-inactivated VACV elicited similar immune responses through the TLR2-MyD88 pathway [24]. TLR2 activation by UV-inactivated viruses that should not induce cell death and thus HMGB1 release suggests that TLR2 activation may instead be mediated by direct binding of an as yet undescribed poxvirus ligand. TLR2 deficiency in conventional DCs (cDCs) and T cells reduced the secretion of IL-6 in response to VACV infection compared to infected wild type cells [24,233]. Additionally, TLR2 mediated signaling is important for NK cell activation after VACV infection and critical to control VACV infection in mice [234].

5.5.1. Poxvirus evasion of TLR2

VACV encodes multiple antagonists of TLR2-mediated signaling, including A46, N1, and E3 (Fig. 1.3). A46 and N1 belong to a family of B-cell lymphoma 2 (Bcl-2)-like proteins and contain experimentally confirmed Bcl-2 folds [219,235,236]. A46 physically interacted with

diverse TIR-domain containing adaptor proteins including MyD88, ultimately preventing TLR2-mediated activation of IRF7 and IFNβ responses [237]. VACV N1 inhibited the TLR2-mediated activation of NF-κB through a direct association with components of the IKK complex [190,236]. Finally, VACV E3 was described to act downstream of this pathway to interact with the DExD/H-box helicase DHX9 to inhibit DHX9-mediated enhancement of NF-κB-dependent IL-6 promoter activation [199].

6. Inflammasome Recognition of Poxviruses and Poxvirus Antagonists

Inflammasomes are multiprotein signaling complexes responsible for the production of proinflammatory cytokines and the induction of pyroptosis, an inflammatory lytic programmed cell death, to halt viral replication and induce nearby cells to adopt antiviral states [238]. Inflammasome activation mediates the conversion of inactive precursor proteins pro-interleukin (IL)-1β and pro-IL-18 into the bioactive forms IL-1β and IL-18, which play important roles in host defense against a variety of bacterial, fungal, and viral infections [239,240]. Certain PRRs have been implicated in canonical inflammasome assembly, including NOD-like receptors and AIM2-like receptors [241,242]. After PAMP and cell damage-associated signal recognition, adaptors are recruited, such as apoptosis-associated speck-like protein (ASC) [243]. This process results in cytokine secretion and pyroptosis as proteolytically active caspases mediate the maturation and secretion of pro-inflammatory cytokines IL-1β and IL-18, while cleavage of gasdermin-D (GSDMD), a key pyroptotic substrate of inflammatory caspases, induces pyroptosis (Fig. 1.4) [244]. Specifically, the inflammasome proteins NACHT, LRR, and PYD domains-containing protein (NLRP3) and AIM2, have been implicated in the recognition of poxvirus infections [29,30,245].

6.1. The NLRP3 inflammasome

NLRP3 acts as the intracellular sensor component of the NLRP3 inflammasome and detects a broad range of both PAMPs and host-derived activating signals (endogenous damage associated molecular patterns DAMPs). NLRP3 is expressed in innate immune cells and non-immune cells, including macrophages, neutrophils, and epithelial cells [246]. This sensor is comprised of an N-terminal pyrin domain (PYD), a central NACHT domain, and C-terminal leucine-rich repeat domains. NLRP3 inflammasomes must be primed before they are activated. This priming step can be mediated by a variety of signals including TLR or NLR ligands, which activate NF-κB. NF-κB then upregulates NLRP3 expression to levels sufficient to permit inflammasome assembly [247–249]. Once the PAMP or DAMP ligand is bound, oligomerized NLRP3 recruits ASC through homotypic PYD-PYD interactions and activates caspase 1, thereby triggering the secretion of the proinflammatory cytokines IL-1β and IL-18 (Fig. 1.4). During MVA infection, crosstalk between the NLRP3 inflammasome and TLR2-TLR6-MyD88 has been documented to mediate the expression and processing of IL-1β in macrophages both in vivo and in vitro [29]. Furthermore, in a keratinocyte model of MVA infection, IL-1β secretion was reduced in the presence of pyrrolidine dithiocarbamate, BAPTA tetrakis (acetoxymethyl ester), and glibenclamide, suggesting that intracellular Ca^{2+} level, and K^{+} efflux may be involved in NLRP3-inflammasome activation [250].

6.1.1. Poxvirus evasion of the NLRP3 inflammasome

To inhibit NLRP3 activity, poxviruses target different stages of inflammasome assembly and processing, as well as inhibiting the secretion or the function of IL-1β and IL-18. Multiple poxviruses encode viral pyrin-only proteins (PYD/vPOP), which have homology with the ASC-PYD domain [18,251]. For example, one of these proteins, MYXV-M013, directly interacts with

ASC-1 to inhibit NLRP3-ASC-1 interactions, thereby inhibiting activation of caspase-1 and the secretion of IL-1β and IL-18 [18,245,252,253]. Similarly, gp013 from rabbit fibroma virus (RFV) interacts with ASC to interfere with PYD-mediated activation of caspase-1 [251]. Poxviruses also encode serine proteinase inhibitor 2 (SPI-2) orthologs, including cytokine response modifier A (CrmA) from cowpox virus and VACV-B13. These proteins act as substrate mimics to inhibit caspase-1 activity, thus preventing proteolytic processing of IL-1β [254–256]. Additionally, poxviruses have evolved secreted viral IL-1β receptors (vIL-1βR), such as VACV-B15, CPXV-B14, and ECTV-191, which prevent IL-1β binding with the host receptors [257,258]. Similarly, viral IL-18 binding proteins (e.g., molluscum contagiosum virus -54L and VACV-C12) compete with the IL-18 cognate receptor for IL-18 binding [259–261].

6.2. The AIM2 inflammasome

AIM2 belongs to the pyrin and HIN protein (PYHIN) family of proteins and is comprised of an N-terminal PYD domain, which recruits ASC through PYD-PYD interactions, and a C-terminal HIN200 domain, which is essential for recognition and binding cytosolic DNA [262–265]. Upon recognition of DNA, AIM2, ASC and procaspase 1 form the AIM2 inflammasome. This inflammasome activates caspase 1 to initiate proinflammatory cytokine processing, resulting in maturation and secretion of IL-1β and IL-18 (Fig. 1.4) [30,266,267].

The AIM2 inflammasome has been shown to recognize multiple viral infections including VACV, mouse cytomegalovirus, and influenza A virus [268–271]. For example, in cells derived from AIM2$^{-/-}$ mice infected with VACV, IL-1β release and maturation, as well as caspase-1 cleavage were all reduced [30,268]. Similarly, AIM2 knockdown in human primary keratinocytes almost completely abolished IL-1β and IL-18 production during MVA infection. In contrast, NLRP3 knockout only slightly reduced IL-1β secretion [250]. While these data clearly

establish a role for the AIM2 inflammasome in response to poxvirus infection, no direct poxvirus inhibitors are currently known. However, the inhibitors of IL-1β and IL-18 activity, discussed in the previous section, are equally effective at preventing the activity of these downstream effectors of AIM2 inflammasome activation.

7. Conclusions

Individual PRRs have unique molecular mechanisms for sensing ligands and triggering antiviral responses via diverse adapters and effectors. Furthermore, redundancy, cooperation, and crosstalk among the various PRRs increase this complexity. This crosstalk and redundancy in immune pathways are also reflected in the viral antagonists, with multiple PRR pathways targeted by the same viral proteins. It is currently an open question as to how Individual PRRs, such as PKR, regulate other signaling pathways, including NF-kB signaling pathway. Investigation of the cooperation and crosstalk between PKR and other pathways will help define the innate immune network(s) elicited by PKR during poxvirus infections.

On the other side of this battle, it is becoming more apparent that the diversity in the poxvirus family is also reflected by the range of activities discovered for individual viral gene orthologs, and their implications for viral host range and virulence. This observation is most strongly supported for rapidly evolving genes like viral immune regulators and their implications for virus host range and virulence [4,72,78,272]. In this thesis, K3 orthologs, as one of such immune regulators, are investigated for their regulatory roles in PKR associated signaling pathways

Author Contributions: Conceptualization: H.Y., G.B., and SR; Writing – original draft: H.Y.; Writing – review & editing (H.Y., R.B., G.B., and S.R.). All authors have read and agreed to the published version of the manuscript.

Acknowledgments

We thank Jeannine Nicole Stroup, Chorong Park, Ana Maria Stoian, Anak Agung Dewi Megawati, Shefali Mrinal Banerjee, Chi Zhang for discussions and suggestions. We apologize to colleagues whose work could not be cited because of space limitations.

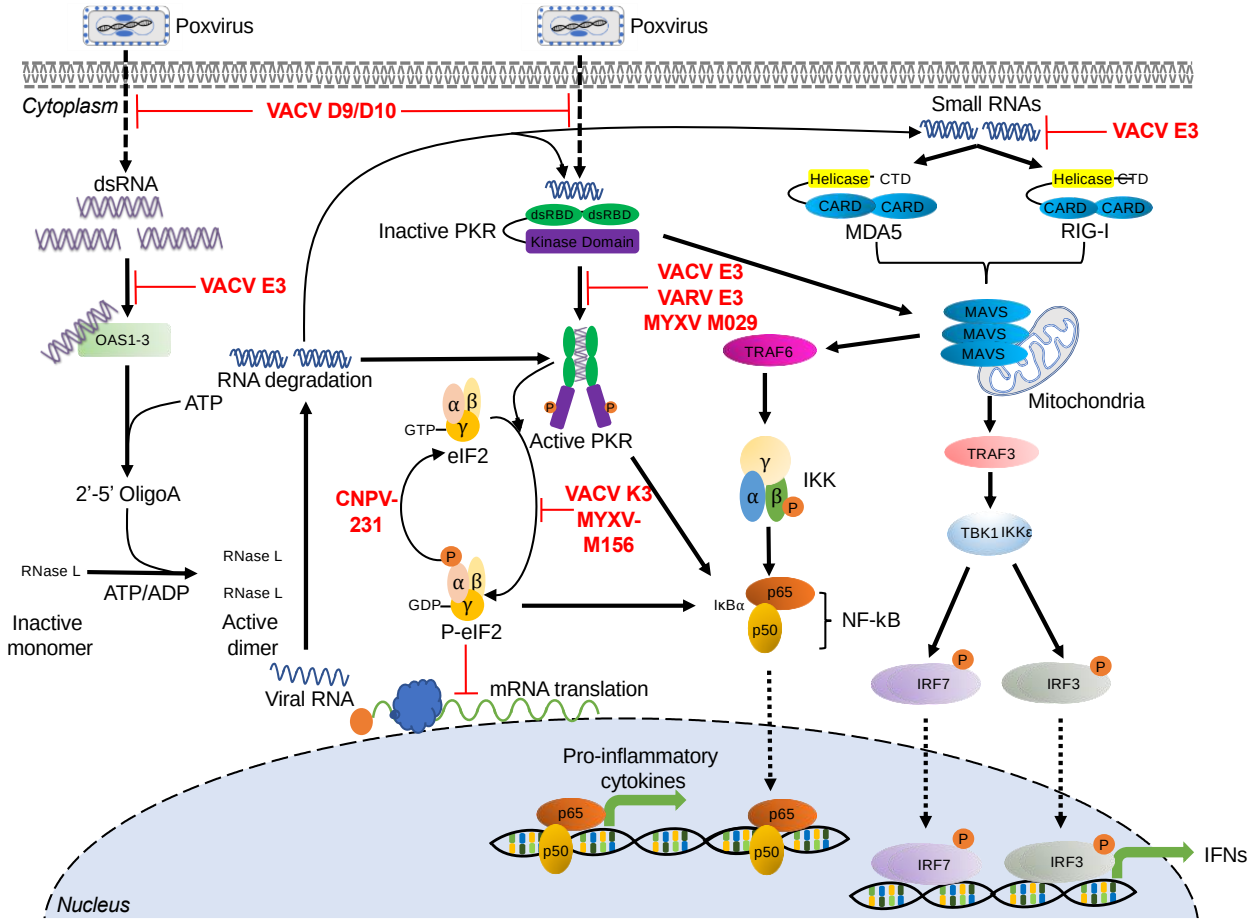

Fig. 1.1 dsRNA sensor-mediated signaling pathways and poxvirus antagonists

The figure presents host sensors involved in recognizing dsRNA species from poxviral infections, and the elicited signaling cascades by these sensors, which are indicated in black. Poxvirus encoded immunomodulatory proteins that inhibit activation of these host pathways are indicated in red. See main text for corresponding details and the underlying molecular mechanisms. Abbreviations used in this figure include ADP: adenosine diphosphate; ATP: adenosine triphosphate; CARD: caspase activation and recruitment domains; CNPV: canarypox virus; CTD: carboxy-terminal domain; dsRBD: dsRNA-binding domain; dsRNA: double-stranded RNA; eIF2: eukaryotic translation initiation factor 2; GDP: guanosine diphosphate; GTP: guanosine-5'-triphosphate; IKKα: IκBα kinase α; IKKβ: IκBα kinase β; IKKε: IκBα

kinase ε; IKKγ: IκBα kinase γ; IL-6: interleukin-6; IRF3/7: interferon regulatory factor 3/7; IκBα: inhibitor κBα; MAVS: mitochondrial antiviral-signaling protein; MDA5: melanoma differentiation-associated protein 5; MYXV: myxoma virus; NF-κB: nuclear factor kappa B; OAS: 2′-5′-oligoadenylate synthetases; p65/p50: NF-κB heterodimer p50/p65 subunit; PKR: protein kinase R; RIG-I: retinoic acid-inducible gene I; RNase L: ribonuclease L; TBK1: TRAF family member-associated NF-κB activator (TANK)-binding kinase 1; TNFα: tumor necrosis factor-alpha; TRAF3/6: tumor necrosis factor receptor-associated factor 3/6; VACV: vaccinia virus; VARV: variola virus.

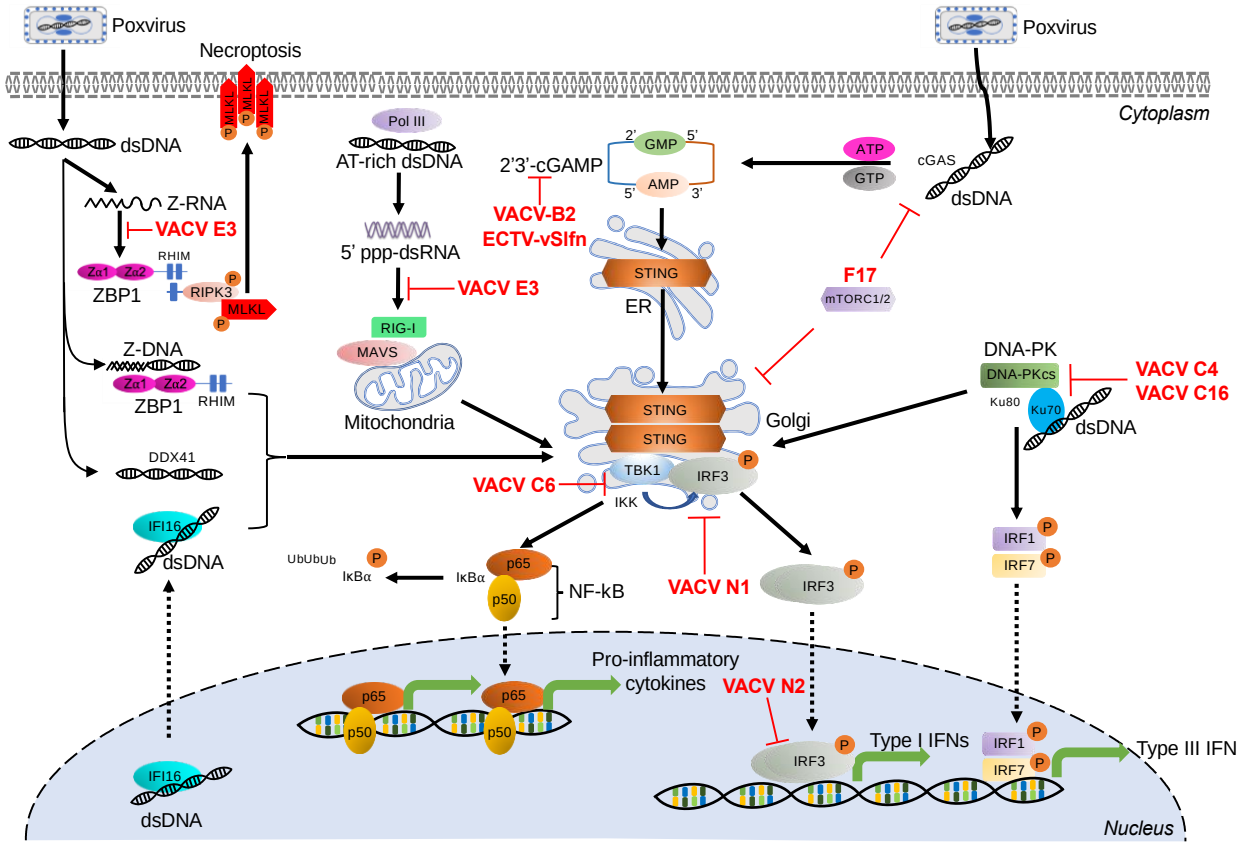

Fig. 1.2 Cytosolic DNA sensor-mediated signaling pathways and poxvirus antagonists

The activation of DNA sensors and the transduction of their triggered signaling cascades are indicated by black arrows. The diverse poxviral inhibitors of these cytosolic DNA sensors are indicated in red. See main text for corresponding details and the underlying molecular mechanisms. Abbreviations used in this figure include ADP: adenosine diphosphate; AMP: adenosine monophosphate; ATP: adenosine triphosphate; cGAS: cyclic GMP-AMP synthase; DDX41: Asp-Glu-Ala-Asp (DEAD) box polypeptide 41; DNA-PK: DNA-dependent protein kinase; DNA-PKcs: DNA-dependent protein kinase catalytic subunit; dsDNA: double-stranded DNA; ECTV: ectromelia virus; ER: endoplasmic reticulum; GMP: guanosine monophosphate; IFI16: interferon-γ inducible protein 16; IL-6: interleukin-6; IRF1/3/7: interferon regulatory factor 1/3/7; IκBα: inhibitor κBα; MAVS: mitochondrial antiviral-signaling protein; MLKL:

mixed lineage kinase-like; mTORC1/2: mammalian target of rapamycin complex 1/2; MVA: modified vaccinia virus Ankara; NF-κB: nuclear factor kappa B; p50/p65: NF-κB heterodimer p50/p65 subunit; RHIM: RIP homotypic interaction motif; RIG-I: retinoic acid-inducible gene I; RIPK: receptor interacting protein kinase; RNA pol III: DNA-dependent RNA polymerase III; STING: stimulator of interferon genes; TBK1: TRAF family member-associated NF-κB activator (TANK)-binding kinase 1; TNFα: tumor necrosis factor-alpha; TRAF: tumor necrosis factor receptor-associated factor; VACV: vaccinia virus; vSlfn: viral Schlafen; ZBP1: Z-nucleic acid-binding protein 1; Zα: Z-nucleic acid-binding domain; 2′3′ cGAMP: 2′3′ cyclic guanosine monophosphate–adenosine monophosphate; 5'ppp-dsRNA: 5' triphosphate double-stranded RNA.

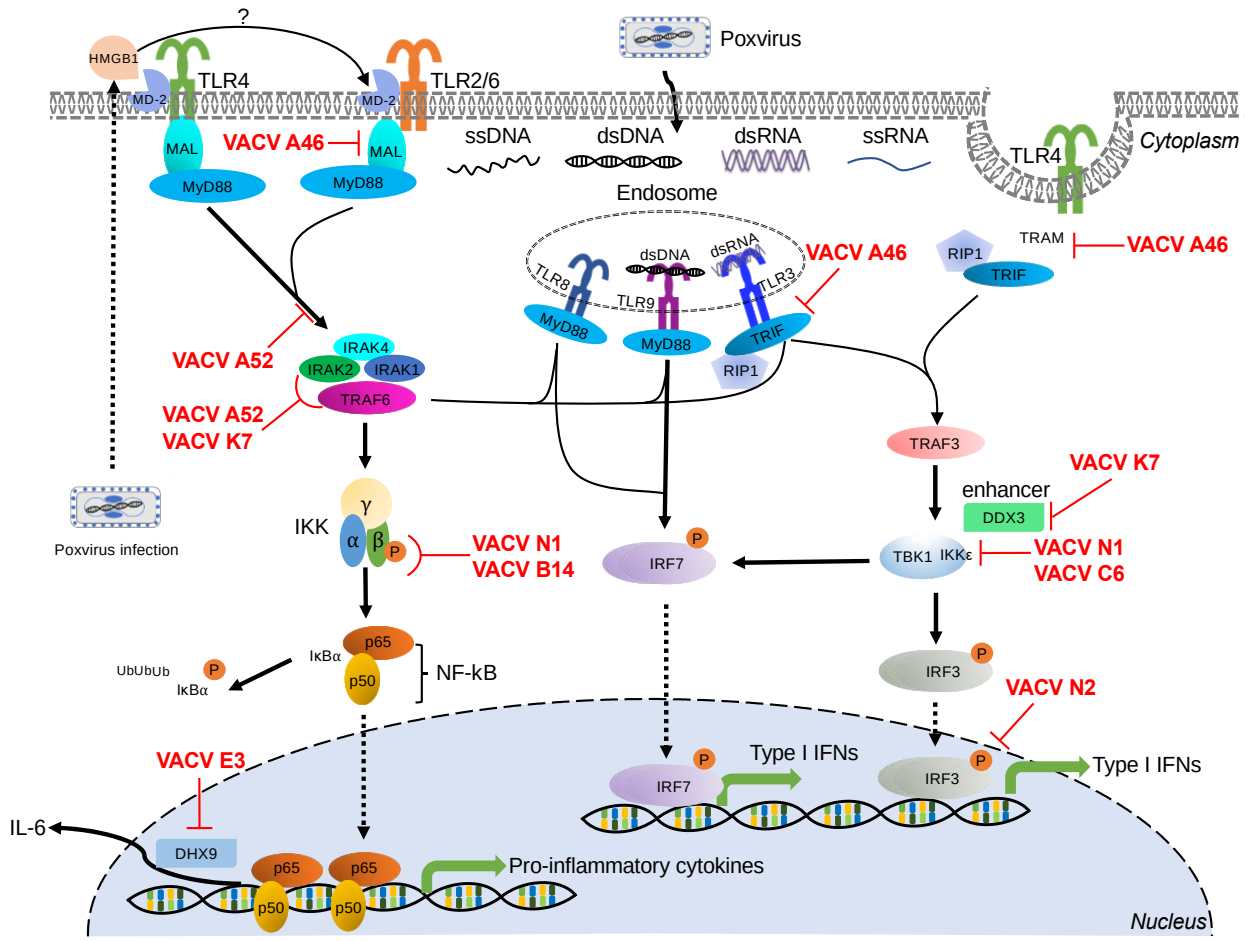

Fig. 1.3 TLR family-mediated signaling pathways and poxvirus antagonists

TLR sensors involved in the recognition of poxviral infections are indicated in their subcellular localization. The signaling cascades induced by these TLRs are denoted by black arrows to indicate transduction or activation. Poxvirus encoded viral antagonists and their targeted signaling molecules are shown in red. Abbreviations used in this figure include DDX3: Asp-Glu-Ala-Asp (DEAD) box polypeptide 3; DHX9: DExH-Box helicase 9; dsDNA: double-stranded DNA; dsRNA: double-stranded RNA; HMGB1: high mobility group box protein 1; IκBα: inhibitor κBα; IKKα: IκBα kinase α; IKKβ: IκBα kinase β; IKKε: IκBα kinase ε; IKKγ: IκBα kinase γ; IL-6: interleukin-6; IRAK1/2/4: interleukin-1 receptor-associated kinase 1/2/4; IRF3/7:

interferon regulatory factor 3/7; Mal: myD88-adapter-like; MD-2: myeloid differentiation factor 2; MyD88: myeloid differentiation primary response gene 88; NF-κB: nuclear factor kappa B; p65/p50: NF-κB heterodimer p50/p65 subunit; RIP1: receptor-interacting protein 1; ssDNA: single-stranded DNA; ssRNA: single-stranded RNA; TBK1: TRAF family member-associated NF-κB activator (TANK)-binding kinase 1; TLR2/3/4/8/9: toll-like receptor 2/3/4/8/9; TNFα: tumor necrosis factor-alpha; TRAF3/6: tumor necrosis factor receptor-associated factor 3/6; TRAM: TRIF-related adapter molecule; TRIF: toll/interleukin-1 receptor domain-containing adapter-inducing interferon-β; VACV: vaccinia virus.

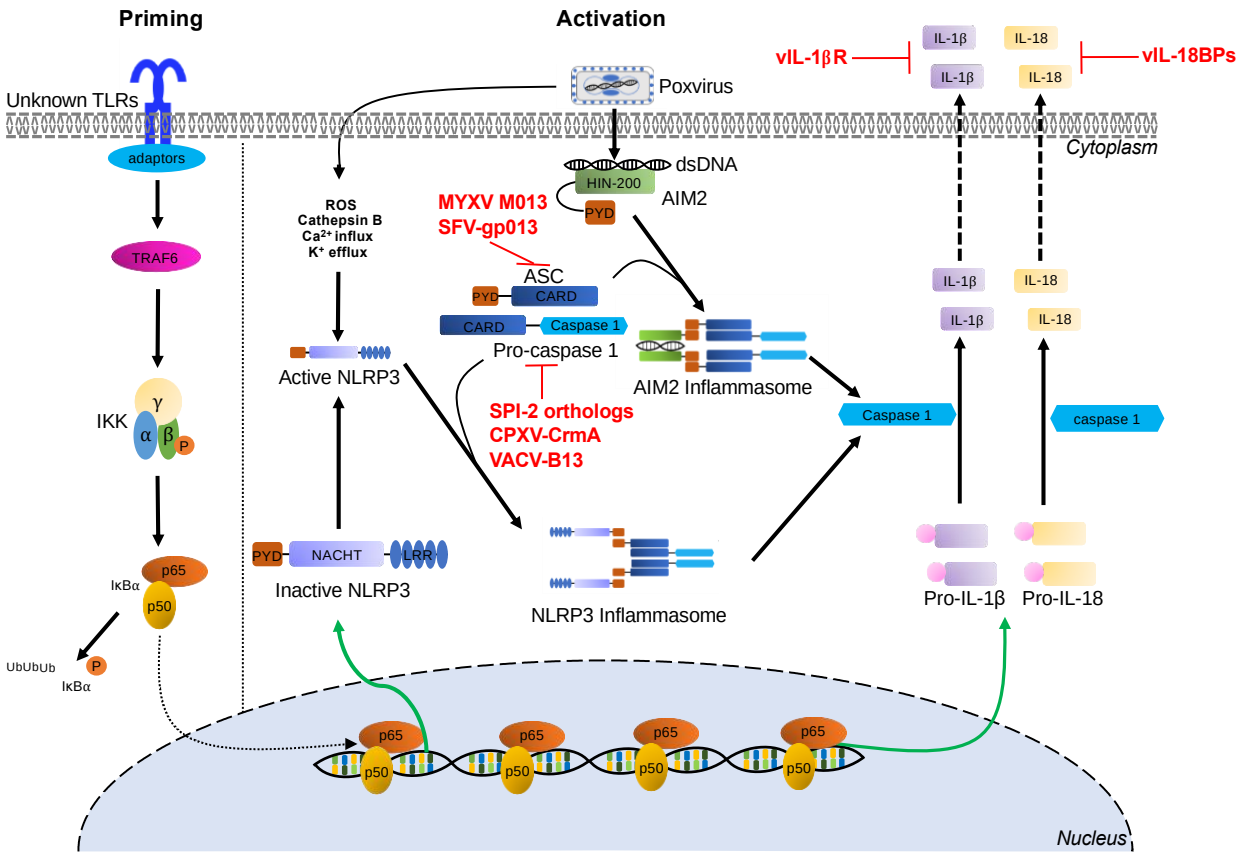

Fig. 1.4 Inflammasome-mediated signaling pathways and poxvirus antagonists

NLRP3- and AIM2-inflammasome-mediated recognition of poxviruses infection and the priming and activation pathways for maturation and secretion of IL-1β and IL-18 effectors is indicated by black arrows. Poxviruses express several viral inhibitors or viral homologs of cellular proteins (shown in red) to interfere with these inflammasome pathways at different stages. Abbreviations used in this figure include AIM2: absent in melanoma 2; ASC: apoptosis-associated speck-like protein containing a CARD; CARD: caspase activating and recruiting domains; CPXV: cowpox virus; CrmA: cytokine response modifier A; dsDNA: double-stranded DNA; HIN-200: hematopoietic interferon-inducible nuclear proteins with a 200 amino acid repeat; IKKα: IκBα kinase α; IKKβ: IκBα kinase β; IKKγ: IκBα kinase γ; IL-18: interleukin-18; IL-1β: interleukin-

1β; IκBα: inhibitor κBα; LRR: leucine-rich repeats; NF-κB: nuclear factor kappa B; NLRP3: NOD-, LRR- and pyrin domain-containing protein 3; NOD; nucleotide-binding and oligomerization domain; p65/p50: NF-κB heterodimer p50/p65 subunit; PYD: pyrin domain; RFV: rabbit fibroma virus; ROS: reactive oxygen species; SPI-2: serine proteinase inhibitor 2; TLRs: toll-like receptors; TRAF6: tumor necrosis factor receptor-associated factor 6; VACV: vaccinia virus.

References

1. Haller, S.L.; Peng, C.; McFadden, G.; Rothenburg, S. Poxviruses and the evolution of host range and virulence. Infect. Genet. Evol. J. Mol. Epidemiol. Evol. Genet. Infect. Dis. 2014, 21, 15–40, doi:10.1016/j.meegid.2013.10.014.

2. Silva, N.I.O.; de Oliveira, J.S.; Kroon, E.G.; Trindade, G. de S.; Drumond, B.P. Here, There, and Everywhere: The Wide Host Range and Geographic Distribution of Zoonotic Orthopoxviruses. Viruses 2020, 13, doi:10.3390/v13010043.

3. Moss, B. Poxvirus DNA replication. Cold Spring Harb. Perspect. Biol. 2013, 5, doi:10.1101/cshperspect.a010199.

4. McFadden, G. Poxvirus tropism. Nat. Rev. Microbiol. 2005, 3, 201–213, doi:10.1038/nrmicro1099.

5. Emergence of monkeypox in West Africa and Central Africa, 1970–2017. Relev. Epidemiol. Hebd. 2018, 93, 125–132.

6. Tuppurainen, E.S.M.; Venter, E.H.; Shisler, J.L.; Gari, G.; Mekonnen, G.A.; Juleff, N.; Lyons, N.A.; De Clercq, K.; Upton, C.; Bowden, T.R.; et al. Review: Capripoxvirus Diseases: Current Status and Opportunities for Control. Transbound. Emerg. Dis. 2017, 64, 729–745, doi:10.1111/tbed.12444.

7. Spiesschaert, B.; McFadden, G.; Hermans, K.; Nauwynck, H.; Van De Walle, G.R. The current status and future directions of myxoma virus, a master in immune evasion. Vet. Res. 2011, 42, 76, doi:10.1186/1297-9716-42-76.

8. Smith, G.L.; Benfield, C.T.O.; Maluquer de Motes, C.; Mazzon, M.; Ember, S.W.J.;

Ferguson, B.J.; Sumner, R.P. Vaccinia virus immune evasion: mechanisms, virulence and immunogenicity. J. Gen. Virol. 2013, 94, 2367–2392, doi:10.1099/vir.0.055921-0.

9. Albarnaz, J.D.; Torres, A.A.; Smith, G.L. Modulating Vaccinia Virus Immunomodulators to Improve Immunological Memory. Viruses 2018, 10, doi:10.3390/v10030101.

10. Staib, C.; Kisling, S.; Erfle, V.; Sutter, G. Inactivation of the viral interleukin 1beta receptor improves CD8+ T-cell memory responses elicited upon immunization with modified vaccinia virus Ankara. J. Gen. Virol. 2005, 86, 1997–2006, doi:10.1099/vir.0.80646-0.

11. Falivene, J.; Del Médico Zajac, M.P.; Pascutti, M.F.; Rodríguez, A.M.; Maeto, C.; Perdiguero, B.; Gómez, C.E.; Esteban, M.; Calamante, G.; Gherardi, M.M. Improving the MVA vaccine potential by deleting the viral gene coding for the IL-18 binding protein. PLoS One 2012, 7, e32220, doi:10.1371/journal.pone.0032220.

12. Smith, G.L.; Moss, B. Infectious poxvirus vectors have capacity for at least 25 000 base pairs of foreign DNA. Gene 1983, 25, 21–28, doi:10.1016/0378-1119(83)90163-4.

13. Liu, R.; Americo, J.L.; Cotter, C.A.; Earl, P.L.; Erez, N.; Peng, C.; Moss, B. One or two injections of MVA-vectored vaccine shields hACE2 transgenic mice from SARS-CoV-2 upper and lower respiratory tract infection. Proc. Natl. Acad. Sci. U. S. A. 2021, 118, doi:10.1073/pnas.2026785118.

14. Wyatt, L.S.; Xiao, W.; Americo, J.L.; Earl, P.L.; Moss, B. Novel Nonreplicating Vaccinia Virus Vector Enhances Expression of Heterologous Genes and Suppresses Synthesis of Endogenous Viral Proteins. MBio 2017, 8, doi:10.1128/mBio.00790-17.

15. Sutter, G.; Moss, B. Nonreplicating vaccinia vector efficiently expresses recombinant genes. Proc. Natl. Acad. Sci. U. S. A. 1992, 89, 10847–10851, doi:10.1073/pnas.89.22.10847.

16. Werden, S.J.; McFadden, G. The role of cell signaling in poxvirus tropism: the case of the M-T5 host range protein of myxoma virus. Biochim. Biophys. Acta 2008, 1784, 228–237, doi:10.1016/j.bbapap.2007.08.001.

17. Pisklakova, A.; McKenzie, B.; Zemp, F.; Lun, X.; Kenchappa, R.S.; Etame, A.B.; Rahman, M.M.; Reilly, K.; Pilon-Thomas, S.; McFadden, G.; et al. M011L-deficient oncolytic myxoma virus induces apoptosis in brain tumor-initiating cells and enhances survival in a novel immunocompetent mouse model of glioblastoma. Neuro. Oncol. 2016, 18, 1088–1098, doi:10.1093/neuonc/now006.

18. Johnston, J.B.; Barrett, J.W.; Nazarian, S.H.; Goodwin, M.; Ricciuto, D.; Wang, G.; McFadden, G. A poxvirus-encoded pyrin domain protein interacts with ASC-1 to inhibit host inflammatory and apoptotic responses to infection. Immunity 2005, 23, 587–598, doi:10.1016/j.immuni.2005.10.003.

19. Urbasic, A.S.; Hynes, S.; Somrak, A.; Contakos, S.; Rahman, M.M.; Liu, J.; MacNeill, A.L. Oncolysis of canine tumor cells by myxoma virus lacking the serp2 gene. Am. J. Vet. Res. 2012, 73, 1252–1261, doi:10.2460/ajvr.73.8.1252.

20. Rahman, M.M.; McFadden, G. Oncolytic Virotherapy with Myxoma Virus. J. Clin. Med. 2020, 9, 171, doi:10.3390/jcm9010171.

21. Burshtyn, D.N. NK cells and poxvirus infection. Front. Immunol. 2013, 4, 7,

doi:10.3389/fimmu.2013.00007.

22. Medeiros-Silva, D.C.; Dos Santos Moreira-Silva, E.A.; Assis Silva Gomes, J. de; da Fonseca, F.G.; Correa-Oliveira, R. CD4 and CD8 T cells participate in the immune memory response against Vaccinia virus after a previous natural infection. Results Immunol. 2013, 3, 104–113, doi:10.1016/j.rinim.2013.10.002.

23. Pütz, M.M.; Midgley, C.M.; Law, M.; Smith, G.L. Quantification of antibody responses against multiple antigens of the two infectious forms of Vaccinia virus provides a benchmark for smallpox vaccination. Nat. Med. 2006, 12, 1310–1315, doi:10.1038/nm1457.

24. Zhu, J.; Martinez, J.; Huang, X.; Yang, Y. Innate immunity against vaccinia virus is mediated by TLR2 and requires TLR-independent production of IFN-beta. Blood 2007, 109, 619–625, doi:10.1182/blood-2006-06-027136.

25. Hutchens, M.; Luker, K.E.; Sottile, P.; Sonstein, J.; Lukacs, N.W.; Núñez, G.; Curtis, J.L.; Luker, G.D. TLR3 increases disease morbidity and mortality from vaccinia infection. J. Immunol. 2008, 180, 483–491, doi:10.4049/jimmunol.180.1.483.

26. Samuelsson, C.; Hausmann, J.; Lauterbach, H.; Schmidt, M.; Akira, S.; Wagner, H.; Chaplin, P.; Suter, M.; O'Keeffe, M.; Hochrein, H. Survival of lethal poxvirus infection in mice depends on TLR9, and therapeutic vaccination provides protection. J. Clin. Invest. 2008, 118, 1776–1784, doi:10.1172/JCI33940.

27. Wolferstätter, M.; Schweneker, M.; Späth, M.; Lukassen, S.; Klingenberg, M.; Brinkmann, K.; Wielert, U.; Lauterbach, H.; Hochrein, H.; Chaplin, P.; et al. Recombinant

modified vaccinia virus Ankara generating excess early double-stranded RNA transiently activates protein kinase R and triggers enhanced innate immune responses. J. Virol. 2014, 88, 14396–14411, doi:10.1128/JVI.02082-14.

28. Rice, A.D.; Turner, P.C.; Embury, J.E.; Moldawer, L.L.; Baker, H. V; Moyer, R.W. Roles of vaccinia virus genes E3L and K3L and host genes PKR and RNase L during intratracheal infection of C57BL/6 mice. J. Virol. 2011, 85, 550–567, doi:10.1128/JVI.00254-10.

29. Delaloye, J.; Roger, T.; Steiner-Tardivel, Q.-G.; Le Roy, D.; Knaup Reymond, M.; Akira, S.; Petrilli, V.; Gomez, C.E.; Perdiguero, B.; Tschopp, J.; et al. Innate immune sensing of modified vaccinia virus Ankara (MVA) is mediated by TLR2-TLR6, MDA-5 and the NALP3 inflammasome. PLoS Pathog. 2009, 5, e1000480, doi:10.1371/journal.ppat.1000480.

30. Hornung, V.; Ablasser, A.; Charrel-Dennis, M.; Bauernfeind, F.; Horvath, G.; Caffrey, D.R.; Latz, E.; Fitzgerald, K.A. AIM2 recognizes cytosolic dsDNA and forms a caspase-1-activating inflammasome with ASC. Nature 2009, 458, 514–518, doi:10.1038/nature07725.

31. El-Jesr, M.; Teir, M.; Maluquer de Motes, C. Vaccinia Virus Activation and Antagonism of Cytosolic DNA Sensing. Front. Immunol. 2020, 11, 568412, doi:10.3389/fimmu.2020.568412.

32. McNab, F.; Mayer-Barber, K.; Sher, A.; Wack, A.; O'Garra, A. Type I interferons in infectious disease. Nat. Rev. Immunol. 2015, 15, 87–103, doi:10.1038/nri3787.

33. Gasteiger, G.; D'Osualdo, A.; Schubert, D.A.; Weber, A.; Bruscia, E.M.; Hartl, D. Cellular Innate Immunity: An Old Game with New Players. J. Innate Immun. 2017, 9, 111–125, doi:10.1159/000453397.

34. Johnston, J.B.; McFadden, G. Poxvirus immunomodulatory strategies: current perspectives. J. Virol. 2003, 77, 6093–6100, doi:10.1128/jvi.77.11.6093-6100.2003.

35. Roberts, W.K.; Hovanessian, A.; Brown, R.E.; Clemens, M.J.; Kerr, I.M. Interferon-mediated protein kinase and low-molecular-weight inhibitor of protein synthesis. Nature 1976, 264, 477–480, doi:10.1038/264477a0.

36. Hovanessian, A.G. On the discovery of interferon-inducible, double-stranded RNA activated enzymes: the 2'-5'oligoadenylate synthetases and the protein kinase PKR. Cytokine Growth Factor Rev. 2007, 18, 351–361, doi:10.1016/j.cytogfr.2007.06.003.

37. Tuazon Kels, M.J.; Ng, E.; Al Rumaih, Z.; Pandey, P.; Ruuls, S.R.; Korner, H.; Newsome, T.P.; Chaudhri, G.; Karupiah, G. TNF deficiency dysregulates inflammatory cytokine production, leading to lung pathology and death during respiratory poxvirus infection. Proc. Natl. Acad. Sci. U. S. A. 2020, 117, 15935–15946, doi:10.1073/pnas.2004615117.

38. Liu, L.; Xu, Z.; Fuhlbrigge, R.C.; Peña-Cruz, V.; Lieberman, J.; Kupper, T.S. Vaccinia virus induces strong immunoregulatory cytokine production in healthy human epidermal keratinocytes: a novel strategy for immune evasion. J. Virol. 2005, 79, 7363–7370, doi:10.1128/JVI.79.12.7363-7370.2005.

39. Ivashkiv, L.B.; Donlin, L.T. Regulation of type I interferon responses. Nat. Rev. Immunol. 2014, 14, 36–49, doi:10.1038/nri3581.

40. Platanitis, E.; Decker, T. Regulatory Networks Involving STATs, IRFs, and NFκB in Inflammation. Front. Immunol. 2018, 9, 2542, doi:10.3389/fimmu.2018.02542.

41. Ullah, M.O.; Sweet, M.J.; Mansell, A.; Kellie, S.; Kobe, B. TRIF-dependent TLR signaling, its functions in host defense and inflammation, and its potential as a therapeutic target. J. Leukoc. Biol. 2016, 100, 27–45, doi:10.1189/jlb.2RI1115-531R.

42. Piras, V.; Selvarajoo, K. Beyond MyD88 and TRIF Pathways in Toll-Like Receptor Signaling. Front. Immunol. 2014, 5, 70, doi:10.3389/fimmu.2014.00070.

43. Thaiss, C.A.; Levy, M.; Itav, S.; Elinav, E. Integration of Innate Immune Signaling. Trends Immunol. 2016, 37, 84–101, doi:10.1016/j.it.2015.12.003.

44. Boone, R.F.; Parr, R.P.; Moss, B. Intermolecular duplexes formed from polyadenylylated vaccinia virus RNA. J. Virol. 1979, 30, 365–374, doi:10.1128/JVI.30.1.365-374.1979.

45. Colby, C.; Jurale, C.; Kates, J.R. Mechanism of synthesis of vaccinia virus double-stranded ribonucleic acid in vivo and in vitro. J. Virol. 1971, 7, 71–76, doi:10.1128/JVI.7.1.71-76.1971.

46. Willis, K.L.; Langland, J.O.; Shisler, J.L. Viral double-stranded RNAs from vaccinia virus early or intermediate gene transcripts possess PKR activating function, resulting in NF-κB activation, when the K1 protein is absent or mutated. J. Biol. Chem. 2011, 286, 7765–7778, doi:10.1074/jbc.M110.194704.

47. Lebleu, B.; Sen, G.C.; Shaila, S.; Cabrer, B.; Lengyel, P. Interferon, double-stranded RNA, and protein phosphorylation. Proc. Natl. Acad. Sci. U. S. A. 1976, 73, 3107–3111, doi:10.1073/pnas.73.9.3107.

48. Hovanessian, A.G.; Brown, R.E.; Kerr, I.M. Synthesis of low molecular weight inhibitor of protein synthesis with enzyme from interferon-treated cells. Nature 1977, 268, 537–540, doi:10.1038/268537a0.

49. Kerr, I.M.; Brown, R.E.; Hovanessian, A.G. Nature of inhibitor of cell-free protein synthesis formed in response to interferon and double-stranded RNA. Nature 1977, 268, 540–542, doi:10.1038/268540a0.

50. Meurs, E.; Chong, K.; Galabru, J.; Thomas, N.S.B.; Kerr, I.M.; Williams, B.R.G.; Hovanessian, A.G. Molecular cloning and characterization of the human double-stranded RNA-activated protein kinase induced by interferon. Cell 1990, 62, 379–390, doi:10.1016/0092-8674(90)90374-N.

51. Rebouillat, D.; Hovanessian, A.G. The human 2',5'-oligoadenylate synthetase family: interferon-induced proteins with unique enzymatic properties. J. Interf. cytokine Res. Off. J. Int. Soc. Interf. Cytokine Res. 1999, 19, 295–308, doi:10.1089/107999099313992.

52. Nanduri, S.; Carpick, B.W.; Yang, Y.; Williams, B.R.; Qin, J. Structure of the double-stranded RNA-binding domain of the protein kinase PKR reveals the molecular basis of its dsRNA-mediated activation. EMBO J. 1998, 17, 5458–5465, doi:10.1093/emboj/17.18.5458.

53. Lemaire, P.A.; Anderson, E.; Lary, J.; Cole, J.L. Mechanism of PKR Activation by dsRNA. J. Mol. Biol. 2008, 381, 351–360, doi:10.1016/j.jmb.2008.05.056.

54. Dey, M.; Cao, C.; Dar, A.C.; Tamura, T.; Ozato, K.; Sicheri, F.; Dever, T.E. Mechanistic link between PKR dimerization, autophosphorylation, and eIF2alpha substrate

recognition. Cell 2005, 122, 901–913, doi:10.1016/j.cell.2005.06.041.

55. Dever, T.E.; Kinzy, T.G.; Pavitt, G.D. Mechanism and Regulation of Protein Synthesis in Saccharomyces cerevisiae. Genetics 2016, 203, 65–107, doi:10.1534/genetics.115.186221.

56. Adomavicius, T.; Guaita, M.; Zhou, Y.; Jennings, M.D.; Latif, Z.; Roseman, A.M.; Pavitt, G.D. The structural basis of translational control by eIF2 phosphorylation. Nat. Commun. 2019, 10, 2136, doi:10.1038/s41467-019-10167-3.

57. Dey, M.; Mann, B.R.; Anshu, A.; Mannan, M.A. Activation of protein kinase PKR requires dimerization-induced cis-phosphorylation within the activation loop. J. Biol. Chem. 2014, 289, 5747–5757, doi:10.1074/jbc.M113.527796.

58. Baird, T.D.; Wek, R.C. Eukaryotic initiation factor 2 phosphorylation and translational control in metabolism. Adv. Nutr. 2012, 3, 307–321, doi:10.3945/an.112.002113.

59. Pfaller, C.K.; Li, Z.; George, C.X.; Samuel, C.E. Protein kinase PKR and RNA adenosine deaminase ADAR1: new roles for old players as modulators of the interferon response. Curr. Opin. Immunol. 2011, 23, 573–582, doi:10.1016/j.coi.2011.08.009.

60. Zamanian-Daryoush, M.; Mogensen, T.H.; DiDonato, J.A.; Williams, B.R. NF-kappaB activation by double-stranded-RNA-activated protein kinase (PKR) is mediated through NF-kappaB-inducing kinase and IkappaB kinase. Mol. Cell. Biol. 2000, 20, 1278–1290, doi:10.1128/mcb.20.4.1278-1290.2000.

61. McAllister, C.S.; Taghavi, N.; Samuel, C.E. Protein kinase PKR amplification of interferon β induction occurs through initiation factor eIF-2α-mediated translational control. J. Biol. Chem. 2012, 287, 36384–36392, doi:10.1074/jbc.M112.390039.

62. Der, S.D.; Lau, A.S. Involvement of the double-stranded-RNA-dependent kinase PKR in interferon expression and interferon-mediated antiviral activity. Proc. Natl. Acad. Sci. U. S. A. 1995, 92, 8841–8845, doi:10.1073/pnas.92.19.8841.

63. Gil, J.; Rullas, J.; García, M.A.; Alcamí, J.; Esteban, M. The catalytic activity of dsRNA-dependent protein kinase, PKR, is required for NF-kappaB activation. Oncogene 2001, 20, 385–394, doi:10.1038/sj.onc.1204109.

64. Pham, A.M.; Santa Maria, F.G.; Lahiri, T.; Friedman, E.; Marié, I.J.; Levy, D.E. PKR Transduces MDA5-Dependent Signals for Type I IFN Induction. PLoS Pathog. 2016, 12, e1005489, doi:10.1371/journal.ppat.1005489.

65. Rojas, M.; Vasconcelos, G.; Dever, T.E. An eIF2α-binding motif in protein phosphatase 1 subunit GADD34 and its viral orthologs is required to promote dephosphorylation of eIF2α. Proc. Natl. Acad. Sci. U. S. A. 2015, 112, E3466-75, doi:10.1073/pnas.1501557112.

66. Chang, H.W.; Jacobs, B.L. Identification of a conserved motif that is necessary for binding of the vaccinia virus E3L gene products to double-stranded RNA. Virology 1993, 194, 537–547, doi:10.1006/viro.1993.1292.

67. Romano, P.R.; Zhang, F.; Tan, S.-L.; Garcia-Barrio, M.T.; Katze, M.G.; Dever, T.E.; Hinnebusch, A.G. Inhibition of Double-Stranded RNA-Dependent Protein Kinase PKR by Vaccinia Virus E3: Role of Complex Formation and the E3 N-Terminal Domain. Mol. Cell. Biol. 1998, 18, 7304–7316, doi:10.1128/mcb.18.12.7304.

68. Myskiw, C.; Arsenio, J.; Hammett, C.; van Bruggen, R.; Deschambault, Y.; Beausoleil,

N.; Babiuk, S.; Cao, J. Comparative analysis of poxvirus orthologues of the vaccinia virus E3 protein: modulation of protein kinase R activity, cytokine responses, and virus pathogenicity. J. Virol. 2011, 85, 12280–12291, doi:10.1128/JVI.05505-11.

69. Langland, J.O.; Jacobs, B.L. The role of the PKR-inhibitory genes, E3L and K3L, in determining vaccinia virus host range. Virology 2002, 299, 133–141, doi:10.1006/viro.2002.1479.

70. Zhang, P.; Jacobs, B.L.; Samuel, C.E. Loss of Protein Kinase PKR Expression in Human HeLa Cells Complements the Vaccinia Virus E3L Deletion Mutant Phenotype by Restoration of Viral Protein Synthesis. J. Virol. 2008, 82, 840–848, doi:10.1128/jvi.01891-07.

71. Rahman, M.M.; Liu, J.; Chan, W.M.; Rothenburg, S.; McFadden, G. Myxoma virus protein M029 is a dual function immunomodulator that inhibits PKR and also conscripts RHA/DHX9 to promote expanded host tropism and viral replication. PLoS Pathog. 2013, 9, e1003465, doi:10.1371/journal.ppat.1003465.

72. Park, C.; Peng, C.; Brennan, G.; Rothenburg, S. Species-specific inhibition of antiviral protein kinase R by capripoxviruses and vaccinia virus. Ann. N. Y. Acad. Sci. 2019, 1438, 18–29, doi:10.1111/nyas.14000.

73. Beattie, E.; Tartaglia, J.; Paoletti, E. Vaccinia virus-encoded eIF-2 alpha homolog abrogates the antiviral effect of interferon. Virology 1991, 183, 419–422, doi:10.1016/0042-6822(91)90158-8.

74. Dar, A.C.; Sicheri, F. X-ray crystal structure and functional analysis of vaccinia virus K3L

reveals molecular determinants for PKR subversion and substrate recognition. Mol. Cell 2002, 10, 295–305, doi:10.1016/S1097-2765(02)00590-7.

75. Ramelot, T.A.; Cort, J.R.; Yee, A.A.; Liu, F.; Goshe, M.B.; Edwards, A.M.; Smith, R.D.; Arrowsmith, C.H.; Dever, T.E.; Kennedy, M.A. Myxoma virus immunomodulatory protein M156R is a structural mimic of eukaryotic translation initiation factor eIF2alpha. J. Mol. Biol. 2002, 322, 943–954, doi:10.1016/s0022-2836(02)00858-6.

76. Rothenburg, S.; Seo, E.J.; Gibbs, J.S.; Dever, T.E.; Dittmar, K. Rapid evolution of protein kinase PKR alters sensitivity to viral inhibitors. Nat. Struct. Mol. Biol. 2009, 16, 63–70, doi:10.1038/nsmb.1529.

77. Peng, C.; Haller, S.L.; Rahman, M.M.; McFadden, G.; Rothenburg, S. Myxoma virus M156 is a specific inhibitor of rabbit PKR but contains a loss-of-function mutation in Australian virus isolates. Proc. Natl. Acad. Sci. U. S. A. 2016, 113, 3855–3860, doi:10.1073/pnas.1515613113.

78. Park, C.; Peng, C.; Rahman, M.J.; Haller, S.L.; Tazi, L.; Brennan, G.; Rothenburg, S. Orthopoxvirus K3 orthologs show virus- and host-specific inhibition of the antiviral protein kinase PKR. PLoS Pathog. 2021, 17, e1009183, doi:10.1371/journal.ppat.1009183.

79. Cao, J.; Varga, J.; Deschambault, Y. Poxvirus encoded eIF2α homolog, K3 family proteins, is a key determinant of poxvirus host species specificity. Virology 2020, 541, 101–112, doi:10.1016/j.virol.2019.12.008.

80. Shors, T.; Keck, J.G.; Moss, B. Down regulation of gene expression by the vaccinia virus

D10 protein. J. Virol. 1999, 73, 791–796, doi:10.1128/JVI.73.1.791-796.1999.

81. Parrish, S.; Moss, B. Characterization of a second vaccinia virus mRNA-decapping enzyme conserved in poxviruses. J. Virol. 2007, 81, 12973–12978, doi:10.1128/JVI.01668-07.

82. Parrish, S.; Resch, W.; Moss, B. Vaccinia virus D10 protein has mRNA decapping activity, providing a mechanism for control of host and viral gene expression. Proc. Natl. Acad. Sci. U. S. A. 2007, 104, 2139–2144, doi:10.1073/pnas.0611685104.

83. Liu, S.-W.; Katsafanas, G.C.; Liu, R.; Wyatt, L.S.; Moss, B. Poxvirus decapping enzymes enhance virulence by preventing the accumulation of dsRNA and the induction of innate antiviral responses. Cell Host Microbe 2015, 17, 320–331, doi:10.1016/j.chom.2015.02.002.

84. Burgess, H.M.; Mohr, I. Cellular 5'-3' mRNA exonuclease Xrn1 controls double-stranded RNA accumulation and anti-viral responses. Cell Host Microbe 2015, 17, 332–344, doi:10.1016/j.chom.2015.02.003.

85. Bratke, K.A.; McLysaght, A.; Rothenburg, S. A survey of host range genes in poxvirus genomes. Infect. Genet. Evol. J. Mol. Epidemiol. Evol. Genet. Infect. Dis. 2013, 14, 406–425, doi:10.1016/j.meegid.2012.12.002.

86. Chebath, J.; Benech, P.; Hovanessian, A.; Galabru, J.; Revel, M. Four different forms of interferon-induced 2',5'-oligo(A) synthetase identified by immunoblotting in human cells. J. Biol. Chem. 1987, 262, 3852–3857.

87. Silverman, R.H. Viral encounters with 2',5'-oligoadenylate synthetase and RNase L

during the interferon antiviral response. J. Virol. 2007, 81, 12720–12729, doi:10.1128/JVI.01471-07.

88. Li, Y.; Dong, B.; Wei, Z.; Silverman, R.H.; Weiss, S.R. Activation of RNase L in Egyptian Rousette Bat-Derived RoNi/7 Cells Is Dependent Primarily on OAS3 and Independent of MAVS Signaling. MBio 2019, 10, doi:10.1128/mBio.02414-19.

89. Li, Y.; Banerjee, S.; Wang, Y.; Goldstein, S.A.; Dong, B.; Gaughan, C.; Silverman, R.H.; Weiss, S.R. Activation of RNase L is dependent on OAS3 expression during infection with diverse human viruses. Proc. Natl. Acad. Sci. U. S. A. 2016, 113, 2241–2246, doi:10.1073/pnas.1519657113.

90. Luthra, P.; Sun, D.; Silverman, R.H.; He, B. Activation of IFN-β expression by a viral mRNA through RNase L and MDA5. Proc. Natl. Acad. Sci. U. S. A. 2011, 108, 2118–2123, doi:10.1073/pnas.1012409108.

91. Malathi, K.; Dong, B.; Gale, M.J.; Silverman, R.H. Small self-RNA generated by RNase L amplifies antiviral innate immunity. Nature 2007, 448, 816–819, doi:10.1038/nature06042.

92. Rong, E.; Wang, X.; Chen, H.; Yang, C.; Hu, J.; Liu, W.; Wang, Z.; Chen, X.; Zheng, H.; Pu, J.; et al. Molecular Mechanisms for the Adaptive Switching Between the OAS/RNase L and OASL/RIG-I Pathways in Birds and Mammals. Front. Immunol. 2018, 9, 1398, doi:10.3389/fimmu.2018.01398.

93. Manivannan, P.; Siddiqui, M.A.; Malathi, K. RNase L Amplifies Interferon Signaling by Inducing Protein Kinase R-Mediated Antiviral Stress Granules. J. Virol. 2020, 94,

doi:10.1128/JVI.00205-20.

94. Díaz-Guerra, M.; Rivas, C.; Esteban, M. Inducible expression of the 2-5A synthetase/RNase L system results in inhibition of vaccinia virus replication. Virology 1997, 227, 220–228, doi:10.1006/viro.1996.8294.

95. Rivas, C.; Gil, J.; Mělková, Z.; Esteban, M.; Díaz-Guerra, M. Vaccinia virus E3L protein is an inhibitor of the interferon (i.f.n.)-induced 2-5A synthetase enzyme. Virology 1998, 243, 406–414, doi:10.1006/viro.1998.9072.

96. Ludwig, H.; Mages, J.; Staib, C.; Lehmann, M.H.; Lang, R.; Sutter, G. Role of viral factor E3L in modified vaccinia virus ankara infection of human HeLa Cells: regulation of the virus life cycle and identification of differentially expressed host genes. J. Virol. 2005, 79, 2584–2596, doi:10.1128/JVI.79.4.2584-2596.2005.

97. Xiang, Y.; Condit, R.C.; Vijaysri, S.; Jacobs, B.; Williams, B.R.G.; Silverman, R.H. Blockade of interferon induction and action by the E3L double-stranded RNA binding proteins of vaccinia virus. J. Virol. 2002, 76, 5251–5259, doi:10.1128/jvi.76.10.5251-5259.2002.

98. Liu, S.-W.; Wyatt, L.S.; Orandle, M.S.; Minai, M.; Moss, B. The D10 decapping enzyme of vaccinia virus contributes to decay of cellular and viral mRNAs and to virulence in mice. J. Virol. 2014, 88, 202–211, doi:10.1128/JVI.02426-13.

99. Liu, R.; Moss, B. Opposing Roles of Double-Stranded RNA Effector Pathways and Viral Defense Proteins Revealed with CRISPR-Cas9 Knockout Cell Lines and Vaccinia Virus Mutants. J. Virol. 2016, 90, 7864–7879, doi:10.1128/JVI.00869-16.

100. Andrejeva, J.; Childs, K.S.; Young, D.F.; Carlos, T.S.; Stock, N.; Goodbourn, S.; Randall, R.E. The V proteins of paramyxoviruses bind the IFN-inducible RNA helicase, mda-5, and inhibit its activation of the IFN-beta promoter. Proc. Natl. Acad. Sci. U. S. A. 2004, 101, 17264–17269, doi:10.1073/pnas.0407639101.

101. Yoneyama, M.; Kikuchi, M.; Natsukawa, T.; Shinobu, N.; Imaizumi, T.; Miyagishi, M.; Taira, K.; Akira, S.; Fujita, T. The RNA helicase RIG-I has an essential function in double-stranded RNA-induced innate antiviral responses. Nat. Immunol. 2004, 5, 730–737, doi:10.1038/ni1087.

102. Hartmann, G. Nucleic Acid Immunity. Adv. Immunol. 2017, 133, 121–169, doi:10.1016/bs.ai.2016.11.001.

103. Uhlén, M.; Fagerberg, L.; Hallström, B.M.; Lindskog, C.; Oksvold, P.; Mardinoglu, A.; Sivertsson, Å.; Kampf, C.; Sjöstedt, E.; Asplund, A.; et al. Proteomics. Tissue-based map of the human proteome. Science 2015, 347, 1260419, doi:10.1126/science.1260419.

104. Luthra, P.; Ramanan, P.; Mire, C.E.; Weisend, C.; Tsuda, Y.; Yen, B.; Liu, G.; Leung, D.W.; Geisbert, T.W.; Ebihara, H.; et al. Mutual antagonism between the Ebola virus VP35 protein and the RIG-I activator PACT determines infection outcome. Cell Host Microbe 2013, 14, 74–84, doi:10.1016/j.chom.2013.06.010.

105. Liu, Y.; Olagnier, D.; Lin, R. Host and Viral Modulation of RIG-I-Mediated Antiviral Immunity. Front. Immunol. 2016, 7, 662, doi:10.3389/fimmu.2016.00662.

106. Chiu, Y.-H.; Macmillan, J.B.; Chen, Z.J. RNA polymerase III detects cytosolic DNA and induces type I interferons through the RIG-I pathway. Cell 2009, 138, 576–591,

doi:10.1016/j.cell.2009.06.015.

107. Wang, F.; Gao, X.; Barrett, J.W.; Shao, Q.; Bartee, E.; Mohamed, M.R.; Rahman, M.; Werden, S.; Irvine, T.; Cao, J.; et al. RIG-I mediates the co-induction of tumor necrosis factor and type I interferon elicited by myxoma virus in primary human macrophages. PLoS Pathog. 2008, 4, e1000099, doi:10.1371/journal.ppat.1000099.

108. Deng, L.; Dai, P.; Parikh, T.; Cao, H.; Bhoj, V.; Sun, Q.; Chen, Z.; Merghoub, T.; Houghton, A.; Shuman, S. Vaccinia virus subverts a mitochondrial antiviral signaling protein-dependent innate immune response in keratinocytes through its double-stranded RNA binding protein, E3. J. Virol. 2008, 82, 10735–10746, doi:10.1128/JVI.01305-08.

109. Brisse, M.; Ly, H. Comparative Structure and Function Analysis of the RIG-I-Like Receptors: RIG-I and MDA5. Front. Immunol. 2019, 10, 1586, doi:10.3389/fimmu.2019.01586.

110. Hornung, V.; Ellegast, J.; Kim, S.; Brzózka, K.; Jung, A.; Kato, H.; Poeck, H.; Akira, S.; Conzelmann, K.-K.; Schlee, M.; et al. 5’-Triphosphate RNA is the ligand for RIG-I. Science 2006, 314, 994–997, doi:10.1126/science.1132505.

111. Myong, S.; Cui, S.; Cornish, P. V; Kirchhofer, A.; Gack, M.U.; Jung, J.U.; Hopfner, K.-P.; Ha, T. Cytosolic viral sensor RIG-I is a 5’-triphosphate-dependent translocase on double-stranded RNA. Science 2009, 323, 1070–1074, doi:10.1126/science.1168352.

112. Rehwinkel, J.; Gack, M.U. RIG-I-like receptors: their regulation and roles in RNA sensing. Nat. Rev. Immunol. 2020, 20, 537–551, doi:10.1038/s41577-020-0288-3.

113. Kato, H.; Takeuchi, O.; Mikamo-Satoh, E.; Hirai, R.; Kawai, T.; Matsushita, K.; Hiiragi,

A.; Dermody, T.S.; Fujita, T.; Akira, S. Length-dependent recognition of double-stranded ribonucleic acids by retinoic acid-inducible gene-I and melanoma differentiation-associated gene 5. J. Exp. Med. 2008, 205, 1601–1610, doi:10.1084/jem.20080091.

114. Seth, R.B.; Sun, L.; Ea, C.-K.; Chen, Z.J. Identification and characterization of MAVS, a mitochondrial antiviral signaling protein that activates NF-kappaB and IRF 3. Cell 2005, 122, 669–682, doi:10.1016/j.cell.2005.08.012.

115. Vazquez, C.; Horner, S.M. MAVS Coordination of Antiviral Innate Immunity. J. Virol. 2015, 89, 6974–6977, doi:10.1128/JVI.01918-14.

116. Myskiw, C.; Arsenio, J.; Booy, E.P.; Hammett, C.; Deschambault, Y.; Gibson, S.B.; Cao, J. RNA species generated in vaccinia virus infected cells activate cell type-specific MDA5 or RIG-I dependent interferon gene transcription and PKR dependent apoptosis. Virology 2011, 413, 183–193, doi:10.1016/j.virol.2011.01.034.

117. Valentine, R.; Smith, G.L. Inhibition of the RNA polymerase III-mediated dsDNA-sensing pathway of innate immunity by vaccinia virus protein E3. J. Gen. Virol. 2010, 91, 2221–2229, doi:10.1099/vir.0.021998-0.

118. Fu, Y.; Comella, N.; Tognazzi, K.; Brown, L.F.; Dvorak, H.F.; Kocher, O. Cloning of DLM-1, a novel gene that is up-regulated in activated macrophages, using RNA differential display. Gene 1999, 240, 157–163, doi:10.1016/s0378-1119(99)00419-9.

119. Schwartz, T.; Behlke, J.; Lowenhaupt, K.; Heinemann, U.; Rich, A. Structure of the DLM-1-Z-DNA complex reveals a conserved family of Z-DNA-binding proteins. Nat. Struct. Biol. 2001, 8, 761–765, doi:10.1038/nsb0901-761.

120. Rothenburg, S.; Schwartz, T.; Koch-Nolte, F.; Haag, F. Complex regulation of the human gene for the Z-DNA binding protein DLM-1. Nucleic Acids Res. 2002, 30, 993–1000, doi:10.1093/nar/30.4.993.

121. Deigendesch, N.; Koch-Nolte, F.; Rothenburg, S. ZBP1 subcellular localization and association with stress granules is controlled by its Z-DNA binding domains. Nucleic Acids Res. 2006, 34, 5007–5020, doi:10.1093/nar/gkl575.

122. Feng, S.; Li, H.; Zhao, J.; Pervushin, K.; Lowenhaupt, K.; Schwartz, T.U.; Dröge, P. Alternate rRNA secondary structures as regulators of translation. Nat. Struct. Mol. Biol. 2011, 18, 169–176, doi:10.1038/nsmb.1962.

123. Takaoka, A.; Wang, Z.; Choi, M.K.; Yanai, H.; Negishi, H.; Ban, T.; Lu, Y.; Miyagishi, M.; Kodama, T.; Honda, K.; et al. DAI (DLM-1/ZBP1) is a cytosolic DNA sensor and an activator of innate immune response. Nature 2007, 448, 501–505, doi:10.1038/nature06013.

124. Wang, Z.; Choi, M.K.; Ban, T.; Yanai, H.; Negishi, H.; Lu, Y.; Tamura, T.; Takaoka, A.; Nishikura, K.; Taniguchi, T. Regulation of innate immune responses by DAI (DLM-1/ZBP1) and other DNA-sensing molecules. Proc. Natl. Acad. Sci. U. S. A. 2008, 105, 5477–5482, doi:10.1073/pnas.0801295105.

125. DeFilippis, V.R.; Alvarado, D.; Sali, T.; Rothenburg, S.; Früh, K. Human cytomegalovirus induces the interferon response via the DNA sensor ZBP1. J. Virol. 2010, 84, 585–598, doi:10.1128/JVI.01748-09.

126. Koehler, H.; Cotsmire, S.; Langland, J.; Kibler, K. V; Kalman, D.; Upton, J.W.; Mocarski,

E.S.; Jacobs, B.L. Inhibition of DAI-dependent necroptosis by the Z-DNA binding domain of the vaccinia virus innate immune evasion protein, E3. Proc. Natl. Acad. Sci. U. S. A. 2017, 114, 11506–11511, doi:10.1073/pnas.1700999114.

127. Rebsamen, M.; Heinz, L.X.; Meylan, E.; Michallet, M.-C.; Schroder, K.; Hofmann, K.; Vazquez, J.; Benedict, C.A.; Tschopp, J. DAI/ZBP1 recruits RIP1 and RIP3 through RIP homotypic interaction motifs to activate NF-kappaB. EMBO Rep. 2009, 10, 916–922, doi:10.1038/embor.2009.109.

128. Upton, J.W.; Kaiser, W.J.; Mocarski, E.S. DAI/ZBP1/DLM-1 complexes with RIP3 to mediate virus-induced programmed necrosis that is targeted by murine cytomegalovirus vIRA. Cell Host Microbe 2012, 11, 290–297, doi:10.1016/j.chom.2012.01.016.

129. Kaiser, W.J.; Upton, J.W.; Mocarski, E.S. Receptor-interacting protein homotypic interaction motif-dependent control of NF-kappa B activation via the DNA-dependent activator of IFN regulatory factors. J. Immunol. 2008, 181, 6427–6434, doi:10.4049/jimmunol.181.9.6427.

130. Koehler, H.S.; Jacobs, B.L. Subversion of Programed Cell Death by Poxviruses. Curr. Top. Microbiol. Immunol. 2021, doi:10.1007/82_2020_229.

131. Brandt, T.A.; Jacobs, B.L. Both carboxy- and amino-terminal domains of the vaccinia virus interferon resistance gene, E3L, are required for pathogenesis in a mouse model. J. Virol. 2001, 75, 850–856, doi:10.1128/JVI.75.2.850-856.2001.

132. Kim, Y.-G.; Muralinath, M.; Brandt, T.; Pearcy, M.; Hauns, K.; Lowenhaupt, K.; Jacobs, B.L.; Rich, A. A role for Z-DNA binding in vaccinia virus pathogenesis. Proc. Natl. Acad.

Sci. U. S. A. 2003, 100, 6974–6979, doi:10.1073/pnas.0431131100.

133. Stetson, D.B.; Medzhitov, R. Recognition of cytosolic DNA activates an IRF3-dependent innate immune response. Immunity 2006, 24, 93–103, doi:10.1016/j.immuni.2005.12.003.

134. Ishii, K.J.; Coban, C.; Kato, H.; Takahashi, K.; Torii, Y.; Takeshita, F.; Ludwig, H.; Sutter, G.; Suzuki, K.; Hemmi, H.; et al. A Toll-like receptor-independent antiviral response induced by double-stranded B-form DNA. Nat. Immunol. 2006, 7, 40–48, doi:10.1038/ni1282.

135. Dempsey, A.; Bowie, A.G. Innate immune recognition of DNA: A recent history. Virology 2015, 479–480, 146–152, doi:10.1016/j.virol.2015.03.013.

136. Sun, L.; Wu, J.; Du, F.; Chen, X.; Chen, Z.J. Cyclic GMP-AMP synthase is a cytosolic DNA sensor that activates the type I interferon pathway. Science 2013, 339, 786–791, doi:10.1126/science.1232458.

137. Gao, P.; Ascano, M.; Wu, Y.; Barchet, W.; Gaffney, B.L.; Zillinger, T.; Serganov, A.A.; Liu, Y.; Jones, R.A.; Hartmann, G.; et al. Cyclic [G(2',5')pA(3',5')p] is the metazoan second messenger produced by DNA-activated cyclic GMP-AMP synthase. Cell 2013, 153, 1094–1107, doi:10.1016/j.cell.2013.04.046.

138. Wu, J.; Sun, L.; Chen, X.; Du, F.; Shi, H.; Chen, C.; Chen, Z.J. Cyclic GMP-AMP is an endogenous second messenger in innate immune signaling by cytosolic DNA. Science 2013, 339, 826–830, doi:10.1126/science.1229963.

139. Abe, T.; Barber, G.N. Cytosolic-DNA-mediated, STING-dependent proinflammatory gene induction necessitates canonical NF-κB activation through TBK1. J. Virol. 2014, 88,

5328–5341, doi:10.1128/JVI.00037-14.

140. Tanaka, Y.; Chen, Z.J. STING specifies IRF3 phosphorylation by TBK1 in the cytosolic DNA signaling pathway. Sci. Signal. 2012, 5, ra20, doi:10.1126/scisignal.2002521.

141. Yum, S.; Li, M.; Fang, Y.; Chen, Z.J. TBK1 recruitment to STING activates both IRF3 and NF-κB that mediate immune defense against tumors and viral infections. Proc. Natl. Acad. Sci. U. S. A. 2021, 118, doi:10.1073/pnas.2100225118.

142. Xu, R.-H.; Wong, E.B.; Rubio, D.; Roscoe, F.; Ma, X.; Nair, S.; Remakus, S.; Schwendener, R.; John, S.; Shlomchik, M.; et al. Sequential Activation of Two Pathogen-Sensing Pathways Required for Type I Interferon Expression and Resistance to an Acute DNA Virus Infection. Immunity 2015, 43, 1148–1159, doi:10.1016/j.immuni.2015.11.015.

143. Cheng, W.-Y.; He, X.-B.; Jia, H.-J.; Chen, G.-H.; Jin, Q.-W.; Long, Z.-L.; Jing, Z.-Z. The cGas-Sting Signaling Pathway Is Required for the Innate Immune Response Against Ectromelia Virus. Front. Immunol. 2018, 9, 1297, doi:10.3389/fimmu.2018.01297.

144. Li, X.-D.; Wu, J.; Gao, D.; Wang, H.; Sun, L.; Chen, Z.J. Pivotal roles of cGAS-cGAMP signaling in antiviral defense and immune adjuvant effects. Science 2013, 341, 1390–1394, doi:10.1126/science.1244040.

145. Dai, P.; Wang, W.; Cao, H.; Avogadri, F.; Dai, L.; Drexler, I.; Joyce, J.A.; Li, X.-D.; Chen, Z.; Merghoub, T.; et al. Modified vaccinia virus Ankara triggers type I IFN production in murine conventional dendritic cells via a cGAS/STING-mediated cytosolic DNA-sensing pathway. PLoS Pathog. 2014, 10, e1003989,

doi:10.1371/journal.ppat.1003989.

146. Georgana, I.; Sumner, R.P.; Towers, G.J.; Maluquer de Motes, C. Virulent Poxviruses Inhibit DNA Sensing by Preventing STING Activation. J. Virol. 2018, 92, doi:10.1128/JVI.02145-17.

147. Meade, N.; King, M.; Munger, J.; Walsh, D. mTOR Dysregulation by Vaccinia Virus F17 Controls Multiple Processes with Varying Roles in Infection. J. Virol. 2019, 93, doi:10.1128/JVI.00784-19.

148. Meade, N.; Furey, C.; Li, H.; Verma, R.; Chai, Q.; Rollins, M.G.; DiGiuseppe, S.; Naghavi, M.H.; Walsh, D. Poxviruses Evade Cytosolic Sensing through Disruption of an mTORC1-mTORC2 Regulatory Circuit. Cell 2018, 174, 1143-1157.e17, doi:10.1016/j.cell.2018.06.053.

149. Eaglesham, J.B.; Pan, Y.; Kupper, T.S.; Kranzusch, P.J. Viral and metazoan poxins are cGAMP-specific nucleases that restrict cGAS-STING signalling. Nature 2019, 566, 259–263, doi:10.1038/s41586-019-0928-6.

150. Hernáez, B.; Alonso, G.; Georgana, I.; El-Jesr, M.; Martín, R.; Shair, K.H.Y.; Fischer, C.; Sauer, S.; Maluquer de Motes, C.; Alcamí, A. Viral cGAMP nuclease reveals the essential role of DNA sensing in protection against acute lethal virus infection. Sci. Adv. 2020, 6, doi:10.1126/sciadv.abb4565.

151. Unterholzner, L.; Sumner, R.P.; Baran, M.; Ren, H.; Mansur, D.S.; Bourke, N.M.; Randow, F.; Smith, G.L.; Bowie, A.G. Vaccinia virus protein C6 is a virulence factor that binds TBK-1 adaptor proteins and inhibits activation of IRF3 and IRF7. PLoS Pathog.

2011, 7, e1002247, doi:10.1371/journal.ppat.1002247.

152. Ferguson, B.J.; Benfield, C.T.O.; Ren, H.; Lee, V.H.; Frazer, G.L.; Strnadova, P.; Sumner, R.P.; Smith, G.L. Vaccinia virus protein N2 is a nuclear IRF3 inhibitor that promotes virulence. J. Gen. Virol. 2013, 94, 2070–2081, doi:10.1099/vir.0.054114-0.

153. Ramsay, E.P.; Abascal-Palacios, G.; Daiß, J.L.; King, H.; Gouge, J.; Pilsl, M.; Beuron, F.; Morris, E.; Gunkel, P.; Engel, C.; et al. Structure of human RNA polymerase III. Nat. Commun. 2020, 11, 6409, doi:10.1038/s41467-020-20262-5.

154. Ablasser, A.; Bauernfeind, F.; Hartmann, G.; Latz, E.; Fitzgerald, K.A.; Hornung, V. RIG-I-dependent sensing of poly(dA:dT) through the induction of an RNA polymerase III-transcribed RNA intermediate. Nat. Immunol. 2009, 10, 1065–1072, doi:10.1038/ni.1779.

155. Almine, J.F.; O'Hare, C.A.J.; Dunphy, G.; Haga, I.R.; Naik, R.J.; Atrih, A.; Connolly, D.J.; Taylor, J.; Kelsall, I.R.; Bowie, A.G.; et al. IFI16 and cGAS cooperate in the activation of STING during DNA sensing in human keratinocytes. Nat. Commun. 2017, 8, 14392, doi:10.1038/ncomms14392.

156. Stratmann, S.A.; Morrone, S.R.; van Oijen, A.M.; Sohn, J. The innate immune sensor IFI16 recognizes foreign DNA in the nucleus by scanning along the duplex. Elife 2015, 4, e11721, doi:10.7554/eLife.11721.

157. Monroe, K.M.; Yang, Z.; Johnson, J.R.; Geng, X.; Doitsh, G.; Krogan, N.J.; Greene, W.C. IFI16 DNA sensor is required for death of lymphoid CD4 T cells abortively infected with HIV. Science 2014, 343, 428–432, doi:10.1126/science.1243640.

158. Orzalli, M.H.; DeLuca, N.A.; Knipe, D.M. Nuclear IFI16 induction of IRF-3 signaling

during herpesviral infection and degradation of IFI16 by the viral ICP0 protein. Proc. Natl. Acad. Sci. U. S. A. 2012, 109, E3008-17, doi:10.1073/pnas.1211302109.

159. Unterholzner, L.; Keating, S.E.; Baran, M.; Horan, K.A.; Jensen, S.B.; Sharma, S.; Sirois, C.M.; Jin, T.; Latz, E.; Xiao, T.S.; et al. IFI16 is an innate immune sensor for intracellular DNA. Nat. Immunol. 2010, 11, 997–1004, doi:10.1038/ni.1932.

160. Walker, J.R.; Corpina, R.A.; Goldberg, J. Structure of the Ku heterodimer bound to DNA and its implications for double-strand break repair. Nature 2001, 412, 607–614, doi:10.1038/35088000.

161. Zhang, X.; Brann, T.W.; Zhou, M.; Yang, J.; Oguariri, R.M.; Lidie, K.B.; Imamichi, H.; Huang, D.-W.; Lempicki, R.A.; Baseler, M.W.; et al. Cutting edge: Ku70 is a novel cytosolic DNA sensor that induces type III rather than type I IFN. J. Immunol. 2011, 186, 4541–4545, doi:10.4049/jimmunol.1003389.

162. Sui, H.; Zhou, M.; Imamichi, H.; Jiao, X.; Sherman, B.T.; Lane, H.C.; Imamichi, T. STING is an essential mediator of the Ku70-mediated production of IFN-λ1 in response to exogenous DNA. Sci. Signal. 2017, 10, doi:10.1126/scisignal.aah5054.

163. Ferguson, B.J.; Mansur, D.S.; Peters, N.E.; Ren, H.; Smith, G.L. DNA-PK is a DNA sensor for IRF-3-dependent innate immunity. Elife 2012, 1, e00047, doi:10.7554/eLife.00047.

164. Peters, N.E.; Ferguson, B.J.; Mazzon, M.; Fahy, A.S.; Krysztofinska, E.; Arribas-Bosacoma, R.; Pearl, L.H.; Ren, H.; Smith, G.L. A mechanism for the inhibition of DNA-PK-mediated DNA sensing by a virus. PLoS Pathog. 2013, 9, e1003649,

doi:10.1371/journal.ppat.1003649.

165. Scutts, S.R.; Ember, S.W.; Ren, H.; Ye, C.; Lovejoy, C.A.; Mazzon, M.; Veyer, D.L.; Sumner, R.P.; Smith, G.L. DNA-PK Is Targeted by Multiple Vaccinia Virus Proteins to Inhibit DNA Sensing. Cell Rep. 2018, 25, 1953-1965.e4, doi:10.1016/j.celrep.2018.10.034.

166. Fahy, A.S.; Clark, R.H.; Glyde, E.F.; Smith, G.L. Vaccinia virus protein C16 acts intracellularly to modulate the host response and promote virulence. J. Gen. Virol. 2008, 89, 2377–2387, doi:10.1099/vir.0.2008/004895-0.

167. Zhang, Z.; Yuan, B.; Bao, M.; Lu, N.; Kim, T.; Liu, Y.-J. The helicase DDX41 senses intracellular DNA mediated by the adaptor STING in dendritic cells. Nat. Immunol. 2011, 12, 959–965, doi:10.1038/ni.2091.

168. Parvatiyar, K.; Zhang, Z.; Teles, R.M.; Ouyang, S.; Jiang, Y.; Iyer, S.S.; Zaver, S.A.; Schenk, M.; Zeng, S.; Zhong, W.; et al. The helicase DDX41 recognizes the bacterial secondary messengers cyclic di-GMP and cyclic di-AMP to activate a type I interferon immune response. Nat. Immunol. 2012, 13, 1155–1161, doi:10.1038/ni.2460.

169. Omura, H.; Oikawa, D.; Nakane, T.; Kato, M.; Ishii, R.; Ishitani, R.; Tokunaga, F.; Nureki, O. Structural and Functional Analysis of DDX41: a bispecific immune receptor for DNA and cyclic dinucleotide. Sci. Rep. 2016, 6, 34756, doi:10.1038/srep34756.

170. Rock, F.L.; Hardiman, G.; Timans, J.C.; Kastelein, R.A.; Bazan, J.F. A family of human receptors structurally related to Drosophila Toll. Proc. Natl. Acad. Sci. U. S. A. 1998, 95, 588–593, doi:10.1073/pnas.95.2.588.

171. Lemaitre, B.; Nicolas, E.; Michaut, L.; Reichhart, J.M.; Hoffmann, J.A. The dorsoventral regulatory gene cassette spätzle/Toll/cactus controls the potent antifungal response in Drosophila adults. Cell 1996, 86, 973–983, doi:10.1016/s0092-8674(00)80172-5.

172. Michel, T.; Reichhart, J.M.; Hoffmann, J.A.; Royet, J. Drosophila Toll is activated by Gram-positive bacteria through a circulating peptidoglycan recognition protein. Nature 2001, 414, 756–759, doi:10.1038/414756a.

173. Lemaitre, B.; Hoffmann, J. The host defense of Drosophila melanogaster. Annu. Rev. Immunol. 2007, 25, 697–743, doi:10.1146/annurev.immunol.25.022106.141615.

174. Liu, G.; Zhang, H.; Zhao, C.; Zhang, H. Evolutionary History of the Toll-Like Receptor Gene Family across Vertebrates. Genome Biol. Evol. 2020, 12, 3615–3634, doi:10.1093/gbe/evz266.

175. Botos, I.; Segal, D.M.; Davies, D.R. The structural biology of Toll-like receptors. Structure 2011, 19, 447–459, doi:10.1016/j.str.2011.02.004.

176. Chaturvedi, A.; Pierce, S.K. How location governs toll-like receptor signaling. Traffic 2009, 10, 621–628, doi:10.1111/j.1600-0854.2009.00899.x.

177. Kawai, T.; Sato, S.; Ishii, K.J.; Coban, C.; Hemmi, H.; Yamamoto, M.; Terai, K.; Matsuda, M.; Inoue, J.; Uematsu, S.; et al. Interferon-alpha induction through Toll-like receptors involves a direct interaction of IRF7 with MyD88 and TRAF6. Nat. Immunol. 2004, 5, 1061–1068, doi:10.1038/ni1118.

178. De Nardo, D.; Balka, K.R.; Cardona Gloria, Y.; Rao, V.R.; Latz, E.; Masters, S.L. Interleukin-1 receptor-associated kinase 4 (IRAK4) plays a dual role in myddosome

formation and Toll-like receptor signaling. J. Biol. Chem. 2018, 293, 15195–15207, doi:10.1074/jbc.RA118.003314.

179. Zhang, J.; Macartney, T.; Peggie, M.; Cohen, P. Interleukin-1 and TRAF6-dependent activation of TAK1 in the absence of TAB2 and TAB3. Biochem. J. 2017, 474, 2235–2248, doi:10.1042/BCJ20170288.

180. Kanarek, N.; London, N.; Schueler-Furman, O.; Ben-Neriah, Y. Ubiquitination and degradation of the inhibitors of NF-kappaB. Cold Spring Harb. Perspect. Biol. 2010, 2, a000166, doi:10.1101/cshperspect.a000166.

181. Liu, T.; Zhang, L.; Joo, D.; Sun, S.-C. NF-κB signaling in inflammation. Signal Transduct. Target. Ther. 2017, 2, 17023-, doi:10.1038/sigtrans.2017.23.

182. Shin, C.H.; Choi, D.-S. Essential Roles for the Non-Canonical IκB Kinases in Linking Inflammation to Cancer, Obesity, and Diabetes. Cells 2019, 8, doi:10.3390/cells8020178.

183. Alexopoulou, L.; Holt, A.C.; Medzhitov, R.; Flavell, R.A. Recognition of double-stranded RNA and activation of NF-kappaB by Toll-like receptor 3. Nature 2001, 413, 732–738, doi:10.1038/35099560.

184. Liu, L.; Botos, I.; Wang, Y.; Leonard, J.N.; Shiloach, J.; Segal, D.M.; Davies, D.R. Structural basis of toll-like receptor 3 signaling with double-stranded RNA. Science 2008, 320, 379–381, doi:10.1126/science.1155406.

185. Son, K.-N.; Liang, Z.; Lipton, H.L. Double-Stranded RNA Is Detected by Immunofluorescence Analysis in RNA and DNA Virus Infections, Including Those by Negative-Stranded RNA Viruses. J. Virol. 2015, 89, 9383–9392, doi:10.1128/JVI.01299-

15.

186. Yamamoto, M.; Sato, S.; Hemmi, H.; Hoshino, K.; Kaisho, T.; Sanjo, H.; Takeuchi, O.; Sugiyama, M.; Okabe, M.; Takeda, K.; et al. Role of adaptor TRIF in the MyD88-independent toll-like receptor signaling pathway. Science 2003, 301, 640–643, doi:10.1126/science.1087262.

187. Israely, T.; Melamed, S.; Achdout, H.; Erez, N.; Politi, B.; Waner, T.; Lustig, S.; Paran, N. TLR3 and TLR9 agonists improve postexposure vaccination efficacy of live smallpox vaccines. PLoS One 2014, 9, e110545, doi:10.1371/journal.pone.0110545.

188. Harte, M.T.; Haga, I.R.; Maloney, G.; Gray, P.; Reading, P.C.; Bartlett, N.W.; Smith, G.L.; Bowie, A.; O'Neill, L.A.J. The poxvirus protein A52R targets Toll-like receptor signaling complexes to suppress host defense. J. Exp. Med. 2003, 197, 343–351, doi:10.1084/jem.20021652.

189. Stack, J.; Haga, I.R.; Schröder, M.; Bartlett, N.W.; Maloney, G.; Reading, P.C.; Fitzgerald, K.A.; Smith, G.L.; Bowie, A.G. Vaccinia virus protein A46R targets multiple Toll-like-interleukin-1 receptor adaptors and contributes to virulence. J. Exp. Med. 2005, 201, 1007–1018, doi:10.1084/jem.20041442.

190. DiPerna, G.; Stack, J.; Bowie, A.G.; Boyd, A.; Kotwal, G.; Zhang, Z.; Arvikar, S.; Latz, E.; Fitzgerald, K.A.; Marshall, W.L. Poxvirus protein N1L targets the I-kappaB kinase complex, inhibits signaling to NF-kappaB by the tumor necrosis factor superfamily of receptors, and inhibits NF-kappaB and IRF3 signaling by toll-like receptors. J. Biol. Chem. 2004, 279, 36570–36578, doi:10.1074/jbc.M400567200.

191. Chen, R.A.-J.; Ryzhakov, G.; Cooray, S.; Randow, F.; Smith, G.L. Inhibition of IkappaB kinase by vaccinia virus virulence factor B14. PLoS Pathog. 2008, 4, e22, doi:10.1371/journal.ppat.0040022.

192. Graham, S.C.; Bahar, M.W.; Cooray, S.; Chen, R.A.-J.; Whalen, D.M.; Abrescia, N.G.A.; Alderton, D.; Owens, R.J.; Stuart, D.I.; Smith, G.L.; et al. Vaccinia virus proteins A52 and B14 Share a Bcl-2-like fold but have evolved to inhibit NF-kappaB rather than apoptosis. PLoS Pathog. 2008, 4, e1000128, doi:10.1371/journal.ppat.1000128.

193. Schröder, M.; Baran, M.; Bowie, A.G. Viral targeting of DEAD box protein 3 reveals its role in TBK1/IKKepsilon-mediated IRF activation. EMBO J. 2008, 27, 2147–2157, doi:10.1038/emboj.2008.143.

194. Hornung, V.; Rothenfusser, S.; Britsch, S.; Krug, A.; Jahrsdörfer, B.; Giese, T.; Endres, S.; Hartmann, G. Quantitative expression of toll-like receptor 1-10 mRNA in cellular subsets of human peripheral blood mononuclear cells and sensitivity to CpG oligodeoxynucleotides. J. Immunol. 2002, 168, 4531–4537, doi:10.4049/jimmunol.168.9.4531.

195. Ishii, N.; Funami, K.; Tatematsu, M.; Seya, T.; Matsumoto, M. Endosomal localization of TLR8 confers distinctive proteolytic processing on human myeloid cells. J. Immunol. 2014, 193, 5118–5128, doi:10.4049/jimmunol.1401375.

196. Ostendorf, T.; Zillinger, T.; Andryka, K.; Schlee-Guimaraes, T.M.; Schmitz, S.; Marx, S.; Bayrak, K.; Linke, R.; Salgert, S.; Wegner, J.; et al. Immune Sensing of Synthetic, Bacterial, and Protozoan RNA by Toll-like Receptor 8 Requires Coordinated Processing by RNase T2 and RNase 2. Immunity 2020, 52, 591-605.e6,

doi:10.1016/j.immuni.2020.03.009.

197. Greulich, W.; Wagner, M.; Gaidt, M.M.; Stafford, C.; Cheng, Y.; Linder, A.; Carell, T.; Hornung, V. TLR8 Is a Sensor of RNase T2 Degradation Products. Cell 2019, 179, 1264-1275.e13, doi:10.1016/j.cell.2019.11.001.

198. Martinez, J.; Huang, X.; Yang, Y. Toll-like receptor 8-mediated activation of murine plasmacytoid dendritic cells by vaccinia viral DNA. Proc. Natl. Acad. Sci. U. S. A. 2010, 107, 6442–6447, doi:10.1073/pnas.0913291107.

199. Dempsey, A.; Keating, S.E.; Carty, M.; Bowie, A.G. Poxviral protein E3-altered cytokine production reveals that DExD/H-box helicase 9 controls Toll-like receptor-stimulated immune responses. J. Biol. Chem. 2018, 293, 14989–15001, doi:10.1074/jbc.RA118.005089.

200. Krieg, A.M. Toll-like receptor 9 (TLR9) agonists in the treatment of cancer. Oncogene 2008, 27, 161–167, doi:10.1038/sj.onc.1210911.

201. Hemmi, H.; Takeuchi, O.; Kawai, T.; Kaisho, T.; Sato, S.; Sanjo, H.; Matsumoto, M.; Hoshino, K.; Wagner, H.; Takeda, K.; et al. A Toll-like receptor recognizes bacterial DNA. Nature 2000, 408, 740–745, doi:10.1038/35047123.

202. Fukui, R.; Yamamoto, C.; Matsumoto, F.; Onji, M.; Shibata, T.; Murakami, Y.; Kanno, A.; Hayashi, T.; Tanimura, N.; Yoshida, N.; et al. Cleavage of Toll-Like Receptor 9 Ectodomain Is Required for In Vivo Responses to Single Strand DNA. Front. Immunol. 2018, 9, 1491, doi:10.3389/fimmu.2018.01491.

203. Park, B.; Brinkmann, M.M.; Spooner, E.; Lee, C.C.; Kim, Y.-M.; Ploegh, H.L. Proteolytic

cleavage in an endolysosomal compartment is required for activation of Toll-like receptor 9. Nat. Immunol. 2008, 9, 1407–1414, doi:10.1038/ni.1669.

204. Uyangaa, E.; Choi, J.Y.; Patil, A.M.; Hossain, F.M.A.; Park, S.O.; Kim, B.; Kim, K.; Eo, S.K. Dual TLR2/9 Recognition of Herpes Simplex Virus Infection Is Required for Recruitment and Activation of Monocytes and NK Cells and Restriction of Viral Dissemination to the Central Nervous System. Front. Immunol. 2018, 9, 905, doi:10.3389/fimmu.2018.00905.

205. Lousberg, E.L.; Diener, K.R.; Fraser, C.K.; Phipps, S.; Foster, P.S.; Chen, W.; Uematsu, S.; Akira, S.; Robertson, S.A.; Brown, M.P.; et al. Antigen-specific T-cell responses to a recombinant fowlpox virus are dependent on MyD88 and interleukin-18 and independent of Toll-like receptor 7 (TLR7)- and TLR9-mediated innate immune recognition. J. Virol. 2011, 85, 3385–3396, doi:10.1128/JVI.02000-10.

206. Dai, P.; Cao, H.; Merghoub, T.; Avogadri, F.; Wang, W.; Parikh, T.; Fang, C.-M.; Pitha, P.M.; Fitzgerald, K.A.; Rahman, M.M.; et al. Myxoma virus induces type I interferon production in murine plasmacytoid dendritic cells via a TLR9/MyD88-, IRF5/IRF7-, and IFNAR-dependent pathway. J. Virol. 2011, 85, 10814–10825, doi:10.1128/JVI.00104-11.

207. Medzhitov, R.; Preston-Hurlburt, P.; Janeway, C.A.J. A human homologue of the Drosophila Toll protein signals activation of adaptive immunity. Nature 1997, 388, 394–397, doi:10.1038/41131.

208. Flo, T.H.; Ryan, L.; Latz, E.; Takeuchi, O.; Monks, B.G.; Lien, E.; Halaas, Ø.; Akira, S.; Skjåk-Braek, G.; Golenbock, D.T.; et al. Involvement of toll-like receptor (TLR) 2 and TLR4 in cell activation by mannuronic acid polymers. J. Biol. Chem. 2002, 277, 35489–

35495, doi:10.1074/jbc.M201366200.

209. Yang, S.; Sugawara, S.; Monodane, T.; Nishijima, M.; Adachi, Y.; Akashi, S.; Miyake, K.; Hase, S.; Takada, H. Micrococcus luteus teichuronic acids activate human and murine monocytic cells in a CD14- and toll-like receptor 4-dependent manner. Infect. Immun. 2001, 69, 2025–2030, doi:10.1128/IAI.69.4.2025-2030.2001.

210. Lai, C.-Y.; Strange, D.P.; Wong, T.A.S.; Lehrer, A.T.; Verma, S. Ebola Virus Glycoprotein Induces an Innate Immune Response In vivo via TLR4. Front. Microbiol. 2017, 8, 1571, doi:10.3389/fmicb.2017.01571.

211. Georgel, P.; Jiang, Z.; Kunz, S.; Janssen, E.; Mols, J.; Hoebe, K.; Bahram, S.; Oldstone, M.B.A.; Beutler, B. Vesicular stomatitis virus glycoprotein G activates a specific antiviral Toll-like receptor 4-dependent pathway. Virology 2007, 362, 304–313, doi:10.1016/j.virol.2006.12.032.

212. Kurt-Jones, E.A.; Popova, L.; Kwinn, L.; Haynes, L.M.; Jones, L.P.; Tripp, R.A.; Walsh, E.E.; Freeman, M.W.; Golenbock, D.T.; Anderson, L.J.; et al. Pattern recognition receptors TLR4 and CD14 mediate response to respiratory syncytial virus. Nat. Immunol. 2000, 1, 398–401, doi:10.1038/80833.

213. Huang, B.; Sikorski, R.; Kirn, D.H.; Thorne, S.H. Synergistic anti-tumor effects between oncolytic vaccinia virus and paclitaxel are mediated by the IFN response and HMGB1. Gene Ther. 2011, 18, 164–172, doi:10.1038/gt.2010.121.

214. Matsumiya, M.; Stylianou, E.; Griffiths, K.; Lang, Z.; Meyer, J.; Harris, S.A.; Rowland, R.; Minassian, A.M.; Pathan, A.A.; Fletcher, H.; et al. Roles for Treg expansion and

HMGB1 signaling through the TLR1-2-6 axis in determining the magnitude of the antigen-specific immune response to MVA85A. PLoS One 2013, 8, e67922, doi:10.1371/journal.pone.0067922.

215. Yang, H.; Wang, H.; Ju, Z.; Ragab, A.A.; Lundbäck, P.; Long, W.; Valdes-Ferrer, S.I.; He, M.; Pribis, J.P.; Li, J.; et al. MD-2 is required for disulfide HMGB1-dependent TLR4 signaling. J. Exp. Med. 2015, 212, 5–14, doi:10.1084/jem.20141318.

216. Hutchens, M.A.; Luker, K.E.; Sonstein, J.; Núñez, G.; Curtis, J.L.; Luker, G.D. Protective effect of Toll-like receptor 4 in pulmonary vaccinia infection. PLoS Pathog. 2008, 4, e1000153, doi:10.1371/journal.ppat.1000153.

217. Kawasaki, T.; Kawai, T. Toll-like receptor signaling pathways. Front. Immunol. 2014, 5, 461, doi:10.3389/fimmu.2014.00461.

218. Lysakova-Devine, T.; Keogh, B.; Harrington, B.; Nagpal, K.; Halle, A.; Golenbock, D.T.; Monie, T.; Bowie, A.G. Viral inhibitory peptide of TLR4, a peptide derived from vaccinia protein A46, specifically inhibits TLR4 by directly targeting MyD88 adaptor-like and TRIF-related adaptor molecule. J. Immunol. 2010, 185, 4261–4271, doi:10.4049/jimmunol.1002013.

219. Fedosyuk, S.; Bezerra, G.A.; Radakovics, K.; Smith, T.K.; Sammito, M.; Bobik, N.; Round, A.; Ten Eyck, L.F.; Djinović-Carugo, K.; Usón, I.; et al. Vaccinia Virus Immunomodulator A46: A Lipid and Protein-Binding Scaffold for Sequestering Host TIR-Domain Proteins. PLoS Pathog. 2016, 12, e1006079, doi:10.1371/journal.ppat.1006079.

220. Stack, J.; Bowie, A.G. Poxviral protein A46 antagonizes Toll-like receptor 4 signaling by targeting BB loop motifs in Toll-IL-1 receptor adaptor proteins to disrupt receptor:adaptor interactions. J. Biol. Chem. 2012, 287, 22672–22682, doi:10.1074/jbc.M112.349225.

221. Kim, Y.; Lee, H.; Heo, L.; Seok, C.; Choe, J. Structure of vaccinia virus A46, an inhibitor of TLR4 signaling pathway, shows the conformation of VIPER motif. Protein Sci. 2014, 23, 906–914, doi:10.1002/pro.2472.

222. Azar, D.F.; Haas, M.; Fedosyuk, S.; Rahaman, M.H.; Hedger, A.; Kobe, B.; Skern, T. Vaccinia Virus Immunomodulator A46: Destructive Interactions with MAL and MyD88 Shown by Negative-Stain Electron Microscopy. Structure 2020, 28, 1271-1287.e5, doi:10.1016/j.str.2020.09.007.

223. Bowie, A.; Kiss-Toth, E.; Symons, J.A.; Smith, G.L.; Dower, S.K.; O'Neill, L.A. A46R and A52R from vaccinia virus are antagonists of host IL-1 and toll-like receptor signaling. Proc. Natl. Acad. Sci. U. S. A. 2000, 97, 10162–10167, doi:10.1073/pnas.160027697.

224. Jin, M.S.; Kim, S.E.; Heo, J.Y.; Lee, M.E.; Kim, H.M.; Paik, S.-G.; Lee, H.; Lee, J.-O. Crystal structure of the TLR1-TLR2 heterodimer induced by binding of a tri-acylated lipopeptide. Cell 2007, 130, 1071–1082, doi:10.1016/j.cell.2007.09.008.

225. Kang, J.Y.; Nan, X.; Jin, M.S.; Youn, S.-J.; Ryu, Y.H.; Mah, S.; Han, S.H.; Lee, H.; Paik, S.-G.; Lee, J.-O. Recognition of lipopeptide patterns by Toll-like receptor 2-Toll-like receptor 6 heterodimer. Immunity 2009, 31, 873–884, doi:10.1016/j.immuni.2009.09.018.

226. Hanzelmann, D.; Joo, H.-S.; Franz-Wachtel, M.; Hertlein, T.; Stevanovic, S.; Macek, B.; Wolz, C.; Götz, F.; Otto, M.; Kretschmer, D.; et al. Toll-like receptor 2 activation depends on lipopeptide shedding by bacterial surfactants. Nat. Commun. 2016, 7, 12304, doi:10.1038/ncomms12304.

227. Fuchs, K.; Cardona Gloria, Y.; Wolz, O.-O.; Herster, F.; Sharma, L.; Dillen, C.A.; Täumer, C.; Dickhöfer, S.; Bittner, Z.; Dang, T.-M.; et al. The fungal ligand chitin directly binds TLR2 and triggers inflammation dependent on oligomer size. EMBO Rep. 2018, 19, doi:10.15252/embr.201846065.

228. Boehme, K.W.; Guerrero, M.; Compton, T. Human cytomegalovirus envelope glycoproteins B and H are necessary for TLR2 activation in permissive cells. J. Immunol. 2006, 177, 7094–7102, doi:10.4049/jimmunol.177.10.7094.

229. Dolganiuc, A.; Oak, S.; Kodys, K.; Golenbock, D.T.; Finberg, R.W.; Kurt-Jones, E.; Szabo, G. Hepatitis C core and nonstructural 3 proteins trigger toll-like receptor 2-mediated pathways and inflammatory activation. Gastroenterology 2004, 127, 1513–1524, doi:10.1053/j.gastro.2004.08.067.

230. Henrick, B.M.; Yao, X.-D.; Rosenthal, K.L. HIV-1 Structural Proteins Serve as PAMPs for TLR2 Heterodimers Significantly Increasing Infection and Innate Immune Activation. Front. Immunol. 2015, 6, 426, doi:10.3389/fimmu.2015.00426.

231. Kokkola, R.; Andersson, A.; Mullins, G.; Ostberg, T.; Treutiger, C.-J.; Arnold, B.; Nawroth, P.; Andersson, U.; Harris, R.A.; Harris, H.E. RAGE is the major receptor for the proinflammatory activity of HMGB1 in rodent macrophages. Scand. J. Immunol. 2005, 61, 1–9, doi:10.1111/j.0300-9475.2005.01534.x.

232. Yu, M.; Wang, H.; Ding, A.; Golenbock, D.T.; Latz, E.; Czura, C.J.; Fenton, M.J.; Tracey, K.J.; Yang, H. HMGB1 signals through toll-like receptor (TLR) 4 and TLR2. Shock 2006, 26, 174–179, doi:10.1097/01.shk.0000225404.51320.82.

233. O'Gorman, W.E.; Sampath, P.; Simonds, E.F.; Sikorski, R.; O'Malley, M.; Krutzik, P.O.; Chen, H.; Panchanathan, V.; Chaudhri, G.; Karupiah, G.; et al. Alternate mechanisms of initial pattern recognition drive differential immune responses to related poxviruses. Cell Host Microbe 2010, 8, 174–185, doi:10.1016/j.chom.2010.07.008.

234. Martinez, J.; Huang, X.; Yang, Y. Direct TLR2 signaling is critical for NK cell activation and function in response to vaccinia viral infection. PLoS Pathog. 2010, 6, e1000811, doi:10.1371/journal.ppat.1000811.

235. González, J.M.; Esteban, M. A poxvirus Bcl-2-like gene family involved in regulation of host immune response: sequence similarity and evolutionary history. Virol. J. 2010, 7, 59, doi:10.1186/1743-422X-7-59.

236. Maluquer de Motes, C.; Cooray, S.; Ren, H.; Almeida, G.M.F.; McGourty, K.; Bahar, M.W.; Stuart, D.I.; Grimes, J.M.; Graham, S.C.; Smith, G.L. Inhibition of apoptosis and NF-κB activation by vaccinia protein N1 occur via distinct binding surfaces and make different contributions to virulence. PLoS Pathog. 2011, 7, e1002430, doi:10.1371/journal.ppat.1002430.

237. Stack, J.; Doyle, S.L.; Connolly, D.J.; Reinert, L.S.; O'Keeffe, K.M.; McLoughlin, R.M.; Paludan, S.R.; Bowie, A.G. TRAM is required for TLR2 endosomal signaling to type I IFN induction. J. Immunol. 2014, 193, 6090–6102, doi:10.4049/jimmunol.1401605.

238. Shrivastava, G.; León-Juárez, M.; García-Cordero, J.; Meza-Sánchez, D.E.; Cedillo-Barrón, L. Inflammasomes and its importance in viral infections. Immunol. Res. 2016, 64, 1101–1117, doi:10.1007/s12026-016-8873-z.

239. Hayward, J.A.; Mathur, A.; Ngo, C.; Man, S.M. Cytosolic Recognition of Microbes and Pathogens: Inflammasomes in Action. Microbiol. Mol. Biol. Rev. 2018, 82, doi:10.1128/MMBR.00015-18.

240. Man, S.M.; Karki, R.; Kanneganti, T.-D. Molecular mechanisms and functions of pyroptosis, inflammatory caspases and inflammasomes in infectious diseases. Immunol. Rev. 2017, 277, 61–75, doi:10.1111/imr.12534.

241. Platnich, J.M.; Muruve, D.A. NOD-like receptors and inflammasomes: A review of their canonical and non-canonical signaling pathways. Arch. Biochem. Biophys. 2019, 670, 4–14, doi:10.1016/j.abb.2019.02.008.

242. Sharma, M.; de Alba, E. Structure, Activation and Regulation of NLRP3 and AIM2 Inflammasomes. Int. J. Mol. Sci. 2021, 22, doi:10.3390/ijms22020872.

243. Nambayan, R.J.T.; Sandin, S.I.; Quint, D.A.; Satyadi, D.M.; de Alba, E. The inflammasome adapter ASC assembles into filaments with integral participation of its two Death Domains, PYD and CARD. J. Biol. Chem. 2019, 294, 439–452, doi:10.1074/jbc.RA118.004407.

244. Shi, J.; Zhao, Y.; Wang, K.; Shi, X.; Wang, Y.; Huang, H.; Zhuang, Y.; Cai, T.; Wang, F.; Shao, F. Cleavage of GSDMD by inflammatory caspases determines pyroptotic cell death. Nature 2015, 526, 660–665, doi:10.1038/nature15514.

245. Rahman, M.M.; McFadden, G. Myxoma virus lacking the pyrin-like protein M013 is sensed in human myeloid cells by both NLRP3 and multiple Toll-like receptors, which independently activate the inflammasome and NF-κB innate response pathways. J. Virol. 2011, 85, 12505–12517, doi:10.1128/JVI.00410-11.

246. Zheng, D.; Liwinski, T.; Elinav, E. Inflammasome activation and regulation: toward a better understanding of complex mechanisms. Cell Discov. 2020, 6, 36, doi:10.1038/s41421-020-0167-x.

247. Bauernfeind, F.G.; Horvath, G.; Stutz, A.; Alnemri, E.S.; MacDonald, K.; Speert, D.; Fernandes-Alnemri, T.; Wu, J.; Monks, B.G.; Fitzgerald, K.A.; et al. Cutting edge: NF-kappaB activating pattern recognition and cytokine receptors license NLRP3 inflammasome activation by regulating NLRP3 expression. J. Immunol. 2009, 183, 787–791, doi:10.4049/jimmunol.0901363.

248. Boaru, S.G.; Borkham-Kamphorst, E.; Van de Leur, E.; Lehnen, E.; Liedtke, C.; Weiskirchen, R. NLRP3 inflammasome expression is driven by NF-κB in cultured hepatocytes. Biochem. Biophys. Res. Commun. 2015, 458, 700–706, doi:10.1016/j.bbrc.2015.02.029.

249. Kelley, N.; Jeltema, D.; Duan, Y.; He, Y. The NLRP3 Inflammasome: An Overview of Mechanisms of Activation and Regulation. Int. J. Mol. Sci. 2019, 20, doi:10.3390/ijms20133328.

250. Strittmatter, G.E.; Sand, J.; Sauter, M.; Seyffert, M.; Steigerwald, R.; Fraefel, C.; Smola, S.; French, L.E.; Beer, H.-D. IFN-γ Primes Keratinocytes for HSV-1-Induced Inflammasome Activation. J. Invest. Dermatol. 2016, 136, 610–620,

doi:10.1016/j.jid.2015.12.022.

251. Dorfleutner, A.; Talbott, S.J.; Bryan, N.B.; Funya, K.N.; Rellick, S.L.; Reed, J.C.; Shi, X.; Rojanasakul, Y.; Flynn, D.C.; Stehlik, C. A Shope Fibroma virus PYRIN-only protein modulates the host immune response. Virus Genes 2007, 35, 685–694, doi:10.1007/s11262-007-0141-9.

252. Rahman, M.M.; Mohamed, M.R.; Kim, M.; Smallwood, S.; McFadden, G. Co-regulation of NF-kappaB and inflammasome-mediated inflammatory responses by myxoma virus pyrin domain-containing protein M013. PLoS Pathog. 2009, 5, e1000635, doi:10.1371/journal.ppat.1000635.

253. Garg, R.R.; Jackson, C.B.; Rahman, M.M.; Khan, A.R.; Lewin, A.S.; McFadden, G. Myxoma virus M013 protein antagonizes NF-κB and inflammasome pathways via distinct structural motifs. J. Biol. Chem. 2019, 294, 8480–8489, doi:10.1074/jbc.RA118.006040.

254. Smith, G.L.; Howard, S.T.; Chan, Y.S. Vaccinia virus encodes a family of genes with homology to serine proteinase inhibitors. J. Gen. Virol. 1989, 70 (Pt 9), 2333–2343, doi:10.1099/0022-1317-70-9-2333.

255. Ray, C.A.; Black, R.A.; Kronheim, S.R.; Greenstreet, T.A.; Sleath, P.R.; Salvesen, G.S.; Pickup, D.J. Viral inhibition of inflammation: cowpox virus encodes an inhibitor of the interleukin-1 beta converting enzyme. Cell 1992, 69, 597–604, doi:10.1016/0092-8674(92)90223-y.

256. Bloomer, D.T.; Kitevska-Ilioski, T.; Pantaki-Eimany, D.; Ji, Y.; Miles, M.A.; Heras, B.; Hawkins, C.J. CrmA orthologs from diverse poxviruses potently inhibit caspases-1 and -8,

yet cleavage site mutagenesis frequently produces caspase-1-specific variants. Biochem. J. 2019, 476, 1335–1357, doi:10.1042/BCJ20190202.

257. Alcamí, A.; Smith, G.L. A soluble receptor for interleukin-1 beta encoded by vaccinia virus: a novel mechanism of virus modulation of the host response to infection. Cell 1992, 71, 153–167, doi:10.1016/0092-8674(92)90274-g.

258. Smith, V.P.; Alcami, A. Expression of secreted cytokine and chemokine inhibitors by ectromelia virus. J. Virol. 2000, 74, 8460–8471, doi:10.1128/jvi.74.18.8460-8471.2000.

259. Xiang, Y.; Moss, B. IL-18 binding and inhibition of interferon gamma induction by human poxvirus-encoded proteins. Proc. Natl. Acad. Sci. U. S. A. 1999, 96, 11537–11542, doi:10.1073/pnas.96.20.11537.

260. Smith, V.P.; Bryant, N.A.; Alcamí, A. Ectromelia, vaccinia and cowpox viruses encode secreted interleukin-18-binding proteins. J. Gen. Virol. 2000, 81, 1223–1230, doi:10.1099/0022-1317-81-5-1223.

261. Meng, X.; Leman, M.; Xiang, Y. Variola virus IL-18 binding protein interacts with three human IL-18 residues that are part of a binding site for human IL-18 receptor alpha subunit. Virology 2007, 358, 211–220, doi:10.1016/j.virol.2006.08.019.

262. Schattgen, S.A.; Fitzgerald, K.A. The PYHIN protein family as mediators of host defenses. Immunol. Rev. 2011, 243, 109–118, doi:10.1111/j.1600-065X.2011.01053.x.

263. Lu, A.; Li, Y.; Yin, Q.; Ruan, J.; Yu, X.; Egelman, E.; Wu, H. Plasticity in PYD assembly revealed by cryo-EM structure of the PYD filament of AIM2. Cell Discov. 2015, 1, 15013-, doi:10.1038/celldisc.2015.13.

264. Wang, B.; Yin, Q. AIM2 inflammasome activation and regulation: A structural perspective. J. Struct. Biol. 2017, 200, 279–282, doi:10.1016/j.jsb.2017.08.001.

265. Bürckstümmer, T.; Baumann, C.; Blüml, S.; Dixit, E.; Dürnberger, G.; Jahn, H.; Planyavsky, M.; Bilban, M.; Colinge, J.; Bennett, K.L.; et al. An orthogonal proteomic-genomic screen identifies AIM2 as a cytoplasmic DNA sensor for the inflammasome. Nat. Immunol. 2009, 10, 266–272, doi:10.1038/ni.1702.

266. Fernandes-Alnemri, T.; Yu, J.-W.; Datta, P.; Wu, J.; Alnemri, E.S. AIM2 activates the inflammasome and cell death in response to cytoplasmic DNA. Nature 2009, 458, 509–513, doi:10.1038/nature07710.

267. Roberts, T.L.; Idris, A.; Dunn, J.A.; Kelly, G.M.; Burnton, C.M.; Hodgson, S.; Hardy, L.L.; Garceau, V.; Sweet, M.J.; Ross, I.L.; et al. HIN-200 proteins regulate caspase activation in response to foreign cytoplasmic DNA. Science 2009, 323, 1057–1060, doi:10.1126/science.1169841.

268. Rathinam, V.A.K.; Jiang, Z.; Waggoner, S.N.; Sharma, S.; Cole, L.E.; Waggoner, L.; Vanaja, S.K.; Monks, B.G.; Ganesan, S.; Latz, E.; et al. The AIM2 inflammasome is essential for host defense against cytosolic bacteria and DNA viruses. Nat. Immunol. 2010, 11, 395–402, doi:10.1038/ni.1864.

269. Fernandes-Alnemri, T.; Yu, J.-W.; Juliana, C.; Solorzano, L.; Kang, S.; Wu, J.; Datta, P.; McCormick, M.; Huang, L.; McDermott, E.; et al. The AIM2 inflammasome is critical for innate immunity to Francisella tularensis. Nat. Immunol. 2010, 11, 385–393, doi:10.1038/ni.1859.

270. Sauer, J.-D.; Witte, C.E.; Zemansky, J.; Hanson, B.; Lauer, P.; Portnoy, D.A. Listeria monocytogenes triggers AIM2-mediated pyroptosis upon infrequent bacteriolysis in the macrophage cytosol. Cell Host Microbe 2010, 7, 412–419, doi:10.1016/j.chom.2010.04.004.

271. Saiga, H.; Kitada, S.; Shimada, Y.; Kamiyama, N.; Okuyama, M.; Makino, M.; Yamamoto, M.; Takeda, K. Critical role of AIM2 in Mycobacterium tuberculosis infection. Int. Immunol. 2012, 24, 637–644, doi:10.1093/intimm/dxs062.

272. Rothenburg, S.; Brennan, G. Species-Specific Host–Virus Interactions: Implications for Viral Host Range and Virulence. Trends Microbiol. 2020, 28, 46–56, doi:10.1016/j.tim.2019.08.007.

Chapter 2-Intermediate Inhibition of PKR by the Myxoma Virus K3 Ortholog M156 Activates the NF-κB Pathway

Huibin Yu[1], Chen Peng[2], Loubna Tazi[1], Greg Brennan[1], Stefan Rothenburg[1*]

[1]Department of Medical Microbiology and Immunology, School of Medicine, University of California, Davis 95618, USA

[2]Key Laboratory of Animal Epidemiology and Zoonosis, College of Veterinary Medicine, China Agricultural University, Beijing 100193, China

*To whom correspondence should be addressed

Stefan Rothenburg

Email: rothenburg@ucdavis.edu. ORCID iD:0000-0002-2525-8230

Abstract

Myxoma virus (MYXV) causes localized cutaneous fibromas in its natural hosts, tapeti and brush rabbits; however, in the non-native European rabbit host MYXV causes the lethal disease myxomatosis. Currently, the molecular mechanisms underlying this increased virulence after cross-species transmission are poorly understood. In this study, we have investigated the interaction between K3 orthologs and the host protein kinase R (PKR) to determine their crosstalk with the pro-inflammatory NF-κB pathway. Our results demonstrated that MYXV-M156 inhibits brush rabbit PKR (bPKR) more strongly than European rabbit PKR (ePKR) and this moderate European rabbit PKR inhibition could be improved by M156R mutants. Based on the symptoms in MYXV infected European rabbits, we hypothesized that the moderate inhibition of European rabbit PKR by M156 might only incompletely suppress the signal transduction pathways modulated by PKR, such as the NF-κB pathway. To test this hypothesis, we analyzed NF-κB pathway activation with a luciferase-based promoter assay. We found that the moderate inhibition of European rabbit PKR by M156 resulted in significantly higher NF-κB activation than complete inhibition of brush rabbit PKR by M156. Consistent with this observation, we found a stronger induction of the NF-κB target genes TNFα and IL-6 in European rabbit PKR expressing cells than in brush rabbit PKR expressing cells. This observation was true in both transfection and infections assays. Further supporting our hypothesis, we found that either hypoactive or hyperactive M156 mutants that were identified in a yeast-based random mutagenesis screen did not activate NF-κB. These observations indicate that M156 is maladapted for European rabbit PKR inhibition and thus M156 only incompletely blocked translation in these hosts. This incomplete inhibition resulted in preferential depletion of short-half-life proteins, such as the NF-κB inhibitor IκBα. This activation of NF-κB, induced by the

intermediate inhibition of European rabbit PKR by M156, may promote systemic dissemination of the virus, and may contribute to the increased virulence of MYXV in European rabbits.

Introduction

The ongoing SARS-CoV-2 pandemic highlights the risk of cross-species transmission events in the modern world. SARS-CoV-2 and other emerging viruses such as monkeypox virus, Middle East respiratory syndrome coronavirus, and Ebola virus, appear to cause enhanced morbidity and mortality in their new hosts compared to their natural hosts. This increased virulence is not a universal feature of cross-species transmission, and the molecular and evolutionary determinants of differential virulence in new hosts are poorly understood [1]. Furthermore, defining the determinants of different host responses is often difficult either because the natural host is unknown or little is known about the virulence of a pathogen in the reservoir species. However, one of the best-known examples of this increased virulence after cross-species transmission is the lagomorph-specific poxvirus, myxoma virus (MYXV).

MYXV naturally circulates in the South and Central American tapeti (forest rabbit, Sylvilagus brasiliensis) and the North American brush rabbit (Sylvilagus bachmani). In these host species, MYXV usually causes innocuous cutaneous fibroma [2]. However, when European rabbits (Oryctolagus cuniculus) are infected, it causes the highly lethal disseminated disease myxomatosis [3]. Symptoms of acute myxomatosis are characterized by an abnormal inflammatory response including fever, edema, mucopurulent conjunctivitis, and rhinitis [4]. In the 1950s, an attempt to reduce the invasive European rabbit population in Australia was undertaken by releasing this extremely pathogenic virus into the wild [5]. Not long after this intentional release, attenuated strains of MYXV began to emerge in wild populations, reducing the case fatality rate from 99.8% to 50-70% in Australian rabbits [6,7]. We previously characterized a naturally occurring mutation in the MYXV PKR inhibitor M156, L98P, that abrogated the ability of M156 to inhibit rabbit PKR and led to MYXV attenuation in cultured

cells [8]. These data indicate that the PKR pathway might contribute to the severe pathogenicity of MYXV in European rabbits.

Double-stranded (ds) RNA-dependent protein kinase R (PKR) is an interferon-stimulated host immune protein, which is activated by dsRNA generated during viral replication [9,10]. Activated PKR exerts its antiviral effect by phosphorylating the alpha subunit of the translation initiation factor (eIF2) at residue serine 51, thus inhibiting cap-dependent translation and inducing apoptosis [11,12]. eIF2α mediated translational repression can have different effects on protein expression including (i) the reduction of protein expression by the inhibition of cap-mediated RNA translation [13]; (ii) the increased translation of RNAs that are eIF2α-independent, e.g. RNAs containing some internal ribosome-entry sites or stem-loops that can directly recruit ribosomes and translation factors [14]; (iii) the increased expression of RNAs that contain inhibitory upstream open reading frames [15]; (iv) the activation of signaling pathways through the enhanced turnover of inhibitor proteins with a short half-life [16]. In addition to the above, PKR can also regulate Nuclear Factor Kappa B (NF-κB) through interactions with the I kappa B kinase complex (IKK) [17–19] or through the rapid turnover of its inhibitor IκB [20].

NF-κB is a family of five structurally related inducible transcription factors which regulate inflammatory, innate and adaptive immune responses in mammals [21,22]. Under resting conditions, inactive NF-κB monomers are held in cytoplasmic protein complexes that include the short-lived inhibitor IκB. In the canonical activation pathway, IKK is activated by a variety of different inflammatory stimuli including cytokines and microbial components [23]. Activated IKK then phosphorylates IκBα, targeting it for ubiquitin-mediated degradation, which results in the release of NF-κB proteins. These monomers rapidly translocate to the nucleus and dimerize,

and induce transcription of target genes, including the NFKBIA gene, which encodes IκBα, and pro-inflammatory genes, such as tumor necrosis factor alpha (TNFα), interleukin (IL)-1, IL-6 and IL-8 [24,25]. Once resolution of the stimulus is achieved, the concurrent transcription of IκBα induces a negative feedback loop to rapidly inactivate NF-κB [26,27].

In this study, we demonstrate that the MYXV PKR antagonist M156 regulates the NF-κB-IκBα complex and NF-κB-dependent inflammatory responses via differential inhibition of the PKR-eIF2α phosphorylation pathway. When PKR was either completely inhibited or fully activated, very little NF-κB activity was observed. Surprisingly, European rabbit PKR was only partially inhibited by M156, despite the severe disease caused by MYXV in these animals. This partial inhibition promoted the translocation of NF-κB and translation of downstream effector molecules, presumably due to more rapid loss of the short-lived IκBα relative to effector molecules while translation was constrained by the partial activation of the PKR pathway. Taken together, this study provides compelling evidence that, at least in the case of MYXV, maladaptation of viral immune regulators to the new host can contribute to an increased inflammatory response.

Results

M156 inhibits PKR from its natural host with highest efficiency

In a previous study, M156 only inhibited PKR from the non-native host European rabbit but did not inhibit PKR from seven other tested mammals [8]. An important outstanding question was how inhibition of European rabbit PKR compared to inhibition of PKR from a natural MYXV host. To answer this, we first cloned PKR from the riparian brush rabbit (Sylvilagus bachmani riparius). Total RNA was prepared from the muscle and connective tissues of rabbit paws from four individual brush rabbits, which died in the field during the Riparian Brush Rabbit Project Recovery Program and who were recovered in Stanislaus and San Joaquin counties (California). The full PKR open reading frame (ORF) was successfully amplified and cloned by RT-PCR with primers adjacent to the ORF from three of these rabbits. Brush rabbit (b) PKR showed 96% and 93% sequence identity compared to European rabbit (e) PKR on the nucleotide and protein level, respectively. Amino acid differences between the two rabbit PKRs are found throughout the protein sequence including the dsRNA binding domains, linker region, and the kinase domain (Fig. 2.1A). Next, we compared the sensitivities of each rabbit PKR to M156 inhibition using an established luciferase-based reporter (LBR) assay. In this assay, PKR-deficient HeLa cells were transiently co-transfected with a luciferase reporter, PKR and potential PKR inhibitors. In this assay, luciferase expression serves as a proxy to quantify relative translation [28]. Whereas M156 alone did not substantially alter luciferase expression, co-transfection of rabbit PKRs with M156R led to significantly increased luciferase expression, indicating PKR inhibition by M156. Notably, brush rabbit PKR was significantly better inhibited than European rabbit PKR by M156 (Fig. 2.2A). Both rabbit PKRs were expressed at comparable levels after transfection (Fig. 2.1B). To extend this analysis and test whether brush rabbit PKR is more sensitive to pseudosubstrate

inhibition, we co-transfected either rabbit PKR with an increasing amount of M156R or vaccinia virus K3L, the latter of which was previously shown to be an effective inhibitor of European rabbit PKR [29]. Both M156 and K3 inhibited rabbit PKRs in dose-dependent manners. Whereas M156 inhibited brush rabbit PKR significantly better at all tested concentrations, no substantial differences were observed for K3, showing that both rabbit PKRs were comparably sensitive to K3 inhibition (Fig. 2.2B and C). We also compared PKR inhibition by M156 from the Californian MSW strain and found comparable PKR inhibition relative to the Lu strain (Fig. 2.2D). Taken together, these results demonstrated that M156 was a more efficient inhibitor of PKR from the natural host and that European rabbit PKR was inhibited sub-optimally. Strikingly, it further shows that the level of PKR inhibition by M156 did not positively correlate with the described virulence of MYXV in its rabbit hosts.

Modulation of PKR-induced NF-κB activity by M156

We hypothesized that the dissimilar inhibition of PKR might result in differential activation of the pro-inflammatory transcription factor NF-κB. This pathway can be activated by PKR and other eIF2α kinases through the depletion of the NF-κB inhibitor IκBα that has a short-half life and is therefore disproportionately depleted after translational inhibition [30]. To test this hypothesis, we first transiently transfected HeLa-PKR^{ko} cells with increasing amounts of either European rabbit PKR or brush rabbit PKR and measured the translational inhibition of PKRs by the LBR assay. Simultaneously, we measured the expression of IκBα and the NF-κB subunit p65 by Western blot analysis. Increasing amounts of either European rabbit PKR or brush rabbit PKR led to comparable translational inhibition as observed by the LBR assay (Fig. 2.3). Increasing amounts of either PKR also resulted in comparably decreased levels of IκBα, whereas

p65 or β-actin (control) levels were barely affected (Fig. 2.4A and B). Lower IκBα protein was not due to a reduction of IκBα transcripts, as those actually increased after PKR transfection (Fig. 2.4C and D), which is consistent with reports that the IκBα encoding gene itself is activated by NF-κB [31,32]. We next assessed whether M156 can modulate the PKR-induced transcription of the NF-κB-activated pro-inflammatory genes, like TNFα and IL-6. Transfection of European rabbit PKR or brush rabbit PKR alone led to increased levels of TNFα and IL-6 transcripts (Fig. 2.4E and F). Whereas co-transfection of M156R with European rabbit PKR led to only moderately reduced TNFα and IL-6 mRNA levels, co-transfection of M156R with brush rabbit PKR resulted in strongly reduced TNFα and IL-6 mRNA levels (Fig. 2.4E and F). We also used an NF-κB-dependent reporter assay to monitor NF-κB dependent responses after differential PKR inhibition. Co-transfection of M156R with European rabbit PKR resulted in a significant increase in luciferase expression as compared to European rabbit PKR-only transfected cells. In contrast, co-transfection of M156R with brush rabbit PKR resulted in significantly decreased luciferase expression compared to brush rabbit PKR-only transfected cells (Fig. 2.4G). In order to analyze the effects of M156 on PKR-dependent IκB levels we co-transfected HeLa-PKR^{ko} cells with M156R and European rabbit PKR or brush rabbit PKR and stimulated cells with poly(I:C), to simulate dsRNA production during virus infection. Transfection of either European rabbit PKR or brush rabbit PKR alone led to reduced IκBα expression (Fig. 2.4H). Whereas co-transfection of brush rabbit PKR with M156R resulted in high IκBα levels, transfection of brush rabbit PKR with M156R led to intermediate IκBα levels. These results show that intermediate PKR inhibition can result in increased NF-κB pathway activation.

PKR-dependent IκBα depletion and NF-κB-activation during MYXV infection

To test the role of PKR in IκBα degradation during MYXV infection, we infected both PKR-competent and PKR^{ko} HeLa and A549 cells with a MYXV construct lacking its two PKR inhibitors, M029 and M156 (MYXVΔM029LΔM156R). At multiple times post-infection, we assayed these cells for phosphorylated PKR, total PKR, phosphorylated eIF2α, total eIF2α, p65, and IκBα by Western blot analyses. The absence of PKR in the HeLa- and A549-PKR^{ko} cells was confirmed using anti-PKR antibodies (Fig. 2.5A and B). Virus infection caused phosphorylation of both PKR and eIF2α in the wild type cells, which was most prominent between 8 and 24 hours post infection (hpi), but not in the PKR deficient cells. Virus infection also led to a PKR-dependent loss of IκBα expression, which was most prominent 12 hpi. IκBα expression recovered 48 hpi, and this recovery correlated with lower levels of PKR and eIF2α phosphorylation. In the PKR-deficient cells, a weaker and later decrease in IκBα expression was observed, which extended to 48 hpi. These data suggest that there were two phases of NF-κB activation, a fast PKR-dependent loss of IκBα expression, followed by a slower and less prominent PKR-independent loss of IκBα expression during infection. To determine whether PKR also directly influences the canonical NF-κB pathway, we tested activity of the NF-κB-dependent luciferase reporter in response to increasing amounts of TNFα in wild type and PKR-deficient HeLa cells and found no substantial differences in NF-κB activation, indicating that PKR did not affect TNFα-induced activation of NF-κB (Fig. 2.6).

We next tested whether IκBα depletion during infection could be inhibited by treatment with AraC, which inhibits poxviral DNA replication, and therefore also inhibits intermediate and late

gene transcription. As a result, AraC treatment leads to a strong reduction in the formation of viral dsRNA, the activator of PKR during infection [33,34]. In HeLa and A549 cells, AraC treatment reduced PKR and eIF2α phosphorylation during infection with MYXVΔM029LΔM156R, and partially restored IκBα expression (Fig. 2.7A and B). We also determined mRNA expression levels of the pro-inflammatory NF-κB target genes TNFα and IL-6 by qRT-PCR during infection in wild type and PKR-deficient HeLa and A549 cells. Infection of the PKR-deficient cell lines with MYXVΔM029LΔM156R led to an increase in TNFα and IL-6 transcript levels. In the PKR-competent cell lines, this increase was significantly higher, whereas AraC treatment led to transcript levels that were comparable to that observed in the PKR-deficient cell lines (Fig. 2.7C, D, E and F). These data support the notion of PKR-dependent and independent mechanisms of NF-κB activation during infection.

Modulation of pro-inflammatory gene expression by M156 during infection of rabbit PKR-expressing cells

Next, we tested whether the expression of pro-inflammatory genes can be affected by M156 during virus infection. We stably transfected PKR-deficient HeLa cells with either empty vector, European rabbit PKR, or brush rabbit PKR under the control of the human PKR promoter and isolated monoclonal cells which expressed European rabbit PKR and brush rabbit PKR at a comparable level (Fig. 2.8A). These cells were then infected with MYXVΔM029L, MYXVΔM029LΔM156R and the revertant virus MYXVΔM029LΔM156R/M156R^{rev}. In HeLa-PKR^{ko} control cells, comparable TNFα and IL-6 induction was observed for all virus infections (Fig. 2.8B and C). In European rabbit PKR- and brush rabbit PKR-expressing cells, infection with MYXVΔM029LΔM156R led to a strong induction of both TNFα and IL-6. When we

infected brush rabbit PKR-expressing cells with the M156 expressing viruses we observed a strong reduction (≈ 6 fold) in both TNFα and IL-6 levels, to levels comparable to the control cells. In contrast, European rabbit PKR-expressing cells infected with these viruses displayed only a 2-fold reduction in TNFα and IL-6 levels (Fig. 2.8B and C). These results indicate that M156 only partially repressed European rabbit PKR-induced NF-κB activation, whereas it strongly inhibited brush rabbit PKR-induced NF-κB activation during infection.

Hyperactive M156 fails to induce European rabbit PKR-mediated NF-κB activation

These preceding data support our hypothesis that preferential depletion of IκBα due to intermediate inhibition of European rabbit PKR by M156, but not strong inhibition of brush rabbit PKR results in NF-κB activation. This hypothesis would also predict that a hyperactive M156 would also not induce European rabbit PKR-mediated NF-κB activation, by fully preventing translational shut-off rather than allowing some translation to occur. To test this hypothesis, we employed a random mutagenesis yeast screen of M156 to identify hyperactive mutants. We used a previously described yeast strain that contains chromosomally integrated, galactose-inducible European rabbit PKR and transformed it with two libraries of mutagenized M156 that were each created from approximately 42,000 E. coli transformants. The finding that VACV K3 inhibited PKR-mediated toxicity better than M156 indicated the feasibility of this approach [8]. In total, we selected 2900 yeast colonies that were transformed with either library and performed replica plating. Plasmids of transformants that showed substantially better growth than those transformed with wild type M156 were isolated, sequenced, and retransformed into the European rabbit PKR-expressing yeast strain. Transformants with single mutations in M156R at four different sites were identified, which facilitated better yeast growth: K21Q (identified

twice from library 1), E28V (identified once from library 1 and twice from library 1), N39D (identified once from library 1), and Q42L (identified three times from library 1) (Fig. 2.10A). Positions of these mutated amino acids projected on the NMR structure of M156 showed that two of the residues (N39 and Q42) are adjacent to residue Y40 which corresponds to the phosphorylation site in eIF2α, and which in M156 has also been shown to be phosphorylated by human PKR [35] (Fig. 2.10B and C). K21 corresponds to the Y32 of eIF2α, which was found to be in direct contact with PKR in a co-crystal structure [36]. When these mutations were introduced into M156R for the LBR assay, M156-K21Q, N39 and Q42 showed significantly increased inhibition of European rabbit PKR compared to wild type M156 (Fig. 2.10D). Because residue K21 was identified as critical for PKR inhibition, we substituted it with every amino acid and measured the effect in the LBR assay. We observed a spectrum of PKR inhibition, ranging from no inhibition, inhibition comparable to wild type M156, to enhanced inhibition comparable to M156-K21Q (K21M and K21Y) (Fig. 2.10E).

We next compared the effects of the hyperactive M156-K21Q and the naturally occurring hypoactive M156-L71P variant on European rabbit PKR and brush rabbit PKR in the LBR assay and in dual luciferase assays using a reporter containing either the ATF-4 upstream open-reading frame (uORF) or the NF-κB-responsive promoter. M156-K21Q only increased luciferase activity when co-transfected with European rabbit PKR but not with brush rabbit PKR (Fig. 2.10F). In the ATF4-uORF assay, firefly luciferase activity is stimulated by eIF2α phosphorylation [15]. In this assay, M156-K21Q led to significantly less luciferase activity than wild type M156 only for European rabbit PKR but not brush rabbit PKR (Fig. 2.10G). Thus, as predicted, the results inversely correlate with the LBR assay. In the NF-κB activity reporter assay, co-transfection of only European rabbit PKR with wild type M156 but not M156-K21Q led to elevated luciferase

activity, whereas no significant difference was detected for brush rabbit PKR (Fig. 2.10H). Western blot analyses revealed that co-transfection of European rabbit PKR with M156-K21Q followed by poly(I:C) stimulation resulted in higher IκBα expression levels than when it was co-transfected with wild type M156, which resulted in intermediate IκBα expression levels (Fig. 2.10I).

Discussion

Myxoma virus infection of European rabbits is one of the best-defined examples of host-virus co-evolution on the population level [4]. This co-evolution is at least in part due to the fact that MYXV gains substantial virulence as a consequence of host switching, resulting in very strong selective pressure on both the host and the virus. Previous work defining the molecular interactions between MYXV and host proteins were primarily performed using cell lines and proteins derived from humans or European rabbits; however, these molecular host-virus interactions had not been well studied in the context of its natural hosts. In this study, we show that, paradoxically, MYXV M156 inhibited brush rabbit PKR much more efficiently than European rabbit PKR, even though MYXV causes a relatively benign, localized lesion in brush rabbits but is highly virulent in European rabbits [2,4]. This observation is even more surprising in light of our previous work demonstrating that attenuation of MYXV isolates from Australia correlated with the emergence of a loss-of-function mutation in M156R against European rabbit PKR [8].

Here we demonstrate that the moderate inhibition of European rabbit PKR by M156 allowed activation of the NF-κB pathway, whereas complete inhibition of brush rabbit PKR by M156 did not. Furthermore, either hyperactive or hypoactive M156 failed to induce European rabbit PKR-mediated NF-κB activation. In all cases, eIF2α phosphorylation coincided with a rapid loss of the NF-κB inhibitor IκBα and thus activation of NF-κB. The maladaptation between M156 and PKR derived from the aberrant European rabbit host resulted in the partial activation PKR and intermediate phosphorylation of eIF2α. As a consequence, some translation could still proceed to enable functional activation of the NF-κB pathway and production of cytokines. In contrast, fully

activated PKR led to high eIF2α phosphorylation levels, which resulted in strong NF-κB activation, but also inhibited translation of the induced mRNAs. A similar outcome was seen with complete PKR inhibition, where NF-κB is not activated, and thus IκBα is not depleted. Taken together, these results demonstrate that intermediate inhibition of PKR is uniquely able to functionally activate the NF-κB pathway and still allow translation of NF-κB target genes. This expression of inflammatory cytokines may explain how MYXV infection becomes systemic in European rabbits and provides a possible explanation for the different disease outcomes in these rabbits.

There are two different mechanisms that have been described for NF-κB activation by PKR: (i) direct association of PKR with IκBα or components of the IKK complex [17,37–41], and (ii) indirectly due to translational repression resulting in more rapid depletion of short half-life proteins relative to more stable proteins. This second mechanism has been demonstrated for the eIF2α kinases PKR, GCN2 and PERK in response to viral infections or other cell stressors. When these kinases are activated, the subsequent translational repression depletes the short half-life protein IκBα more rapidly than NF-κB thus relieving its inhibitory effect on NF-κB and activating the NF-κB pathway [16,20,30,42,43]. Our observation that NF-κB activation was blocked by strong PKR inhibition of both rabbit PKRs indicates that the enzymatic activity of PKR and possibly the phosphorylation status of eIF2α is important for this process. Both brush rabbit and European rabbit PKR caused comparable activation of NF-κB in the absence of PKR inhibitors. In transfection assays, both PKRs led to reduced IκBα protein levels, and increased mRNA expression of the NF-κB targets IκBα, TNFα and IL-6. Similarly, infection of transgenic HeLa cells that express either brush rabbit or European rabbit PKR instead of endogenous PKR

with MYXV devoid of its two native PKR inhibitors led to a comparable, PKR-dependent induction of TNFα and IL-6. Using two different PKR-deficient cell lines, we also demonstrate that MYXV infection can induce the NF-κB pathway in both a PKR-dependent and a PKR-independent manner. The PKR-dependent IκBα depletion occurred rapidly and reached a maximum at approximately 12 hours post infection, whereas the PKR-independent IκBα depletion was not as pronounced and occurred more slowly (Fig. 2.5). Induction of TNFα and IL-6 was also more pronounced when the NF-κB pathway was activated through the PKR-dependent mechanism relative to PKR-independent NF-κB activation. These data emphasize the important role of PKR in NF-κB activation during poxvirus infection.

One of the most profound differences between brush rabbits and European rabbits during the course of MYXV infection is that MYXV produces a localized skin infection in its natural host, while in European rabbits it rapidly disseminates systemically. While many virus spillover events are likely dead ends due to maladaptation between host and pathogen [44], here we demonstrate an example of molecular maladaptation that correlates with increased host virulence and virus dissemination in the aberrant host. Because European rabbit PKR was only partially inhibited by M156, the functional activation of NF-κB and the resulting expression of inflammatory cytokines like IL-6 and TNFα may promote the systemic spread of MYXV in European rabbits. For example, in MYXV infection of European rabbits, leukocytes play an essential role in the systemic dissemination of viruses [4,45]. In fact, the NF-κB-induced cytokine TNFα "activates" the endothelium to initiate the multistep adhesion cascade to recruit neutrophils [46,47]. Therefore, the continued expression of TNFα in MYXV infected European rabbits suggests a potential mechanism to initiate and promote systemic spread of the virus. This

maladaptation of M156 and PKR as a contributor to virulence is supported by our previous observation of an M156 loss of function mutation evolving in a substantial proportion of Australian rabbits which correlated with MYXV attenuation [8]. As an extension of this observation, our work also supports the hypothesis that evolution of a hyperactive M156 should have a similar attenuating effect on MYXV disease in European rabbits and may evolve in natural populations as well. Together with earlier studies, these data show that PKR-dependent pathways in infection should be considered when studying NF-κB activation.

To the best of our knowledge, this report is the first study demonstrating limited cap-dependent translation after activation of the PKR pathway and the impact this modest translation inhibition has in shaping cellular pro-inflammatory responses. While it is clear that poxviruses must inhibit PKR to prevent the antiviral effect of translation inhibition, nuanced PKR inhibition may play a pivotal role in determining disease outcome. While strong PKR inhibition prevents PKR-dependent NF-κB activation, and no PKR inhibition leads to strong NF-κB activation, resulting in increased transcription but no translation of induced mRNAs, only intermediate PKR inhibition allows both the activation of NF-κB, as well as the translation of NF-κB-induced mRNAs (Fig. 2.11). High expression of the NF-κB luciferase reporter only after intermediate PKR inhibition suggests that PKR activation is not an "on-off switch" for translation. Rather, PKR may initiate a spectrum of translation inhibition, at least in certain situations. This attenuated translation may result in differential proteomic profiles during infection based on half-life or other intrinsic properties of the proteins, beyond the changes to TNFα and IL-6 that we demonstrate in this study. Currently, it's unclear whether this phenomenon is specific to the rabbit/MYXV system, or if it's a more generalizable phenotype. If this is a general mechanism of a more measured translational shutoff by PKR, this may represent a mechanism to fine tune the

intracellular environment, which could conceivably be manipulated by either the host or the virus depending on context.

Materials and Methods

Plasmids, Yeast Strains and Cell Lines

Cloning of European rabbit PKR (ePKR) and MYXV M156R was described previously [8]. Brush rabbit PKR (bPKR), MSW-M156R and M156R mutants were cloned into pSG5 for expression in mammalian cells. HeLa-PKR knock-out (PKR^{ko}) cells (a kind gift of Dr. Adam Geballe [48]) were stably transfected with European rabbit PKR and brush rabbit PKR under the control of the human PKR promoter. See SI Materials and Methods for details.

Luciferase-based Reporter (LBR) Assays

Single or dual luciferase assays were performed as previously described [8]. Briefly, 5×10^4 HeLa-PKR^{ko} cells or HeLa-PKR^{kd} cells were seeded in 24-well plates 24 hours prior to the experiment. Cells were transfected with the indicated plasmids using GenJet (Signagen) following the manufacturer's protocol. After 48h, cell lysates were harvested using mammalian lysis buffer (GE Healthcare) and pGL3-firefly luciferase, NF-κB- or ATF4-firefly luciferase and renilla luciferase were measured. See SI Materials and Methods for details.

Western Blot Analyses

HeLa-PKR^{ko} cells were transfected with either European rabbit PKR or bPKR alone or in combination with K3L, M156R or M156R mutants. In separate experiments, 4×10^5 HeLa, HeLa-PKR^{ko}, A549, or A549-PKR^{ko} cells were seeded in six-well plates and infected with MYXVΔM029LΔM156R at a MOI of 3 for the times indicated in the figures. Cells were lysed in 1% sodium dodecyl sulfate (SDS) in PBS (VWR) and sonicated at 50% amplitude for 10 seconds twice. The lysates were separated by 12% SDS/PAGE, blotted on PVDF membranes

and incubated with diluted primary and secondary antibodies as described in the SI Materials and Methods. See SI Materials and Methods for details.

Quantitative RT-PCR

Transfected or infected cells were collected and lysed with TRIzol Reagent (Invitrogen). Total cellular RNA was isolated using Direct-zol™ RNA Kits (Zymo Research), then cDNA was synthesized using protoScript® II reverse transcriptase (NEB). qRT-PCR was performed using EvaGreen dye (Biotium) and measured using CFX Connect Real-Time PCR Detection System (Bio-Rad). See SI Materials and Methods for details

Yeast Growth Assays

Experiments were performed as previously described [8,49]. See SI Materials and Methods for details.

Statistical Analysis

Statistical analyses were performed using Prism 8 Software (GraphPad). The data were analyzed using paired Student's t-test. A p value of <0.05 was considered significant. * $p < 0.5$, ** $p<0.01$, *** $p< 0.001$, **** $p< 0.0001$; ns, not significant. All values are presented as the means ± SD.

Supporting Information

SI Materials and Methods

Plasmids, Yeast Strains, Cell Lines and Viruses

Brush rabbit PKR was cloned from total RNA isolated from muscle and connective tissues of the paws of brush rabbits (kindly provided by Dr. Patrick Kelly and Dr. Matthew Lloyd), which died in the field during the Riparian Brush Rabbit Recovery project. For transient expression in mammalian cells, all PKRs and viral proteins were cloned into pSG5 vector as previously described [8]. Generation of yeast strains stably transformed with empty vector (J673) or European rabbit PKR (O8) under the control of a yeast GAL-CYC1 hybrid promoter was also previously described [8,49].

Random mutagenesis of M156 was performed with the GeneMorph II Random Mutagenesis Kit (Agilent) and 10 ng (library 1) or 2 ng (library 2) pYX113-M156R plasmid template for libraries 1 and 2, respectively. PCR products were cloned into the vector pYX113 (R&D Systems), which contains the GAL-CYC1 hybrid promoter and the selectable marker URA3. Plasmid libraries 1 and 2 were created from 41,574 and 43,520 E. coli transformants, respectively. After transformation into yeast strain O8, 2900 yeast colonies were randomly selected for replica printing on glucose-containing SD (non-inducing) and galactose-containing (inducing) agar plates. Plasmids of transformants that showed increased growth under inducing conditions were isolated, cloned into E. coli and retested in O8. Plasmids that conferred better yeast growth were sequenced. Identified single mutations were introduced into pYX113-M156R by site-directed mutagenesis and retested in O8. For each transformation, four independent clones were picked, colony purified on SD plates, and replica plated on glucose- or galactose-containing agar plates.

The M156R mutations (E28V, N39D, Q42L, K21Q, K21Q, K21A, K21R, K21N, K21D, K21C, K21E, K21G, K21H, K21I, K21L, K21M, K21F, K21P, K21S, K21T, K21W, K21Y, K21V) were generated by site-directed mutagenesis PCR using Phusion High-Fidelity DNA polymerase (NEB). PCR was performed using the pSG5-M156R short construct as the template with primers containing the corresponding mutation flanked by 15 nucleotides identical to the template up- and downstream of the mutation. All ORFs were sequenced by Sanger sequencing to confirm correct sequences. The NF-κB reporter plasmid (kindly provided by Dr. Bastian Opitz) contains a firefly luciferase gene driven by six NF-κB binding sites followed by a minimal beta-globin promoter [50]. The ATF4-reporter plasmid (kindly provided by Dr. Ron Wek) contains a full-length mouse ATF4 mRNA leader sequence which drives the expression of a firefly luciferase gene [15]. For dual luciferase assays pRL-TK renilla (Promega) luciferase was used.

HeLa-PKR knock-out (PKR^{ko}) cells were kindly provided by Dr. Adam Geballe [48]. To generate HeLa-PKR^{ko} cells expressing rabbit PKRs, the European rabbit PKR gene or brush rabbit PKR gene were cloned into a plasmid that drives PKR expression under the control of the human PKR promoter as previously described [8,51]. HeLa-PKR^{ko} cells were transfected using GenJet-HeLa (SignaGen Laboratories) according to the manufacturer's instructions. Cells were trypsinized 48 h after transfection and cultured in the presence of 700 µg/ml geneticin (Invitrogen) for 14 days. To select clones, cells were seeded on 96-well plates at densities of either 0.3 cells or one cell per well, and wells were screened for single colonies. Clones were then grown, and proteins were isolated to detect the expression of European rabbit PKR or brush rabbit PKR with an anti-PKR antibody B10 antibodies (Sc-6282, Santa Cruz Biotechnology). Clones HeLa-European rabbit PKR-C6, containing European rabbit PKR, and HeLa-brush rabbit PKR-C4, containing brush rabbit PKR showed comparable PKR expression and were used for

subsequent experiments. HeLa cells (human, ATCC #CCL-2), HeLa-PKR knock-down (PKR^{kd}) cells (kindly provided by Dr. Charles Samuel [52], A549 cells and A549-PKR^{ko} cells (kindly provided by Dr. Bernard Moss [53]), were propagated in Dulbecco's Modified Eagle's Medium (DMEM) supplemented with 2 mML-glutamine, 100 IU/ml penicillin/streptomycin (Gibco) and containing 5% fetal bovine serum (FBS) (BT cells). HeLa-PKR^{kd} cells were maintained in media additionally supplemented with 1 µg/ml puromycin (Sigma). RK13+E3L+K3L [54] cells were maintained in medium additionally supplemented with 500 µg/ml geneticin (G418) and 300 µg/ml zeocin (Life Technologies). All cells were grown at 37°C in a humidified 5% CO_2 incubator. The construction of MYXVΔM029L, MYXVΔM029LΔM156R and MYXVΔM029LΔM156R/$M156R^{revertant(rev)}$ were described previously [8]. The viruses were propagated in RK13+E3L+K3L cells.

Antibodies, Cytokines and Chemicals

The mouse anti-IκBα monoclonal antibodies (mAb) (L35A5), rabbit anti-NF-κB p65 mAb (D14E12), rabbit anti-Phospho-NF-κB p65 (Ser536) mAb (93H1), and rabbit anti-Phospho-eIF2α (Ser51) polyclonal antibody (9721) were purchased from Cell Signaling Technologies. The mouse anti-PKR B10 polyclonal antibody (Sc-6282), and rabbit anti-eIF2α polyclonal antibody (sc-11386) was purchased from Santa Cruz Biotechnology. Mouse anti-flag M2 mAb (F3165) and mouse anti-β-actin mAb (A1978) were purchased from Sigma. Rabbit anti-PKR (phospho T446) antibody (E120) (ab32036) was purchased from Abcam. The horseradish peroxidase (HRP)-conjugated goat anti-mouse, goat anti-rabbit secondary antibodies fluorescein isothiocyanate (FITC)-conjugated goat anti-mouse IgG (H+L), and tetramethyl rhodamine isocyanate (TRITC)-conjugated goat anti-mouse antibodies were purchased from Thermo Fisher Scientific. Recombinant human TNFα (300-01A) was purchased from PeproTech and used at the

indicated concentrations in the figures. Cytosine β-D-arabinofuranoside (AraC) (C1768) and poly (I:C) (P1530) were purchased from Sigma and used at 50 μg/ml and 5 μg/ml, respectively.

Luciferase-based reporter (LBR) Assays

Single luciferase assays were used to measure PKR inhibition by K3, M156 or M156 mutants. 5×10^4 HeLa-PKR^{ko} cells were seeded in 24-well plates 24 hours prior to the transfection. For each transfection, firefly luciferase (pGL3 plasmid, 50 ng, Promega) and pSG5 plasmids encoding European rabbit PKR or brush rabbit PKR, K3, lu-M156, MSW-M156, M156-K21Q (E28V, N39D, Q42L, K21Q, K21Q, K21A, K21R, K21N, K21D, K21C, K21E, K21G, K21H, K21I, K21L, K21M, K21F, K21P, K21S, K21T, K21W, K21Y, K21V), M156-E28V, M156-N39D, M156-Q42L, were transfected using GenJet-HeLa (SignaGen Laboratories) for HeLa-PKR^{ko} cells. The same amount of pSG5 empty vector was transfected as a control. Each transfection was conducted in triplicate.

Dual luciferase assays were used to measure NF-κB and ATF4 responses. 5×10^4 HeLa-PKR^{ko} cells or HeLa-PKR^{kd} cells were seeded in 24-well plates 24 hours prior to transfection. For NF-κB or ATF4 activity assays, transient co-transfections were carried out in triplicate using the NF-κB-luc (50 ng) or ATF4-luc (50 ng) reporter along with the pRL-TK renilla luciferase reporter for normalization. Plasmid transfections were performed using the GenJet-HeLa (SignaGen Laboratories). After 48 hours, cell lysates were harvested using mammalian lysis buffer (GE Healthcare) and luciferase activities were measured using single or dual luciferase assays (Promega) in a GloMax luminometer (Promega). Each experiment was conducted three times independently and representative results are shown. Error bars represent the standard deviations of three replicate transfections.

Western blot analyses

HeLa-PKR^{ko} cells were transfected with European rabbit PKR, brush rabbit PKR only or together with M156R or M156R mutants. After 24 hours, the collected cells were washed with PBS and lysed with 1% sodium dodecyl sulfate (SDS) in PBS. For infection assays, 4×10^5 of HeLa, HeLa-PKR^{ko}, A549, and A549-PKR^{ko}cells were seeded in six-well plates and infected with MYXVΔM029LΔM156R at a MOI of 3 for the times indicated in the figures. All protein lysates were sonicated at 50% amplitude for 10 seconds twice. Protein concentrations were determined by NanoDrop One spectrophotometer (Thermo Scientific). Equal amount of protein samples was separated on 12% SDS-polyacrylamide gels and transferred to polyvinyl difluoride (PVDF, GE Healthcare) membranes using a methanol-based wet transfer apparatus (Bio-Rad). Membranes were blocked with 5% non-fat milk in TBST buffer (20M Tris, 150mM NaCl, 0.1% Tween 20, pH 7.4) for 1 hour. Blots were probed overnight at 4℃ using the primary antibodies listed above diluted 1:1000 in TBST containing 5% BSA. After washing with TBST 3 times for 10 mins, membranes were incubated for 1 hour at room temperature with donkey-anti-rabbit or donkey-anti-mouse secondary antibodies indicated above diluted 1:10,000 in TBST containing 5% (w/v) nonfat milk. The membranes were then washed, and proteins were detected with AmershamTM ECL^T (GE Healthcare). Images were taken using the iBright Imaging System (Invitrogen).

Quantitative RT-PCR

Transfected or infected cells were lysed with TRIzol Reagent (Invitrogen), and total cellular RNA was isolated using Direct-zol RNA Kits (Zymo Research). To remove residual genomic DNA contamination, 2 μg of RNA was treated with ribonuclease-free DNase I (0.5 U μg^{-1} RNA:

NEB). 1 µg of RNA was reverse transcribed to produce cDNA utilizing the ProtoScript II Reverse Transcriptase (NEB) according to the manufacturer's protocol. Quantitative PCR reactions were carried out with 50 ng of cDNA sample from each reaction in a 20 µl reactions containing 0.25 mM of dNTPs, 2.5 mM $MgCl_2$, 1X OneTaq® standard reaction buffer (NEB), 1X EvaGreen dye (Biotium), 325 nM each of forward and reverse primers, one unit of OneTaq® DNA polymerases. Primers used to amplify 18 S rRNA from HeLa and A549 cells for RT-PCR analysis were 18S-qPCR-F: 5′-AGGAATTGACGGAAGGGCAC-3′ and 18S-qPCR-R: 5′-GGACATCTAAGGGCATCACA-3′. Primers used to amplify TNFα (134 bp) from HeLa and A549 cells were TNFα-qPCR-F: 5′-AGCCCATGTTGTAGCAAACC-3′ and TNFα-qPCR-R: 5′-TGAGGTACAGGCCCTCTGAT-3′. Primers used to amplify IL-6 (175 bp) from HeLa and A549 cells were IL-6-qPCR-F: 5′-TACCCCCAGGAGAAGATTCC-3′ and IL-6-qPCR-R: 5′-TTTTCTGCCAGTGCCTCTTT-3′′. Primers used to amplify IκBα (102 bp) from HeLa cells were IκBα-qPCR-F: 5′-GATCCGCCAGGTGAAGGG-3′ and IκBα-qPCR-R: 5′-GCAATTTCTGGCTGGTTGG-3′. PCR cycling was performed at 95°C, 2 min, followed by 40 cycles of 95°C, 5 s; 60°C, 8 s (12 s for IL-6) on a CFX Connect Real-Time PCR Detection System (Bio-Rad), with the fluorescence acquired at the end of each cycle. Melt curve analyses were performed to confirm that there is only a single product amplified in each reaction. Relative expression levels for tested mRNAs were determined using 18 S rRNA as an internal reference using comparative Ct ($2^{-\Delta\Delta Ct}$) method. Values are average of three experiments with standard deviations as indicated.

Author contributions

H.Y. C.P., and S.R. designed and performed research; H.Y. G.B., and S.R. analyzed data and wrote the paper; H.Y. C.P. L.T. G.B., and S.R. contributed new reagents/analytic tools/review & editing.

Figure legend

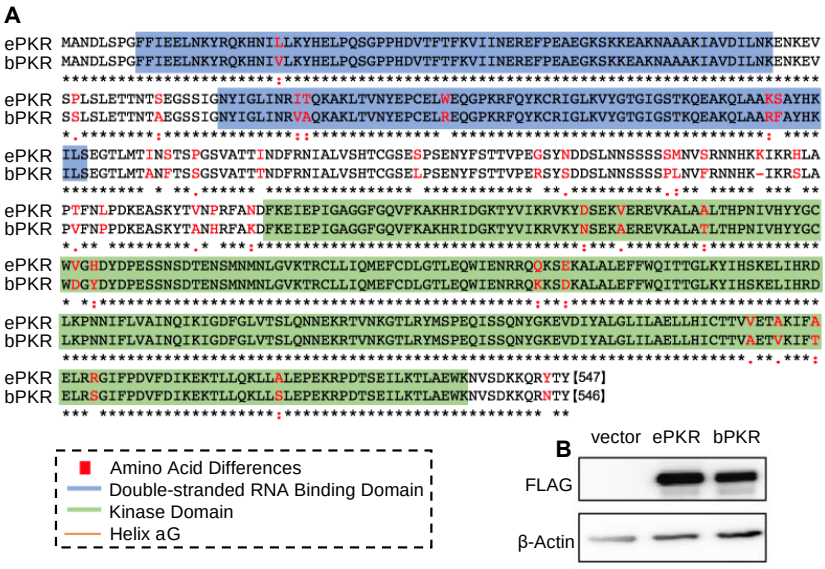

Fig. 2.1 Multiple sequence alignment of PKRs from European rabbit or Brush rabbit

(A) Differences between the two PKRs are found throughout the protein sequence including the dsRNA binding domains, linker region, kinase domain, and the αG-helix region. (B) HeLa-PKR^{ko} cells were transfected with either 3 µg of vector, flag-tagged European rabbit PKR (ePKR) or brush rabbit PKR (bPKR) plasmids. After 48 h, collected cell lysates were separated on 12% SDS-PAGE gels and analyzed by immunoblot analysis with anti-flag and anti-β-actin antibodies.

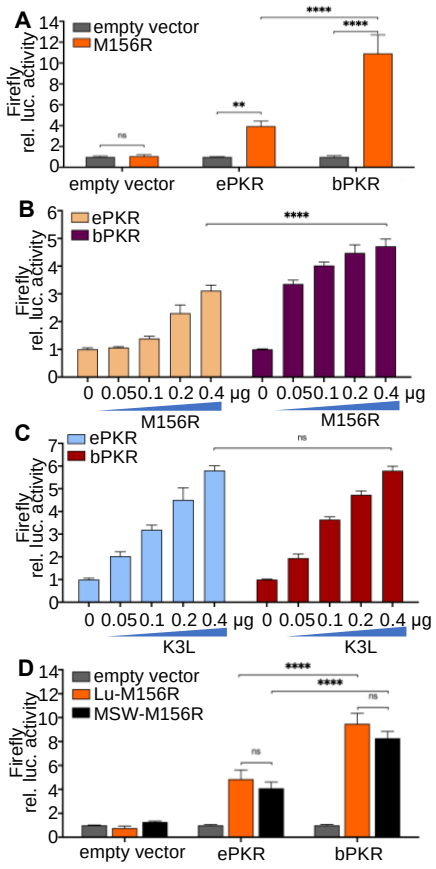

Fig. 2.2 Differential inhibition of European rabbit and brush rabbit PKR by M156

(A) HeLa PKR^{ko} cells were transfected with expression vectors for firefly luciferase reporter (0.05 µg), M156 (0.4 µg), and PKR (0.2 µg) from either European rabbits (ePKR) or brush rabbits (bPKR). Luciferase activity was measured 48 hours post-transfection (hpt) and normalized to the empty vector control in each group. (B, C) 0.2 µg European rabbit PKR or brush rabbit PKR were co-transfected with increasing amounts of M156R (B) or VACV K3L, indicated in the figure (C), along with the firefly luciferase reporter (0.05 µg). Luciferase activity was determined 48 hpt and normalized to PKR-only transfected cells. (D) Lu-M156R (0.4 µg) or MSW-M156R (0.4 µg) were co-transfected with vectors encoding firefly luciferase (0.05 µg), European rabbit PKR (0.2 µg) or brush rabbit PKR (0.2 µg) for 48 h. Relative luciferase activity

is shown. Experiments were performed in triplicate and the results are representative of three independent experiments. Error bars indicate the standard deviations (SD).

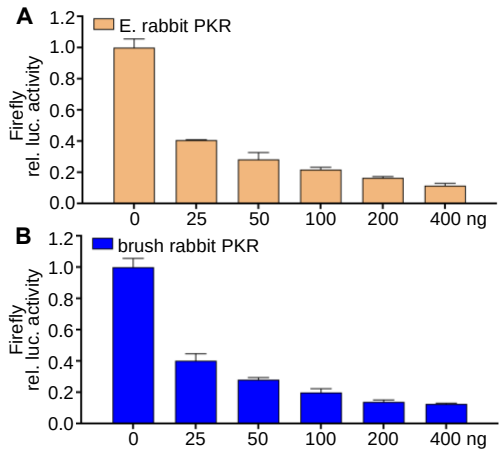

Fig. 2.3 PKR-mediated translational inhibition is equivalent between European rabbit PKR and brush rabbit PKR

(A, B) HeLa-PKR^{ko} cells were transfected with an increasing amount of either European rabbit PKR (ePKR) (A) or brush rabbit PKR (bPKR) (B) as indicated. Firefly luciferase activity was measured 48 hpt and normalized to vector-only transfected cells to obtain relative luciferase activities. Error bars represent the standard deviations from three independent transfections. Results shown are representative of three independent experiments.

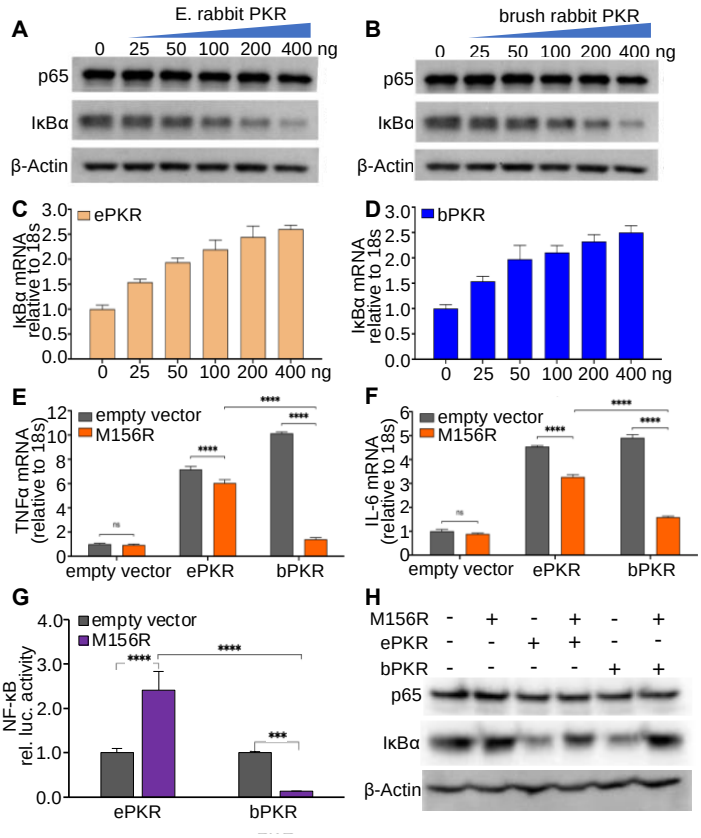

Fig. 2.4 Modulation of NF-κB activity by differential inhibition of rabbit PKRs

(A, B, C, D) HeLa-PKR^{ko} cells were transfected with increasing amounts of European rabbit PKR (ePKR) (A, C) or brush rabbit PKR (bPKR) (B, D) as indicated. After 24 h, total protein lysates were collected and subjected to Western blot analyses for NF-κB-p65, IκBα, and β-actin (A, B). IκBα mRNA levels (C, D) were measured by qRT-PCR at 24 hpt in parallel experiments. (E, F) HeLa PKR^{ko} cells were co-transfected with M156R (0.3 μg) and either European rabbit PKR (0.3 μg) or brush rabbit PKR (0.3 μg). After 24 h, total RNA was isolated from the transfected cells and subjected to qRT-PCR for TNFα (E) and IL-6 (F). (G) HeLa-PKR^{ko} cells were co-transfected with expression vectors encoding M156 (0.3 μg), the indicated PKRs (0.3 μg) and both the NF-κB-responsive firefly luciferase and constitutively active renilla luciferase reporters (0.05 μg

each). After 48 h, NF-κB firefly luciferase activity was measured and normalized to renilla luciferase values in the same well to obtain internally controlled luciferase activity. The obtained values were further normalized to PKR-only transfected cells to calculate relative NF-κB-specific luciferase activities. The results are representative of three independent experiments. (H) In order to analyze the effects of M156 on PKR-dependent IκB levels, we co-transfected HeLa-PKR^{ko} cells with M156R and European rabbit PKR or brush rabbit PKR and stimulated cells with poly(I:C) to mimic dsRNA production during a virus infection. In details, HeLa-PKR^{ko} cells were co-transfected with M156R (0.8 µg) and the indicated PKRs (0.4 µg). After 16 hours, cells were stimulated with 5 µg/ml poly(I:C) for 8 hours. 24 hpt total proteins were isolated subjected to immunoblotting using antibodies specific for NF-κB-p65, IκBα, and β-actin.

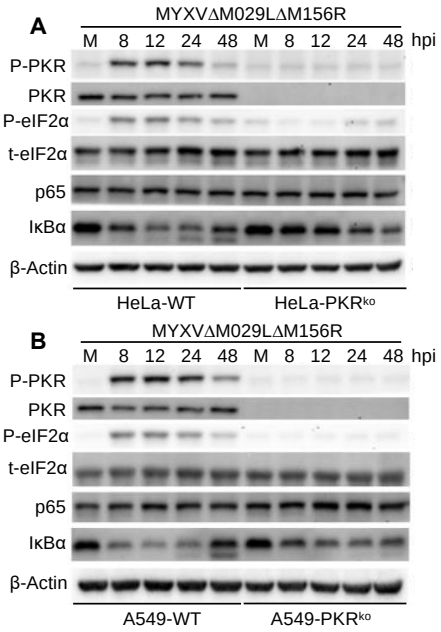

Fig. 2.5 Activated PKR mediated IκBα depletion during MYXV infection

(A, B) HeLa wild type (WT) or PKR^{ko} (A), and A549 WT or PKR^{ko} (B) cells were infected with MYXVΔM029LΔM156R at a MOI of 3 for 8, 12, 24, or 48 h. Total protein lysates were collected and subjected to Western blot analyses for phosphorylated (P) PKR, total (t) PKR, phosphorylated (P) eIF2α, total (t) eIF2α, NF-κB-p65, IκBα and β-actin. Lysates of mock-infected cells were included as controls.

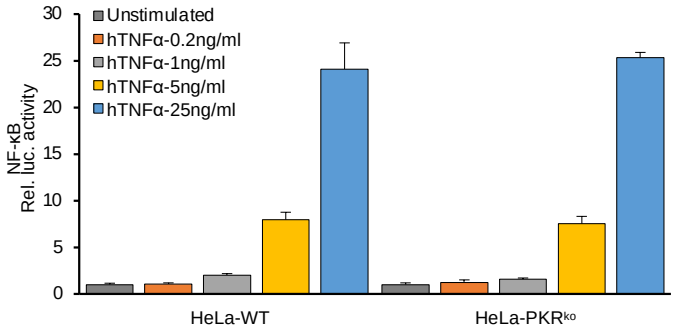

Fig. 2.6 PKR does not affect TNFα stimulated canonical NF-κB activation

PKR WT and PKR^{ko} HeLa cells were co-transfected with NF-κB reporter (0.05 µg) and TK renilla reporter (0.05 µg). At 42 hpt, cells were mock stimulated or stimulated with increasing amounts of human TNFα for 6 h. NF-κB firefly and renilla luciferase activities were measured at 48 hpt. Measured NF-κB firefly luciferase values were normalized to renilla luciferase activities. Obtained values were then further normalized t to non-stimulated control to calculate NF-κB relative luciferase activities. Results shown are representative of three independent experiments. Error bars indicate the SD.

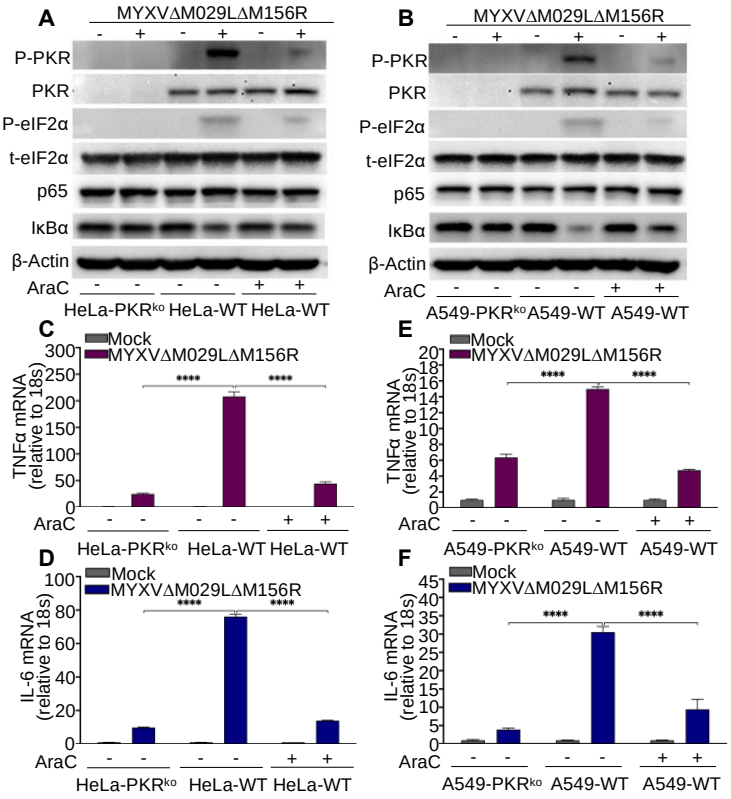

Fig. 2.7 PKR-mediated amplification of pro-inflammatory cytokine expression during MYXV infection

HeLa-WT and HeLa-PKR^{ko} (A, C, D) or A549 WT and A549-PKR^{ko} (B, E, F) were infected with MYXVΔM029LΔM156R at a MOI of 3. As indicated, some HeLa-WT or A549-WT cells were also treated with 50 μg/mL AraC. Total protein lysates were collected at 8 hpi to monitor the expression of indicated proteins using indicated antibodies (A, B). At 12 hpi, the total RNA was isolated from the indicated cells and subjected to qRT-PCR for TNFα (C, E) and IL-6 (D, F), respectively.

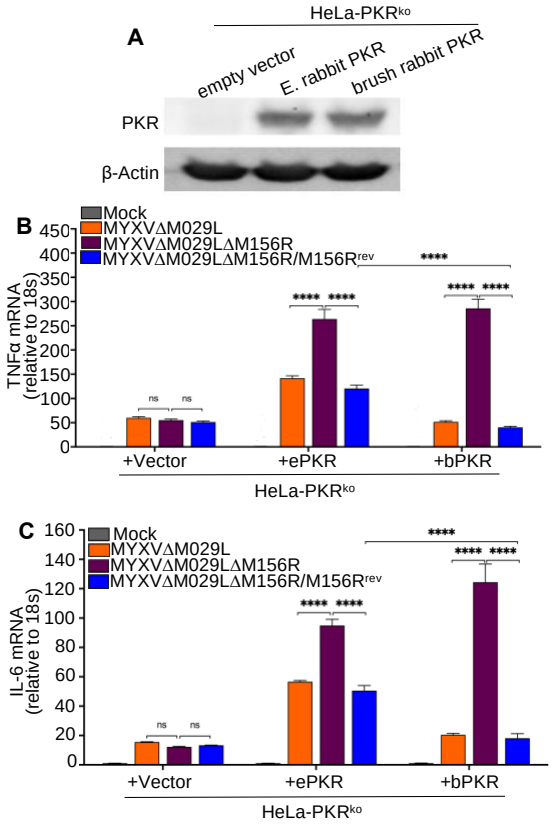

Fig. 2.8 PKR-dependent modulation of pro-inflammatory gene expression during infection of MYXV infection

(A) HeLa-PKR^{ko} cells were stably transfected with empty vector, European rabbit PKR (ePKR), or brush rabbit PKR (bPKR) under the control of the human PKR promoter. The expression of European rabbit PKR and brush rabbit PKR was measured by Western blot analyses using anti-PKR antibodies. (B, C) Congenic HeLa-PKR^{ko} cell lines which stably express vector control, European rabbit PKR or brush rabbit PKR were mock infected or infected with MYXVΔM029L, MYXVΔM029LΔM156R and MYXVΔM029LΔM156R/M156R$^{revertant(rev)}$ at a MOI of 3. At 12 hpi, total RNA was isolated from the indicated cell lines and subjected to qRT-PCR for TNFα (B) and IL-6 (C).

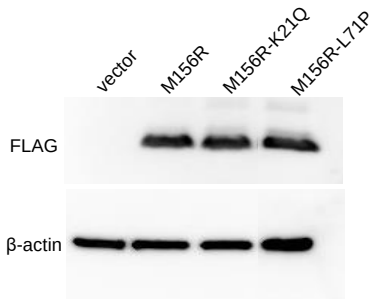

Fig. 2.9 Expression of M156 and M156 mutants in transfected HeLa-PKR^{kd} cells

Plasmids (3 μg) expressing flag-tagged M156, M156-K21Q, M156-L71P were transfected into HeLa PKR^{kd} cells. After 48 h, cell lysates from transfected cells were separated on 12% SDS-PAGE gels and analyzed by immunoblot analysis with anti-flag and anti-β-actin antibodies.

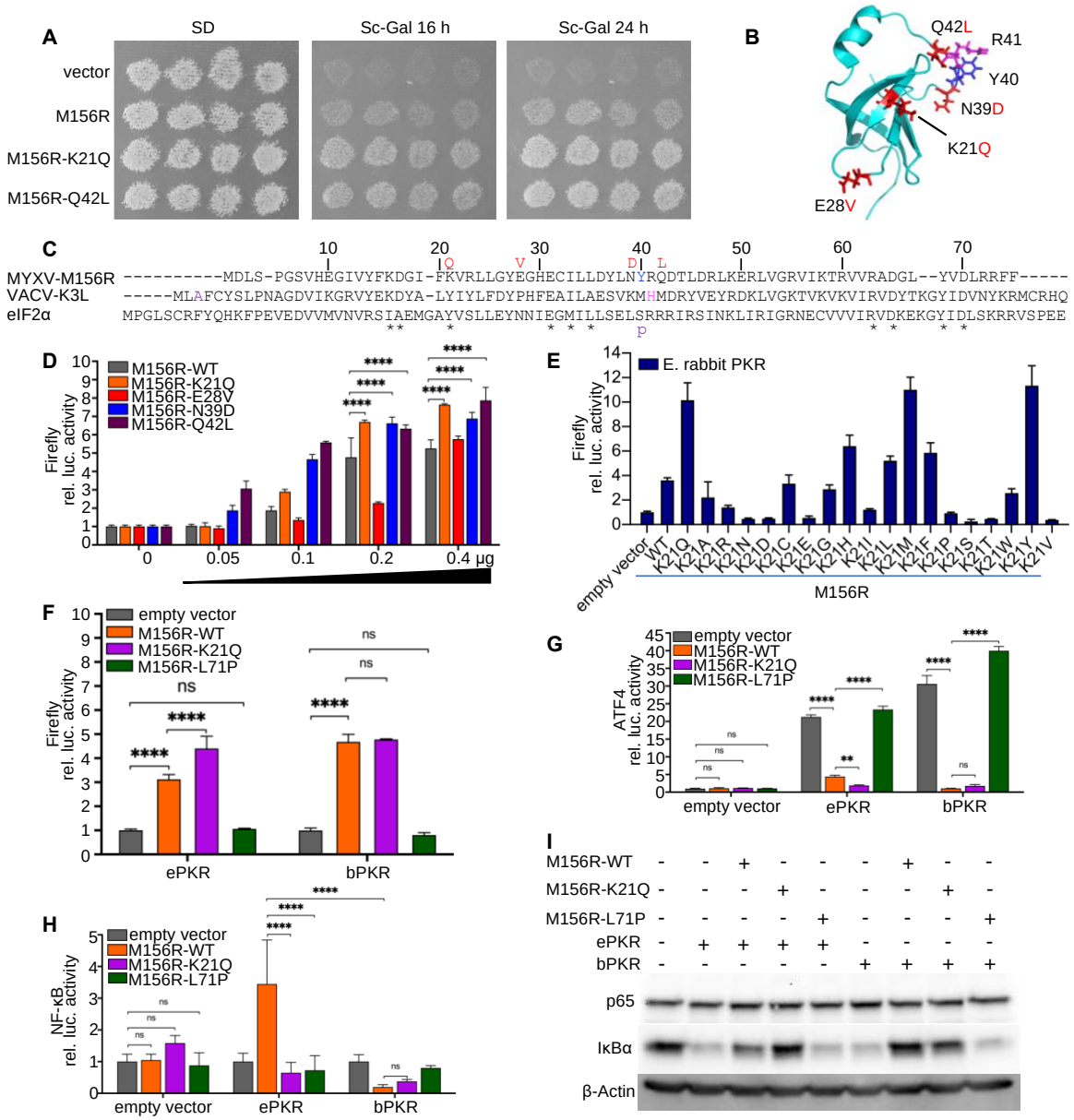

Fig. 2.10 Activation of the NF-κB pathway after intermediate inhibition of PKR by M156

(A) Plasmids encoding empty vector, M156, M156-K21Q or M156-Q42L under the control of a galactose-inducible promoter were transformed into a yeast strain which has European rabbit PKR stably integrated at the LEU2 locus under the control of the GAL-CYC1 hybrid promoter. For each transformant, four colonies were purified and grown under non-inducing (SD) or

inducing conditions (Sc-Gal) at 30°C for 16 or 24 hours. (B) Crystal structure of M156 (REF). Positions of mutations identified in a random mutagenesis screen in M156 that conferred hyper-inhibition of European rabbit PKR (ePKR) in yeast growth assays are shown in red. Residues Y40 and R51 are also highlighted. (C) Multiple sequence alignment of MYXV-Lu M156, VACV K3, and human eIF2α. Mutations that conferred hyperactivity of M156 in the yeast assay are shown in red. Asterisks denote eIF2α residues that contact human PKR in the co-crystal structure [36]. (D) HeLa-PKR^{ko} cells were co-transfected with increasing amounts of either M156R WT or the indicated M156R mutants, firefly luciferase (0.05 μg), and European rabbit PKR (0.2 μg). 48 hpt, luciferase activity was measured and normalized to PKR-only transfected cells to obtain relative luciferase activity. (E) HeLa-PKR^{ko} cells were co-transfected with expression vectors encoding firefly luciferase (0.05 μg), with the indicated M156R mutants (0.4 μg), and European rabbit PKR (0.2 μg). Luciferase activity was measured 48 hpt and normalized to PKR-only transfected cells. (F) European rabbit PKR (0.2 μg) or brush rabbit PKR (bPKR) (0.2 μg) and firefly luciferase reporter (0.05 μg) were co-transfected with either M156R or the indicated mutants of M156R (0.4 μg). (G, H) HeLa PKR^{kd} cells were co-transfected with expression vectors encoding MYXV M156 (0.4 μg), or indicated M156 mutants (0.4 μg), European rabbit PKR or brush rabbit PKR (0.2 μg), renilla luciferase (0.05 μg), along with ATF4-firefly luciferase (0.05 μg), which contains the mouse ATF4 mRNA-5'UTR sequence (D) or NF-κB-dependent firefly luciferase (0.05 μg) (E). After 48, firefly luciferase activities were measured and normalized to renilla luciferase activities. Obtained values were then further normalized to vector control of each group to calculate relative luciferase activity. Results shown are representative of three independent experiments. Error bars indicate the standard deviations from three independent transfections. (I) M156R (0.8 μg) or indicated M156R mutants was co-

transfected with indicated PKRs (0.4 µg) in the HeLa-PKR^{ko} cells. After 16 hours, cells were stimulated with 5 µg/ml poly(I:C) for 8 hours. 24 hpt, total protein lysates were analyzed by immunoblotting with the indicated antibodies.

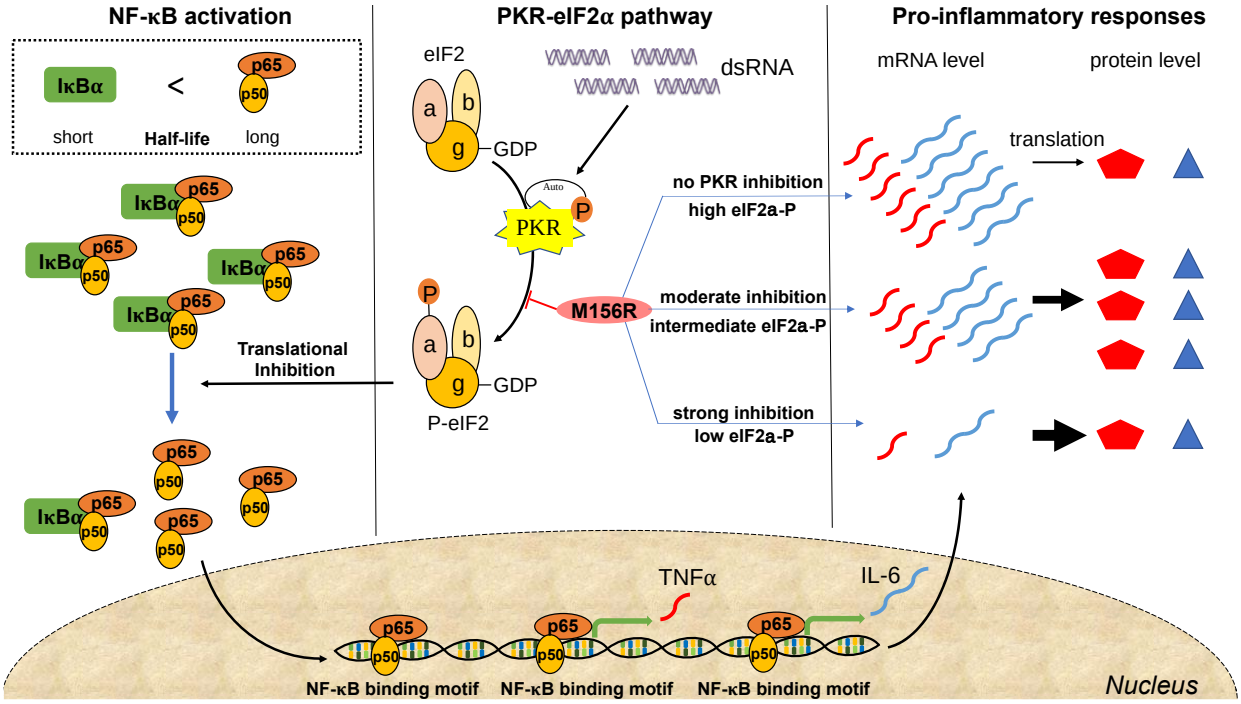

Fig. 2.11 Effects of intermediate PKR inhibition on the NF-κB pathway

References

1. Geoghegan, J.L.; Holmes, E.C. The phylogenomics of evolving virus virulence. Nat. Rev. Genet. 2018, 19, 756–769, doi:10.1038/s41576-018-0055-5.
2. Regnery, D.C.; Miller, J.H. A myxoma virus epizootic in a brush rabbit population. J. Wildl. Dis. 1972, 8, 327–331, doi:10.7589/0090-3558-8.4.327.
3. Kerr, P.J.; Best, S.M. Myxoma virus in rabbits. OIE Rev. Sci. Tech. 1998, 17, 256–268, doi:10.20506/rst.17.1.1081.
4. Kerr, P.J. Myxomatosis in Australia and Europe: a model for emerging infectious diseases. Antiviral Res. 2012, 93, 387–415, doi:10.1016/j.antiviral.2012.01.009.
5. MYERS, K. Studies in the epidemiology of infectious myxomatosis of rabbits. II. Field experiments, August-November 1950, and the first epizootic of myxomatosis in the Riverine Plain of south-eastern Australia. J. Hyg. (Lond). 1954, 52, 47–59, doi:10.1017/s0022172400027248.
6. MARSHALL, I.D.; FENNER, F. Studies in the epidemiology of infectious myxomatosis of rabbits. V. Changes in the innate resistance of Australian wild rabbits exposed to myxomatosis. J. Hyg. (Lond). 1958, 56, 288–302, doi:10.1017/s0022172400037773.
7. MARSHALL, I.D.; DOUGLAS, G.W. Studies in the epidemiology of infectious myxomatosis of rabbits. VIII. Further observations on changes in the innate resistance of Australian wild rabbits exposed to myxomatosis. J. Hyg. (Lond). 1961, 59, 117–122, doi:10.1017/s0022172400038766.
8. Peng, C.; Haller, S.L.; Rahman, M.M.; McFadden, G.; Rothenburg, S. Myxoma virus M156 is a specific inhibitor of rabbit PKR but contains a loss-of-function mutation in Australian virus isolates. Proc. Natl. Acad. Sci. U. S. A. 2016, 113, 3855–3860,

doi:10.1073/pnas.1515613113.

9. Meurs, E.; Chong, K.; Galabru, J.; Thomas, N.S.; Kerr, I.M.; Williams, B.R.; Hovanessian, A.G. Molecular cloning and characterization of the human double-stranded RNA-activated protein kinase induced by interferon. Cell 1990, 62, 379–390, doi:10.1016/0092-8674(90)90374-n.
10. Weber, F.; Wagner, V.; Rasmussen, S.B.; Hartmann, R.; Paludan, S.R. Double-stranded RNA is produced by positive-strand RNA viruses and DNA viruses but not in detectable amounts by negative-strand RNA viruses. J. Virol. 2006, 80, 5059–5064, doi:10.1128/JVI.80.10.5059-5064.2006.
11. Li, S.; Peters, G.A.; Ding, K.; Zhang, X.; Qin, J.; Sen, G.C. Molecular basis for PKR activation by PACT or dsRNA. Proc. Natl. Acad. Sci. U. S. A. 2006, 103, 10005–10010, doi:10.1073/pnas.0602317103.
12. Dey, M.; Cao, C.; Dar, A.C.; Tamura, T.; Ozato, K.; Sicheri, F.; Dever, T.E. Mechanistic link between PKR dimerization, autophosphorylation, and eIF2alpha substrate recognition. Cell 2005, 122, 901–913, doi:10.1016/j.cell.2005.06.041.
13. Gordiyenko, Y.; Llácer, J.L.; Ramakrishnan, V. Structural basis for the inhibition of translation through eIF2α phosphorylation. Nat. Commun. 2019, 10, 2640, doi:10.1038/s41467-019-10606-1.
14. Fitzgerald, K.D.; Semler, B.L. Bridging IRES elements in mRNAs to the eukaryotic translation apparatus. Biochim. Biophys. Acta 2009, 1789, 518–528, doi:10.1016/j.bbagrm.2009.07.004.
15. Vattem, K.M.; Wek, R.C. Reinitiation involving upstream ORFs regulates ATF4 mRNA translation in mammalian cells. Proc. Natl. Acad. Sci. U. S. A. 2004, 101, 11269–11274,

doi:10.1073/pnas.0400541101.

16. Deng, J.; Lu, P.D.; Zhang, Y.; Scheuner, D.; Kaufman, R.J.; Sonenberg, N.; Harding, H.P.; Ron, D. Translational Repression Mediates Activation of Nuclear Factor Kappa B by Phosphorylated Translation Initiation Factor 2. Mol. Cell. Biol. 2004, 24, 10161–10168, doi:10.1128/mcb.24.23.10161-10168.2004.

17. Gil, J.; Alcamí, J.; Esteban, M. Activation of NF-kappa B by the dsRNA-dependent protein kinase, PKR involves the I kappa B kinase complex. Oncogene 2000, 19, 1369–1378, doi:10.1038/sj.onc.1203448.

18. Gil, J.; García, M.A.; Gomez-Puertas, P.; Guerra, S.; Rullas, J.; Nakano, H.; Alcamí, J.; Esteban, M. TRAF family proteins link PKR with NF-kappa B activation. Mol. Cell. Biol. 2004, 24, 4502–4512, doi:10.1128/MCB.24.10.4502-4512.2004.

19. Yu, H.; Bruneau, R.C.; Brennan, G.; Rothenburg, S. Battle Royale: Innate Recognition of Poxviruses and Viral Immune Evasion. Biomedicines 2021, 9.

20. McAllister, C.S.; Taghavi, N.; Samuel, C.E. Protein kinase PKR amplification of interferon β induction occurs through initiation factor eIF-2α-mediated translational control. J. Biol. Chem. 2012, 287, 36384–36392, doi:10.1074/jbc.M112.390039.

21. Hayden, M.S.; West, A.P.; Ghosh, S. NF-κB and the immune response. Oncogene 2006, 25, 6758–6780, doi:10.1038/sj.onc.1209943.

22. Liu, T.; Zhang, L.; Joo, D.; Sun, S.-C. NF-κB signaling in inflammation. Signal Transduct. Target. Ther. 2017, 2, 17023-, doi:10.1038/sigtrans.2017.23.

23. Zhang, H.; Sun, S.-C. NF-κB in inflammation and renal diseases. Cell Biosci. 2015, 5, 63, doi:10.1186/s13578-015-0056-4.

24. Zandi, E.; Rothwarf, D.M.; Delhase, M.; Hayakawa, M.; Karin, M. The IkappaB kinase

complex (IKK) contains two kinase subunits, IKKalpha and IKKbeta, necessary for IkappaB phosphorylation and NF-kappaB activation. Cell 1997, 91, 243–252, doi:10.1016/s0092-8674(00)80406-7.

25. Hl, P. Activators and target genes of Rel/NF-kappaB transcription factors. Oncogene 1999, 18, 6853–66.

26. Hoffmann, A.; Levchenko, A.; Scott, M.L.; Baltimore, D. The IkappaB-NF-kappaB signaling module: temporal control and selective gene activation. Science 2002, 298, 1241–1245, doi:10.1126/science.1071914.

27. Shih, V.F.-S.; Kearns, J.D.; Basak, S.; Savinova, O. V; Ghosh, G.; Hoffmann, A. Kinetic control of negative feedback regulators of NF-kappaB/RelA determines their pathogen- and cytokine-receptor signaling specificity. Proc. Natl. Acad. Sci. U. S. A. 2009, 106, 9619–9624, doi:10.1073/pnas.0812367106.

28. Rothenburg, S.; Seo, E.J.; Gibbs, J.S.; Dever, T.E.; Dittmar, K. Rapid evolution of protein kinase PKR alters sensitivity to viral inhibitors. Nat. Struct. Mol. Biol. 2009, 16, 63–70, doi:10.1038/nsmb.1529.

29. Park, C.; Peng, C.; Rahman, M.J.; Haller, S.L.; Tazi, L.; Brennan, G.; Rothenburg, S. Orthopoxvirus K3 orthologs show virus- and host-specific inhibition of the antiviral protein kinase PKR. PLoS Pathog. 2021, 17, e1009183, doi:10.1371/journal.ppat.1009183.

30. Wek, R.C.; Jiang, H.-Y.; Anthony, T.G. Coping with stress: eIF2 kinases and translational control. Biochem. Soc. Trans. 2006, 34, 7–11, doi:10.1042/BST20060007.

31. Sun, S.C.; Ganchi, P.A.; Ballard, D.W.; Greene, W.C. NF-kappa B controls expression of inhibitor I kappa B alpha: evidence for an inducible autoregulatory pathway. Science

1993, 259, 1912–1915, doi:10.1126/science.8096091.

32. Brown, K.; Park, S.; Kanno, T.; Franzoso, G.; Siebenlist, U. Mutual regulation of the transcriptional activator NF-kappa B and its inhibitor, I kappa B-alpha. Proc. Natl. Acad. Sci. U. S. A. 1993, 90, 2532–2536, doi:10.1073/pnas.90.6.2532.

33. Frey, T.R.; Lehmann, M.H.; Ryan, C.M.; Pizzorno, M.C.; Sutter, G.; Hersperger, A.R. Ectromelia virus accumulates less double-stranded RNA compared to vaccinia virus in BS-C-1 cells. Virology 2017, 509, 98–111, doi:10.1016/j.virol.2017.06.010.

34. Liu, S.-W.; Katsafanas, G.C.; Liu, R.; Wyatt, L.S.; Moss, B. Poxvirus decapping enzymes enhance virulence by preventing the accumulation of dsRNA and the induction of innate antiviral responses. Cell Host Microbe 2015, 17, 320–331, doi:10.1016/j.chom.2015.02.002.

35. Ramelot, T.A.; Cort, J.R.; Yee, A.A.; Liu, F.; Goshe, M.B.; Edwards, A.M.; Smith, R.D.; Arrowsmith, C.H.; Dever, T.E.; Kennedy, M.A. Myxoma virus immunomodulatory protein M156R is a structural mimic of eukaryotic translation initiation factor eIF2alpha. J. Mol. Biol. 2002, 322, 943–954, doi:10.1016/s0022-2836(02)00858-6.

36. Dar, A.C.; Dever, T.E.; Sicheri, F. Higher-order substrate recognition of eIF2alpha by the RNA-dependent protein kinase PKR. Cell 2005, 122, 887–900, doi:10.1016/j.cell.2005.06.044.

37. Kumar, A.; Haque, J.; Lacoste, J.; Hiscott, J.; Williams, B.R. Double-stranded RNA-dependent protein kinase activates transcription factor NF-kappa B by phosphorylating I kappa B. Proc. Natl. Acad. Sci. U. S. A. 1994, 91, 6288–6292, doi:10.1073/pnas.91.14.6288.

38. Koromilas, A.E.; Cantin, C.; Craig, A.W.; Jagus, R.; Hiscott, J.; Sonenberg, N. The

interferon-inducible protein kinase PKR modulates the transcriptional activation of immunoglobulin kappa gene. J. Biol. Chem. 1995, 270, 25426–25434, doi:10.1074/jbc.270.43.25426.

39. Zamanian-Daryoush, M.; Mogensen, T.H.; DiDonato, J.A.; Williams, B.R. NF-kappaB activation by double-stranded-RNA-activated protein kinase (PKR) is mediated through NF-kappaB-inducing kinase and IkappaB kinase. Mol. Cell. Biol. 2000, 20, 1278–1290, doi:10.1128/mcb.20.4.1278-1290.2000.

40. Gil, J.; Rullas, J.; García, M.A.; Alcamí, J.; Esteban, M. The catalytic activity of dsRNA-dependent protein kinase, PKR, is required for NF-kappaB activation. Oncogene 2001, 20, 385–394, doi:10.1038/sj.onc.1204109.

41. Bonnet, M.C.; Weil, R.; Dam, E.; Hovanessian, A.G.; Meurs, E.F. PKR stimulates NF-kappaB irrespective of its kinase function by interacting with the IkappaB kinase complex. Mol. Cell. Biol. 2000, 20, 4532–4542, doi:10.1128/mcb.20.13.4532-4542.2000.

42. Jiang, H.-Y.; Wek, S.A.; McGrath, B.C.; Scheuner, D.; Kaufman, R.J.; Cavener, D.R.; Wek, R.C. Phosphorylation of the Subunit of Eukaryotic Initiation Factor 2 Is Required for Activation of NF- B in Response to Diverse Cellular Stresses. Mol. Cell. Biol. 2003, 23, 5651–5663, doi:10.1128/mcb.23.16.5651-5663.2003.

43. Jiang, H.-Y.; Wek, R.C. GCN2 phosphorylation of eIF2alpha activates NF-kappaB in response to UV irradiation. Biochem. J. 2005, 385, 371–380, doi:10.1042/BJ20041164.

44. Dennehy, J.J. Evolutionary ecology of virus emergence. Ann. N. Y. Acad. Sci. 2017, 1389, 124–146, doi:10.1111/nyas.13304.

45. FENNER, F.; WOODROOFE, G.M. The pathogenesis of infectious myxomatosis; the mechanism of infection and the immunological response in the European rabbit

(Oryctolagus cuniculus). Br. J. Exp. Pathol. 1953, 34, 400–411.

46. Leick, M.; Azcutia, V.; Newton, G.; Luscinskas, F.W. Leukocyte recruitment in inflammation: basic concepts and new mechanistic insights based on new models and microscopic imaging technologies. Cell Tissue Res. 2014, 355, 647–656, doi:10.1007/s00441-014-1809-9.

47. Bevilacqua, M.P.; Gimbrone, M.A.J. Inducible endothelial functions in inflammation and coagulation. Semin. Thromb. Hemost. 1987, 13, 425–433, doi:10.1055/s-2007-1003519.

48. Carpentier, K.S.; Esparo, N.M.; Child, S.J.; Geballe, A.P. A Single Amino Acid Dictates Protein Kinase R Susceptibility to Unrelated Viral Antagonists. PLoS Pathog. 2016, 12, e1005966, doi:10.1371/journal.ppat.1005966.

49. Rothenburg, S.; Chinchar, V.G.; Dever, T.E. Characterization of a ranavirus inhibitor of the antiviral protein kinase PKR. BMC Microbiol. 2011, 11, 56, doi:10.1186/1471-2180-11-56.

50. Krüll, M.; Klucken, A.C.; Wuppermann, F.N.; Fuhrmann, O.; Magerl, C.; Seybold, J.; Hippenstiel, S.; Hegemann, J.H.; Jantos, C.A.; Suttorp, N. Signal transduction pathways activated in endothelial cells following infection with Chlamydia pneumoniae. J. Immunol. 1999, 162, 4834–4841.

51. Kuhen, K.L.; Samuel, C.E. Isolation of the interferon-inducible RNA-dependent protein kinase Pkr promoter and identification of a novel DNA element within the 5'-flanking region of human and mouse Pkr genes. Virology 1997, 227, 119–130, doi:10.1006/viro.1996.8306.

52. Zhang, P.; Jacobs, B.L.; Samuel, C.E. Loss of Protein Kinase PKR Expression in Human HeLa Cells Complements the Vaccinia Virus E3L Deletion Mutant Phenotype by

Restoration of Viral Protein Synthesis. J. Virol. 2008, 82, 840–848, doi:10.1128/jvi.01891-07.

53. Liu, R.; Moss, B. Opposing Roles of Double-Stranded RNA Effector Pathways and Viral Defense Proteins Revealed with CRISPR-Cas9 Knockout Cell Lines and Vaccinia Virus Mutants. J. Virol. 2016, 90, 7864–7879, doi:10.1128/JVI.00869-16.

54. Rahman, M.M.; Liu, J.; Chan, W.M.; Rothenburg, S.; McFadden, G. Myxoma virus protein M029 is a dual function immunomodulator that inhibits PKR and also conscripts RHA/DHX9 to promote expanded host tropism and viral replication. PLoS Pathog. 2013, 9, e1003465, doi:10.1371/journal.ppat.1003465.

Chapter 3-PKR-regulated proinflammatory responses are antagonized by K3 orthologs from poxviruses

Huibin Yu[1], Chen Peng[2], Ryan C. Bruneau[1], Jeannine Nicole Stroup[1], Greg Brennan[1], Stefan Rothenburg[1*]

[1]Department of Medical Microbiology and Immunology, School of Medicine, University of California, Davis 95618, USA

[2]Key Laboratory of Animal Epidemiology and Zoonosis, College of Veterinary Medicine, China Agricultural University, Beijing 100193, China

*To whom correspondence should be addressed

Stefan Rothenburg

Email: rothenburg@ucdavis.edu. ORCID iD:0000-0002-2525-8230

Abstract

Protein kinase R (PKR), an interferon (IFN)-inducible gene product, is a major antiviral protein and an important host restriction factor, which also plays an essential role in the mediation of IFN responses and NF-κB activities. PKR has been described to be involved in the regulation of NF-κB activities using different mechanisms. The regulation of NF-κB activities from different species and potential regulation of PKR associated NF-κB activities by poxviruses immunomodulatory protein, K3 orthologs, are still largely unknown. Here we successfully knocked out rabbit PKR in RK13 cells using CRISPR-Cas9 technology and found that the replication of MYXVΔM029LΔM156R, which lacks both PKR inhibitors, was significantly increased in RK13-PKR^{ko} cells when compared to that in RK13 wild type cells. Additionally, knockout of PKRs from different human cell lines significantly facilitated the replication of MYXVΔM029LΔM156R, indicating the antiviral functions of those PKRs during MYXV infection. In HeLa and A549 cells, the antiviral effect of PKR was associated with its autophosphorylation at the residue Thr446. During MYXV infection, the absence of PKR significantly reduced NF-κB dependent TNFα and IL-6 transcripts, while complementation of either human PKR or rabbit PKR in PKR knock out cell lines restored and increased transcriptional levels of TNFα and IL-6 genes. Furthermore, we tested PKRs from 17 mammalian species for their regulatory role in transient transfection assays. Along with PKR mediated translational inhibition, they all upregulated ATF4 responses and NF-κB transcriptional activities. K3 ortholog M156, increased its inhibition on brush rabbit PKR when compared to E. rabbit PKR, which dependents on helix αG region. Swapping four amino acids of helix αG region from European rabbit PKR to brush rabbit PKR reduced PKR inhibition by M156, resulting in increased ATF4 responses and NF-κB activation correspondingly.

Additionally, four tested K3 orthologs from other different poxviruses were shown to highly inhibit both human PKR and rabbit PKR, and high inhibition of PKRs by those K3 orthologs significantly reduced NF-κB activation. Taken together, these results demonstrate that dual regulatory functions of PKRs from different species, antiviral function and NF-κB regulatory function. Poxviruses K3 orthologs antagonize PKR activation and therefore regulate PKR-associated ATF4 response and NF-κB transcriptional activities.

Keywords: poxviruses; myxoma virus; K3; PKR; NF-κB; ATF4; inflammatory responses;

Introduction

Interferon (IFN) production plays an essential role in antiviral defenses of mammalian cells and, subsequently, induces the upregulation of IFN-stimulated genes (ISGs). Among those gene products, dsRNA-dependent protein kinase R (PKR) is an antiviral protein, which serves as a pattern recognition receptor for the recognition of double-strand RNA (dsRNA) generated as a byproduct during viral transcription and replication [1,2]. After binding to dsRNA, activated and phosphorylated PKR halts protein synthesis by phosphorylating the α subunit of the translation initiation factor (eIF2) at residue serine 51 [3,4]. eIF2α phosphorylation enables the cell to regulate the translation rate of cellular or viral mRNAs and adjust to rapid changes in the cellular environment. As a node for translational control, eIF2α phosphorylation has been suggested as a mechanism linking NF-κB activation in response to diverse stress conditions, such as ER stress, amino acid starvation, and UV irradiation [5–7]. In addition, eIF2α phosphorylation preferentially increases the translation of selected genes, such as activating transcription factor 4 (ATF4), which is a transcriptional activator and regulator during the integrated stress response (ISR) [8,9]. The eIF2α/ATF4 axis paly an essential role in the regulation of cellular homeostasis and cellular recovery during different environmental stresses, including virus infection [10]. The crosstalk between PKR/eIF2α/ATF4 pathway and other signaling pathways, such as NF-κB pathway, are still not well understood. It has been reported that there are both PKR kinase-dependent and kinase-independent NF-κB activation mechanisms, perhaps due to differences of assay systems [11,12].

Nuclear factor kappa B (NF-κB) is a rapid response transcription factor and plays a key role in regulating the inflammatory, innate and adaptive immune responses in mammals [13,14]. Under

resting conditions, NF-κB is held in a latent form by binding with the short-lived inhibitor IκBα in the cytoplasm. Upon activation by viral infection or stimulation with inflammatory stimuli, degradation of IκBα can be initiated and released NF-κB dimers then translocate to the nucleus where they induce transcription of numerous target genes, including the NFKBIA gene, which encodes IκBα, and pro-inflammatory genes, such as tumor necrosis factor alpha (TNFα), Interleukin (IL)-1, IL-6 and IL-8 [15,16]. Once the resolution of the stimulus is achieved, transcriptional activation of new IκBα synthesis acts as a tight negative feedback loop to reset the latent state of NF-κB in a timely manner [17,18]. Appropriate inflammatory response and sufficient cytokine production are important to eliminate of the pathogens. As a result of NF-κB's importance for host health, The NF-κB pathway is often targeted for inhibition as a key player in the battle between host and pathogen.

Poxviruses are a family of large double-stranded DNA viruses. As a result of antiviral selective pressures, most members of *chordopoxvirinae* subfamily have evolved to encode viral antagonists targeting the PKR-eIF2α phosphorylation pathway. One member of the *Leporipoxviruses* genus of note is Myxoma virus (MYXV), which encodes two PKR antagonists M029 and M156, orthologs of vaccinia virus (VACV) E3 and K3, respectively [19,20]. MYXV M029 and VACV E3 bind viral dsRNA and prevent PKR dimerization and activation [21]. MYXV M156 and VACV K3 are structural mimics of eIF2α. These viral pseudosubstrate inhibitors can compete with eIF2α for PKR binding to reduce eIF2α phosphorylation, allowing protein synthesis to continue [22–24]. Additionally, M156 has been reported as a species-specific inhibitor for European rabbit PKR [20].

In the present study, we successfully generated rabbit PKR knock out RK13 cells using the CRISPR/Cas9 system. Knock out rabbit PKR enhanced the replication of MYXV lacking PKR inhibitors in RK13 cells. Activation of PKRs from different species resulted in inhibition of MYXV replication and the antiviral effects of PKR dependent on its autophosphorylation. Following with inhibition of MYXV infection exerted by PKR, increased TNFα and IL-6 responses at the transcriptional level were detected. 17 tested PKRs from different species upregulated the transcriptional level of proinflammatory cytokines in transient transfection assay. Additionally, ATF4 expression was significantly upregulated following PKR mediated protein synthesis inhibition, which indirectly reflected the eIF2α phosphorylation after PKR activation. We provide evidence showing that human PKR and rabbit PKR are highly antagonized by K3 orthologs from four tested poxviruses, including raccoonpox virus (RCPV), sheeppox virus (SPPV), skunkpox virus (SKPV), and camelpox virus (CMLV). Generally, high inhibition of PKRs by those K3 orthologs significantly reduced NF-κB activation.

Results

Generation of rabbit PKR knockout RK13 cells using RNA-programmable CRISPR-Cas9 technology

The clustered regularly interspaced short palindromic repeat-Cas9 (CRISPR-Cas9) technology originates from type II CRISPR-Cas systems, which provide bacteria with adaptive immunity to viruses and plasmids [25,26]. It has been widely used to modify genes in model systems including animal zygotes and other cells [27]. The CRISPR-associated protein Cas9 is an endonuclease that uses a guide sequence (termed guide RNA or gRNA) that is formed from an RNA duplex consisting of tracrRNA which acts a binding scaffold for the CAS nuclease and crRNA which binds to the target site, enabling Cas9 to introduce a site-specific double-strand break (DSBs) in the DNA [28]. DSBs can be repaired by either non-homologous end joining (NHEJ), or homologous recombination directed repair (HDR), resulting in indels or precise repair, respectively [29,30].

To investigate the role of European rabbit (*Oryctolagus cuniculus*) PKR during MYXV infection, we first knocked out European rabbit PKR in RK13 cells using the CRISPR-Cas9 system. The rabbit PKR gene is located on chromosome 2 and has 16 exons, including 1 non-coding exon and 15 coding exons (Fig. 3.6A). Using online tools developed by chopchop (http://chopchop.cbu.uib.no/#), we designed and generated gRNA that targeted coding exon 2 of rabbit PKR (Fig. 3.1A). The Cas9 nuclease with gRNA was co-transfected into cells using Lipofectamine CRISPRMAX protein transfection reagent (Invitrogen). After 48 hours of incubation, single cells were isolated to allow single-colony formation. After 14 days of culturing, we used VC-R4 infection for pre-screening of potential positive clones, VC-R4 lacking K3L and E3L could replicate in potential PKR deficient cells and express eGFP as

selection marker. Then, we extracted genomic DNA from potential positive clones for PCR amplification of the target region. The PCR products were subsequently subcloned for sequence analysis to determine the integrity of the rabbit PKR gene, we found either 1 bp deletion or 2 bp insertion within two alleles, resulting in a frame-shift event and premature stop codon (Fig. 3.1A and 3.1B). Western blot analysis showed that rabbit PKR was knocked out successfully in these RK13-PKR^{ko} cells (Fig. 3.1C). Rabbit PKR expression was not detected in the RK13-PKR^{ko} cells even after treatment with type I IFN, which increased the rabbit PKR expression in RK13 wild type cells (Fig. 3.1D). Overall, we successfully generated RK13-PKR^{ko} cells using the CRISPR-Cas9 system.

Knock out of rabbit PKR facilitates the replication of MYXV lacking PKR inhibitors

To directly test the antiviral effect of rabbit PKR from European rabbits (*Oryctolagus cuniculus*) in limiting the growth of MYXV, RK13-WT, RK13-PKR^{ko}, and RK13+E3L+K3L cells, the latter of which constitutively express VACV E3 and K3, were infected with MYXVΔM029LΔM156R at MOI of 1 for 48 hours. MYXVΔM029LΔM156R is devoid of both PKR inhibitors M029 and M156 and expresses EGFP under the control of a synthetic early/late poxvirus promoter. At 48 hours post infection (hpi), the replication of MYXVΔM029LΔM156R was observed as reflected by EGFP expression. E3 and K3 from VACV have been reported to inhibit the rabbit PKR in single luciferase assays (unpublished data) [20,31]. EGFP fluorescence was observed in both RK13-PKR^{ko} and RK13+E3L+K3L cells, but not in RK13-WT cells, indicating either PKR deficiency or inhibition of PKR activation is essential for MYXV replication (Fig. 3.2B).

Next, multi-step replication curves were performed to assess viral replication. Wild type RK13, RK13-PKR^{ko}, and RK13+E3L+K3L cells were infected with MYXVΔM029LΔM156R at an

MOI of 0.1, and then the cells were collected at 2, 12, 24, and 48 hpi. The virus titers were determined in triplicate following serial dilutions on RK13-PKR^{ko} cells (Fig. 3.2C). The results showed that knock out of rabbit PKR rescued the replication of MYXVΔM029LΔM156R in the RK13-PKR^{ko} cells when compared to that in RK13-WT cells. Additionally, the replication of MYXVΔM029LΔM156R increased in the RK13 cells expressing K3 and E3 when compared to that in RK13-PKR^{ko} cells.

Antiviral effect of PKRs from different species on the infection of MYXVΔM029LΔM156R

To characterize whether PKR from other species plays an essential role in the restriction of MYXVΔM029LΔM156R replication, we tested the antiviral effect of human PKR from different human cell lines. Human PKR was previously knocked out in HeLa and A549 cells human cell lines, including, as described before [32,33]. HeLa wild type, and HeLa-PKR^{ko} cells, or A549-RNaseL^{ko}, and A549-RNaseL^{ko}PKR^{ko} were infected with MYXVΔM029LΔM156R to analyze if knock out human PKR allows MYXV replication. After 36 hpi, green fluorescence was observed in HeLa-PKR^{ko} and A549-RNaseL^{ko}PKR^{ko} cells, whereas the expression of EGFP was strongly suppressed in HeLa wild type and A549-RNaseL^{ko} cells, which contain intact human PKR genes (Fig. 3.3A and 3.4A). These results demonstrate that human PKR restricts replication of MYXV, which lacks PKR inhibitors.

To test whether human PKR was activated during early MYXV infection, we directly measured the phosphorylation level of PKR using Western blot assays in HeLa-wild type, HeLa-PKR^{ko}, A549-RNaseL^{ko} and A549-RNaseL^{ko}PKR^{ko} cells following infection with MYXVΔM029LΔM156R. In the MYXV infected cells, phosphorylation of PKR was detected in HeLa-wild type and A549-RNaseL^{ko} cells at 12 hours post infection (Fig. 3.3B and 3.4B). In contrast, PKR phosphorylation was not detectable in HeLa-PKR^{ko} and A549-RNaseL^{ko}PKR^{ko}

cells. β-Actin was used as an internal gel-loading control and was detected at a similar level for all lanes.

In order to directly compare the effects of E. rabbit and human PKR during infection, we made congenic RK13 cells, which are based on RK13-PKR^{ko} cells, which we stably transfected with plasmid constructs for either E. rabbit PKR or human PKR. The constructs contain the human PKR promoter, which drives the expression of PKRs, followed by the rabbit β-globin intron and a multiple cloning site, into which we inserted E. rabbit PKR or human PKR gene. RK13-PKR^{ko} cells were stably transfected with the empty vector or plasmids expressing either PKR were subsequently sub-cloned cloned. For subsequent experiments, human PKR expressing clone (h3) and rabbit PKR expressing clone (r10) were chosen since they exhibited similar inhibitory ability to inhibit the eGFP expression during viral infection selection. We infected RK13 wild type cells, as well as RK13-PKR^{ko} cells that were stably transfected with vector, human, or rabbit PKR with MYXVΔM029LΔM156R expressing EGFP at an MOI of 1 for 36 hours. In RK13 wild type cells, there was no MYXV-EGFP expression indicating that rabbit PKR suppressed viral replication. EGFP was detected in RK13-PKR^{ko} vector control cells, whereas it was strongly suppressed in RK13-PKR^{ko} cells expressing human or E. rabbit PKR (Fig. 3.5). Those results indicated that the complementation of PKRs in RK13 cells suppressed MYXV replication.

PKR associated pro-inflammatory responses during MYXV infection

In addition to its established role in restricting viral replication, PKR has also been implicated as a component in the regulation of inflammation and immune responses through several signaling pathways [34–36]. Previous studies suggested the involvement of PKR in activating NF-κB signaling pathways [5]. As a pivotal mediator of inflammatory responses, NF-κB activation

triggers up-regulation of pro-inflammatory cytokines such as TNFα, IL-6 and IL-1β in response to different stimuli [16]. To examine whether human PKR could induce NF-κB activities in HeLa cells during MYXV infection, HeLa-wild type and HeLa-PKR^{ko} cells were assayed for NF-κB dependent pro-inflammatory responses, including TNFα and IL-6 induction after MYXVΔM029LΔM156R infection. At 12 hours post infection, the cell lysates were collected and subjected to qRT-PCR for measuring TNFα and IL-6 transcripts. Whereas we detected transcriptional upregulation of TNFα and IL-6 after infection of MYXVΔM029LΔM156R in the HeLa-PKR^{ko} cells compared with mock infection control, the transcription of both TNFα and IL-6 was substantially upregulated in the presence of PKR when compared with that in PKR deficient cells (Fig. 3.6). These results indicate the requirement of PKR activation for full induction of TNFα and IL-6 transcripts during MYXV infection.

To further determine whether E. rabbit PKR and human PKR induce comparable NF-κB activation, HeLa-PKR^{kd} cells expressing empty vector or FLAG-tagged PKRs from the two species, were infected with MYXVΔM029LΔM156R [20]. Western blot showed comparable expression of human PKR and E. rabbit PKR (Fig. 3.7A). Then we infected HeLa-PKR^{kd} cells expressing empty vector, human PKR, or E. rabbit PKR with MYXVΔM029LΔM156R at an MOI of 3 for 12 hours, RNAs were extracted from infected cells and subjected to RT-qPCR for analyzing TNFα and IL-6 responses. Infection of HeLa-PKR^{kd} cells expressing empty vector with MYXVΔM029LΔM156R upregulated the TNFα and IL-6 when compared to mock infected control, while stable expression of either human PKR or rabbit PKR significantly increased TNFα and IL-6 transcripts in HeLa-PKR^{kd} cells (Fig. 3.7B and 3.7C). These results show that

both tested PKR can induce NF-κB-dependent pro-inflammatory gene expression upon MYXV infection.

Activation of PKRs from different species regulates ATF4 and NF-κB signaling pathways in transient transfection assays

To test global protein synthesis inhibition by PKRs from other species, we used a single luciferase assay to monitor the translational level of the luciferase reporter. In this assay, HeLa-PKR^{ko} cells are transiently co-transfected with plasmids encoding a luciferase reporter, and PKR for 48 hours. With the activation of PKR during transient transfection, luciferase expression is strongly reduced due to PKR mediated translational inhibition. First, we tested PKRs from the following 17 different mammalian species: human (Homo sapiens), orangutan (Pongo borneo), gibbon (Hylobates leucogenys), Rhesus macaque (Macaca mulatta), tamarin (Saguinus labiatus), mouse (Mus musculus), brown rat (Rattus norvegicus), Syrian hamster (Mesocricetus auratus), Guinea pig (Cavia porcellus), European rabbit (Oryctolagus cuniculus), cat (Felis catus), dog (Canis lupus), horse (Equus caballus), pig (Sus scrofa), cow (Bos Taurus), camel (Camelus dromedaries), sheep (Ovis aries). We observed that transfection of PKRs from all tested species significantly reduced the translation of the luciferase reporter, suggesting PKRs exerted a similar inhibition protein synthesis inhibition (Fig. 3.8). After PKR activation, phosphorylation of eIF2α inhibits global protein synthesis, however, it was also reported to coincidently promote preferential translation of a subset of transcripts, including those that contain inhibitory upstream open reading frames (uORF) such as activating transcription factor 4 (ATF4) in response to different environmental stresses [37,38]. Next, we measured ATF4 responses after PKR transfection utilizing an ATF4-dual luciferase assay, which can indirectly reflect the levels of PKR dependent eIF2α phosphorylation [8]. Transient transfection of PKRs from different

species resulted in significant activation of ATF4-uORF-containing reporter. (Fig. 3.9A). This result indicates that the tested PKRs have a similar function in the upregulation of ATF4. Because PKR has also been involved in the regulation of NF-κB activities, we further tested NF-κB dependent pro-inflammatory responses after PKR activation using qRT-PCR. All tested PKRs lead to upregulation of TNFα and IL-6 transcripts at the transcriptional level (Fig. 3.10A and 3.10B). Additionally, activation PKRs also upregulate the transcriptional levels of IκBα, which is an inhibitor of the NF-κB pathway and is essential for the regulation and recovery of NF-κB homeostasis. All those results indicate that PKRs from 17 tested different species induced ATF4 responses and also the NF-κB dependent signaling pathway.

The levels of PKR inhibition by M156 affect ATF4 and NF-κB activities

K3 orthologs have been reported to target the PKRs in a species-specific manner, including M156 from MYXV [20,24,31,39]. To extend our research to rabbit cells, we utilized the RK13-PKR^{ko} cell line to study the inhibition of E. rabbit PKR by M156 using a single luciferase assay. RK13-PKR^{ko} cells were co-transfected with rabbit PKR and an increasing amount of M156R, we found M156 inhibits E. rabbit PKR in a dose dependent manner (Fig. 3.12). We further confirmed that MYXV M156 showed higher inhibition on PKR from the natural host, brush rabbit, than that on PKR from E. rabbit (Fig. 3.13B).

To further identify which amino acids in rabbits PKRs are responsible for their differential sensitivity to M156 inhibition, we concentrated on helix αG, which directly contacts eIF2α [40]. Residues in helix αG have been previously shown to influence PKR sensitivity to K3 [41–43]. Four amino acid residues differ between E. rabbit and brush rabbit PKR in helix αG (Fig. 3.13A). We exchanged these four residues in between the two PKRs and measured the

sensitivities of the mutants to M156 using the single luciferase assay (Fig. 3.13B). We found that swapping of four aa residues between European rabbit PKR and brush rabbit PKR did not affect the level of translational inhibition, indicating that mutations in helix αG regions of PKRs did not impact PKR mediated phosphorylation of eIF2α. The European rabbit PKR quad. Mutant showed increased susceptibility to M156 inhibition, which was comparable to that of brush rabbit PKR. Conversely, the brush rabbit PKR quad. mutant showed reduced sensitivity to M156, which was comparable to E. rabbit PKR (Fig. 3.13B). These results suggest that these four residues, either alone or in combinations with one another, within the helix αG region of rabbit PKR contribute to the differential sensitives to inhibition by M156.

After supporting the hypothesis that activation of PKRs affects the ATF4 and NF-κB activities. Next, we tested whether swapping the four residues of helix αG region between European and brush rabbit PKRs could alter ATF4 and NF-κB responses in the transient transfection assay. ATF4 responses (ATF4 firefly Luc/TK renilla-Luc ratios) were normalized to the empty vector transfection group. M156-mediated PKR inhibition significantly reduced ATF4 reporter activities when compared to the PKR transfection only group. Importantly, higher inhibition of brush rabbit PKR by M156 correlated with a further reduction of ATF4 activity compared to moderate inhibition of European rabbit PKR by M156, whereas swapping of the four residues in helix αG reversed the ATF4 response (Fig. 3.14A). We further tested whether alteration of the inhibitory sensitivities of PKR mutants by M156 changes NF-κB activation. In consistent with the results as showed in chapter 2, co-transfection of M156R with brush rabbit PKR substantially reduced NF-κB activity compared to that with European rabbit PKR (Fig. 3.14B). Additionally, co-transfection of M156R with European rabbit PKR quad. mutant containing helix αG residues

from brush rabbit PKR caused reduced NF-κB induction compared to that with European rabbit PKR wild type, while reduced inhibition of the brush rabbit PKR quad. mutant by M156 significantly augmented NF-κB activity (Fig. 3.14B). These data demonstrated that M156 showed higher inhibition of brush rabbit PKR than that of European rabbit PKR, resulting in reduced ATF4 and NF-κB responses and swapping of four residues of helix αG between two PKR reversed the patterns.

High inhibition of PKRs by other K3 orthologs reduces NF-κB activation

To extend our study, we further investigated the inhibition of rabbit or human PKR by K3 orthologs from other four tested poxviruses in the single luciferase assay, including raccoonpox virus (RCPV), skunkpox virus (SKPV), sheeppox virus (SPPV), camelpox virus (CMLV). These K3 orthologs are highly diverse from different poxvirus genera and display as low as 31.7 % sequence identity with one another. Specifically, K3 ortholog from RCPV displays 73.2%, 31.7%, 61.0% sequence identity with that from SKPV, SPPV, and CMLV respectively. SKPV K3 ortholog is 32.9%, 65.9% identical to K3 orthologs from SPPV and CMLV respectively. SPPV K3 has 35.7% sequence identity with K3 from CMLV. We found that four tested K3 orthologs from RCPV, SKPV, SPPV, CMLV showed high inhibition on both human PKR and rabbit PKR (Fig. 3.15A and 3.15B). Next, we tested NF-κB activation following high inhibition of PKRs by these K3 orthologs using the NF-κB reporter assay. The NF-κB promoter assay showed that high inhibition of human PKR or rabbit PKR by K3 orthologs substantially reduced NF-κB activation (Fig. 3.15C and 3.15D).

Discussion

Activation of PKR-eIF2α pathway not only suppresses general translation but also influences the regulation of other signaling pathways, such as NF-κB, inflammation, and IFN responses, via different mechanisms [11,34,44]. K3 orthologs are encoded by diverse poxviruses to antagonize PKR activities. To date, a systematic investigation of other regulatory roles of PKRs from different species are lacking. Also, whether K3 orthologs antagonize the PKR-associated NF-κB activation and which residues within PKR are responsible for regulated NF-κB responses by K3 ortholog are still unknown. In addition to showing that the PKRs from different species play essential roles in restricting replication of MYXV lacking PKR inhibitors, we demonstrated that MYXV infection induced PKR activation and upregulated transcription of pro-inflammatory genes, including TNFα and IL-6 (figure 3.7). In a transient transfection assay, activation of PKRs from 17 tested species resulted in increased expression of a reporter gene containing the 5' region of the untranslated region of the mouse ATF4 mRNA and NF-κB transcriptional activities. PKR associated NF-κB activation was suppressed by PKR antagonists (K3 orthologs) from diverse poxviruses. Importantly, our findings highlight the multiple functions of PKR activation during MYXV infection and illustrate regulatory functions of K3 orthologs for the PKR-regulated NF-κB signaling pathway.

It has been reported that MYXV lacking two PKR inhibitors, M029L and M156R, showed a severe replication defect in RK13 cells [20]. However, there was no direct evidence to show whether endogenous rabbit PKR plays major role in this restriction of MYXV replication in RK13 cells. The generated RK13-PKR^{ko} cells can be used as a good tool to directly investigate the antiviral function of endogenous PKR. They also allow us to test directly the relevance of

rabbit PKR by viral inhibitors in cells more relevant to natural MYXV infections. To the best of our knowledge, this is the first study generating rabbit PKR knock out cells using the CRISPR/Cas9 system. Absence of endogenous PKR in RK13-PKR^{ko} cells rescued the replication of MYXVΔM029LΔM156R, and thus provides direct evidence for the involvement of rabbit PKR in restricting MYXV replication. Additionally, stable expression of both VACV E3 and K3, which have the ability to inhibit European rabbit PKR (chapter 2 and unpublished data) [20], also facilitated MYXVΔM029LΔM156R's replication in RK13 cells, suggesting that endogenous rabbit PKR was inhibited in the presence of E3 and K3 inhibitors. Of note, MYXV infection formed larger focus sizes in RK13+K3L+E3L cells than that in RK13-PKR^{ko} cells, thus, K3 or E3 may target additional antiviral host proteins in addition to PKR (figure 3.2). Viral protein synthesis has been shown to be inhibited in MYXVΔM029LΔM156R infected RK13 cells compared to wild type MYXV infected RK13 cells, and phosphorylation of PKR and resulting translational inhibition may contribute to this diminished production of viral proteins [20]. In HeLa and A549 cells, restricted MYXV replication correlated with increased PKR phosphorylation (figure 3.3 and 3.4). This may lead to halted viral protein synthesis.

In addition to PKR, activation of other kinases, such as HRI, GCN2 and PERK, results in eIF2α phosphorylation in response to diverse stimuli [45–49]. These eIF2α kinases suppress protein synthesis from most mRNAs through phosphorylation of eIF2α but selectively upregulate translation of the transcription factor ATF4, resulting in downstream gene expression reprogramming [50,51]. Specifically, PKR is required for ATF4 expression after poly (I:C) stimulation [52]. HRI activates the ATF4 stress response pathway for adaptation to oxidative stress [53,54]. Knock out GCN2 impairs ATF4 accumulation during amino acid deprivation, and PERK is required for ATF4 induction during ER stress [9,54]. These studies highlight the

important role of the eIF2α kinase-eIF2α-ATF4 pathway during integrated stress responses, including virus infection. The results from the transient transfection assay shown here demonstrated the involvement of PKR in eIF2α phosphorylation mediated translation inhibition and corresponding ATF4 induction. The 17 tested PKRs from different species showed similar abilities to inhibit the translation of a luciferase reporter and to upregulate the ATF4 reporter. A negative correlation between PKR mediated translation inhibition and ATF4 reporter induction was observed as expected. Our results suggest that upregulated translation of the ATF4 reporter may serve as a good indirect indicator for the level of eIF2α phosphorylation after PKR activation.

eIF2α phosphorylation mediated translation repression has been reported to activate NF-κB signaling pathways through affecting the protein synthesis of IκBα [5,6]. For instance, GCN2 or PERK dependent eIF2α phosphorylation was critical for decreased levels of IκBα in response to UV irradiation [7,55] and IKK complex mediated IκBα phosphorylation was not responsible for the increased IκBα turnover [56,57]. During VACV infection, PKR phosphorylation activates NF-κB, and the catalytic activity of PKR is necessary for NF-κB activation instead of protein-protein interaction of PKR with the IKK complex [11,58]. Other studies showed that inhibition of the PKR catalytic activity by an inhibitor, 2-aminopurine, abolished the PKR induced NF-κB activation [59–61]. The important role of kinase-dependent translational suppression in NF-κB activation was highlighted in those studies. Here we show that the transient transfection of PKRs from different species initiated NF-κB dependent transcriptional activities. Following MYXVΔM029LΔM156R infection, PKR-dependent NF-κB transcriptional activities were also observed, including upregulation of TNFα and IL-6 transcripts. dsRNA, a byproduct during

MYXV infection, may play major role in PKR phosphorylation and then NF-κB activation. As a critical node for linking PKR kinase and NF-κB signaling, eIF2α phosphorylation is upregulated as indirectly reflected by ATF4 reporter results following transient transfection of PKR, consistent with other research that showed upregulation of negative feedback regulator IκBα in response to diverse NF-κB activators, such as TNF and LPS [62–65], we also detected PKR-dependent upregulation of IκBα transcripts. Considering the PKR-mediated translational inhibition, the protein synthesis of IκBα transcripts may be limited or but help replenish IκBα once eIF2a phosphorylation subsided.

As poxvirus immunomodulators, K3 orthologs share a few conserved residues within the S1 domain of eIF2α, which interacts with PKR [23,41]. PKRs from European rabbits and brush rabbit share 93% sequence identity at the protein level. M156 evolved to highly inhibit PKR from its natural brush rabbit host, whereas European rabbit PKR was sub-optimally inhibited by M156 as tested in RK13-PKR^{ko} cells. Given that the helix αG region of PKR is essential for eIF2α binding and M156 competes with eIF2α for PKR binding, helix αG of rabbit PKR may serve as a key region for determining the sensitivity of PKR to M156 inhibition. We showed that 4 amino acids of rabbit PKRs, which map to the helix αG region of the PKR kinase domain are responsible for the sensitivity of M156 inhibition. Our result is also consistent with other research that demonstrated that mutations in the helix αG region of PKR confer resistance to K3 inhibition [66]. If PKR-eIF2α phosphorylation is responsible for NF-κB activities, we would expect that K3 orthologs could regulate NF-κB through affecting PKR activation. High inhibition of brush rabbit PKR by M156 significantly reduced NF-κB activation, while swapping of 4 residues from European rabbit PKR to brush rabbit PKR increased ATF4 responses and NF-

κB activation after M156 inhibition. Additionally, other 4 tested K3 from different poxviruses also diminished the NF-κB activation correlated with high inhibition on PKR from human and rabbit species. Therefore, the levels of PKR inhibition by K3 affect ATF4 responses and NF-κB activities. Poxviruses might employ this regulatory function for infection progression and pathogenesis in vivo. This interplay between PKR activation, NF-κB activity, and viral antagonists of PKR associated signaling pathways may indicate the importance of these interactions in infection progression and its pathogenesis in vivo, an area of research need to be explored further.

Materials and methods

Cells, viruses, and antibodies

HeLa cells, HeLa-PKR^{ko} cells, A549 cells, A549-RNaseL^{ko} cells and A549-RNaseL^{ko}PKR^{ko} cells [33], RK13 cells, and RK13 PKR^{ko} cells were cultured in Dulbecco's Modified Eagle's Medium (DMEM) supplemented with 2mML-glutamine, 100 IU/ml penicillin/streptomycin (Gibco), and 5 % heat-inactivated fetal bovine serum (FBS). HeLa-PKR^{kd} and HeLa-PKR^{ko} cells expressing human PKR or E. rabbit PKR were generated as described previously [20,67]. HeLa-PKR^{KD} cells were maintained in media additionally supplemented with 1 μg/ml puromycin (Sigma). RK13+E3L+K3L cells were maintained in media supplemented with 500 μg/ml geneticin (G418) and 300 μg/ml zeocin (Life Technologies). All cells were grown at 37°C in an incubator containing 5% CO_2. MYXVΔM029LΔM156R was described before (CITATION) and propagated in RK13+E3L+K3L cells. The mouse anti-Flag monoclonal antibody (mAb) and the mouse anti-β-Actin mAb (A1978) were purchased from Sigma. The mouse anti-PKR B10 polyclonal antibody (Sc-6282) was purchased from Santa Cruz Biotechnology. The rabbit anti-PKR (phosphor T446) mAb (ab32036) was purchased from Abcam.

Plasmids

As described before, PKR from different mammalian species and K3L orthologs genes were cloned into the pSG5 vector (Stratagene) for transient expression in the indicated cell lines [20,31]. The NF-κB reporter plasmid contains a firefly luciferase gene driven by six NF-κB binding sites followed by a minimal beta-globin promoter [68]. The ATF4 reporter plasmid contains a firefly luciferase gene driven by a full-length mouse ATF4 mRNA leader sequence [8]. The renilla luciferase vector was driven by the TK promoter. Site-directed mutagenesis PCR was used to generate E. rabbit and brush rabbit quadruple-mutant PKR containing the swapped

helix αG region. pSG5-European rabbit PKR and pSG5-brush rabbit PKR were used as templates for PCR amplification by Pfu Ultra High-Fidelity DNA polymerase (Invitrogen). The PCR primers contain the designed mutations flanked by 15 nucleotides identical to the template up- and downstream of the mutation. All open reading frames were sequenced to confirm correct sequences.

Generation of RK13 PKR knock-out (KO) cell lines using CRISPR-Cas9 technology

CRISPR-Cas 9 system was used to knock out PKR in RK13 cells (European rabbit kidney cells). Targeting sequences were chosen using online tools developed by chopchop (http://chopchop.cbu.uib.no/#). The exon 2 of rabbit PKR was targeted for knockout and gRNA PKR-ATCATGAACTGCCCCAGTCG was used. The gRNA was generated using the TrueGuide Synthetic gRNA service (Invitrogen) in a 2-piece modified (TrueGuide crRNA:tracrRNA) format. TrueCut Cas9 Protein v2 was purchased from Invitrogen and used for genome editing. The Cas9 protein was co-transfected with gRNA into RK13 cells using Lipofectamine CRISPRMAX protein transfection reagent (Invitrogen). At 48 hours post transfection, single cells were isolated to allow single-colony formation. Aliquots of individual colonies were collected and screening for their ability to permit VC-R4 infection. VC-R4 lacks both PKR antagonists K3L and E3L and expresses EGFP from the E3L locus [69]. VC-R4 replication can be monitored by the expression of EGFP. Because VC-R4 lacks K3L and E3L, it cannot replicate in cells with intact PKR but may replicate and express EGFP in potential PKR knock out cells. Clones in which VC-R4 could replicate were then subjected to Western blotting to confirm the absence of rabbit PKR in RK13 cells.

Validation of RK13 PKR gene knock out by genomic DNA amplification and sequencing

Genomic DNA was extracted from one? individual cell clone and subjected to direct PCR amplification with the NEB OneTaq DNA polymerase (NEB) using designed primers flanking the targeted region, PKR-Exon2 F 5′-GAGATTTCGCACACTACACCA-3′ and PKR-Exon2 R 5′-CTAAGGACGAGTGCTCCAATT-3′. The PCR products encompassing the CRISPR/Cas9 target sites were cloned into a pCR™-Blunt II-TOPO™ Vector from Zero Blunt™ TOPO™ PCR Cloning Kit (Invitrogen) and 18 positives colonies were randomly chosen for Sanger sequencing. Clone sequencing showed 1bp deletion (7 colonies) in one allele and a 2 bp i insertion (11 colonies) in another allele (figure 3.1A). To further validate the correct sequencing, we designed mismatch primer pair for further validation, oligonucleotide primers were F: 5′-TCATGAACTGCCCCAGTC-3′ and R: 5′-AGGACGAGTGCTCCAATT-3′ (figure 3.1B).

Viral Infection

To test replication of MYXVΔM029LΔM156R, RK13 cells, RK13 PKR^{ko} cells, and RK13+E3L+K3L cells were seeded into six-well plates and were mock infected with PBS or infected with MYXVΔM029LΔM156R at an MOI of 0.1. After 1 hour of incubation, unbound virus was removed by washing the cells twice with prewarmed phosphate-buffered saline (PBS). The cells were then incubated at 37℃ at 5 % CO_2 atmosphere in DMEM supplemented with 2 % FBS. The virus-infected cells were harvested at 2, 12, 24, and 48 hpi and then tittered in RK13 cells that stably express E3 and K3 [19]. The viral replication kinetics assays were performed in triplicate.

Generation of stable cell lines expressing human PKR and European rabbit PKR

To generate RK13-PKR^{ko} cells that express human PKR or E. rabbit PKR, a plasmid was previously constructed that contains the human PKR promoter [20]. Human PKR or E. rabbit PKR were cloned into this vector. RK13-PKR^{ko} cells were transfected using GenJet-HeLa (SignaGen Laboratories) according to the manufacturer's instructions. Cells were trypsinized 48 h after transfection and cultured in the presence of 1 μg/ml geneticin (Invitrogen) for 14 d. To select clones, cells were seeded on 96-well plates at a density of 0.3 and one cell per well until single colonies appeared.

Luciferase assay

Single luciferase assay for PKR inhibition was described previously [20,31]. RK13-PKR^{ko} or HeLa-PKR^{ko} cells were seeded in 24-well plates at a density of 5×10^4 cells per well. After 24 h, the cells were transiently transfected with firefly luciferase reporter (pGL3 plasmid, 50 ng, Promega) and pSG5 plasmids encoding PKRs from indicated different species, European rabbit (e) PKR, brush rabbit (b) PKR, European rabbit PKR mutant, brush rabbit PKR mutant, along with M156R, or K3L orthologs from other four poxviruses, RCPV, SPPV, SKPV, CMLV using GenJet-HeLa (SignaGen) for Hela-PKR^{ko} cells, and lipofectamine 2000 (Invitrogen) for RK13-PKR^{ko} cells. For controls, empty pSG5 vector was transfected using the same amount. Each transfection was conducted in triplicate.

For NF-κB or ATF4 activity assays, transient co-transfections were carried out in triplicate using the NF-κB-Luc (50 ng) or ATF4-Luc (50 ng) reporter along with the renilla TK-luciferase plasmid for normalization. Plasmid transfections were performed using the GenJet-HeLa

(SignaGen). After 48 h, luciferase activity was determined with the dual luciferase reporter assay system (Promega) in a luminometer (Promega).

Quantitative RT-PCR

After transfections or infections, RNA was extracted using TRIzol reagent (Invitrogen). Ribonuclease-free DNase I (0.5 U μg^{-1} RNA; NEB) was used to remove residual genomic DNA contamination. 1 μg of RNA was reverse transcribed to produce cDNA utilizing the ProtoScript® II Reverse Transcriptase (NEB) according to the manufacturer's protocol. 50 ng of obtained cDNA was amplified in 20 μL reactions using EvaGreen dye (Biotium). Oligonucleotide primers were 18S-qPCR-F: 5′-AGGAATTGACGGAAGGGCAC-3′ and 18S-qPCR-R: 5′-GGACATCTAAGGGCATCACA-3′; TNFα-qPCR-F: 5′-AGCCCATGTTGTAGCAAACC-3′ and TNFα-qPCR-R: 5′-TGAGGTACAGGCCCTCTGAT-3′; IL-6-qPCR-F: 5′-TACCCCCAGGAGAAGATTCC-3′ and IL-6-qPCR-R: 5′-TTTTCTGCCAGTGCCTCTTT-3′′.

PCR cycling was performed at 95 °C, 2 min, followed by 40 cycles of 95 °C, 5 s; 60 °C, 12 s on a CFX Connect Real-Time PCR Detection System (Bio-Rad). Relative expression levels for tested mRNAs were determined using 18S as an internal reference using comparative Ct ($2^{-\Delta\Delta Ct}$) method.

Western blot

Cells were harvested and lysed with 1% sodium dodecyl sulfate (SDS) and sonicated at 50% amplitude for 10 seconds twice. Proteins were separated by SDS-PAGE and transferred to polyvinyl difluoride membranes (PVDF, GE Healthcare). The membranes were blocked with 5% nonfat milk and incubated with indicated primary antibodies for overnight at 4℃. The membranes were then incubated with donkey-anti-rabbit or donkey-anti-mouse secondary

antibodies and detected with AmershamTM ECLTM (GE Healthcare). Images were collected with an iBright Imaging System (Invitrogen). A mouse anti-β-Actin antibody was used to detect endogenous β-Actin, which served as a protein-loading control.

Statistical analysis

The Values were expressed as the means ± SD. Statistical analysis was performed using GraphPad Prism Software. The data were analyzed using Student's t-test. A p value of <0.05 was considered significant. * $p < 0.5$, ** $p<0.01$, *** $p< 0.001$, ****$p< 0.0001$.

Author contributions

H.Y. and S.R. designed research; H.Y. performed research and wrote the original draft; H.Y. C.P. R.B. J.N.S. G.B. and S.R. contributed new reagents/analytic tools/review & editing; H.Y. and S.R. analyzed data.

Figure legend

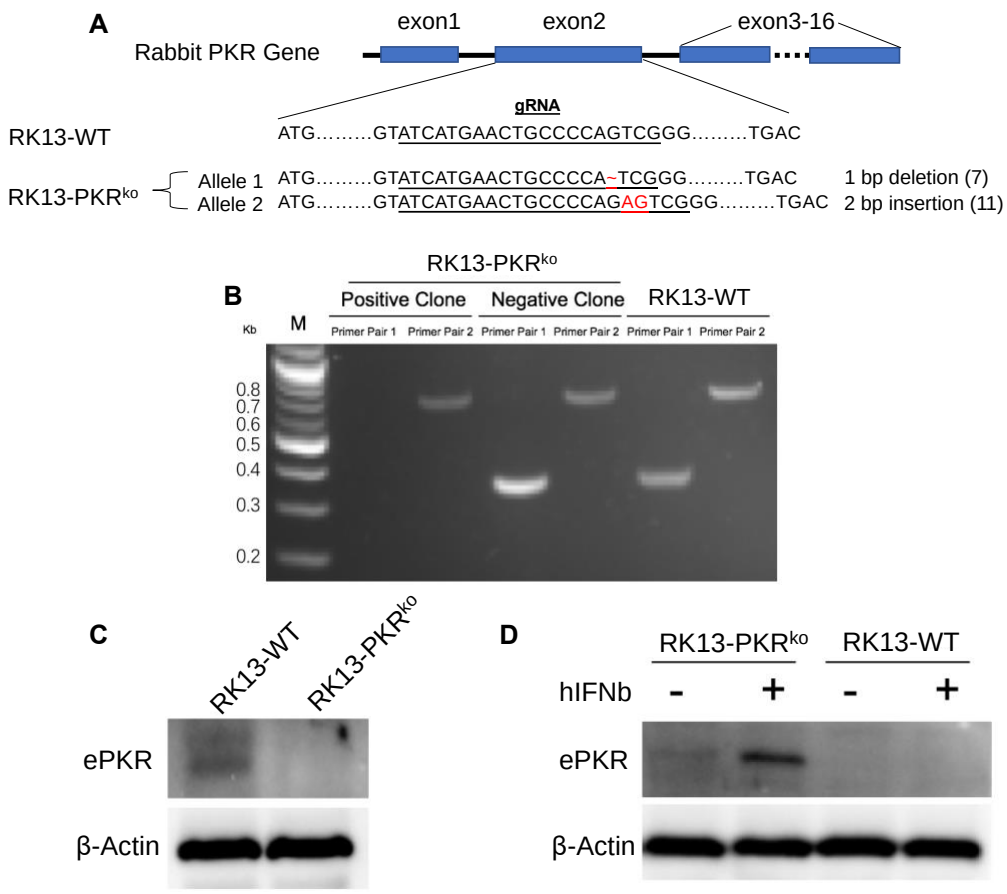

Fig. 3.1 Generation and validation of RK13 PKR knockout (KO) cell lines using the CRISPR-Cas9 system

(A) Schematic representation of the PKR gene and indels induced by CRISPR-Cas9. Guide RNA (gRNA) was designed to target exon 2 of Rabbit PKR. Sequence analysis of a positive clone showed both alleles contain a deletion or insertion (indel), respectively, as indicated in the target sites. (B) Validation of CRISPR/Cas9-induced indels by PCR. Single-cell clones (one positive clone as shown in A, one negative clone contains intact allele) were characterized by isolation of genomic DNA and the existence of specific PKR gene indels was determined by PCR using

mismatch primer, RK13 wild type cells were used as a control. (C, D) Western blot analysis of endogenous PKR protein levels in cell lysates from RK13-wild type (WT) and positive RK13-PKR^{ko} cells (C) and Human IFN-β (hIFN-β/500 Unit) stimulated RK13-wild type (WT) and RK13-PKR^{ko} for 18 hours (D).

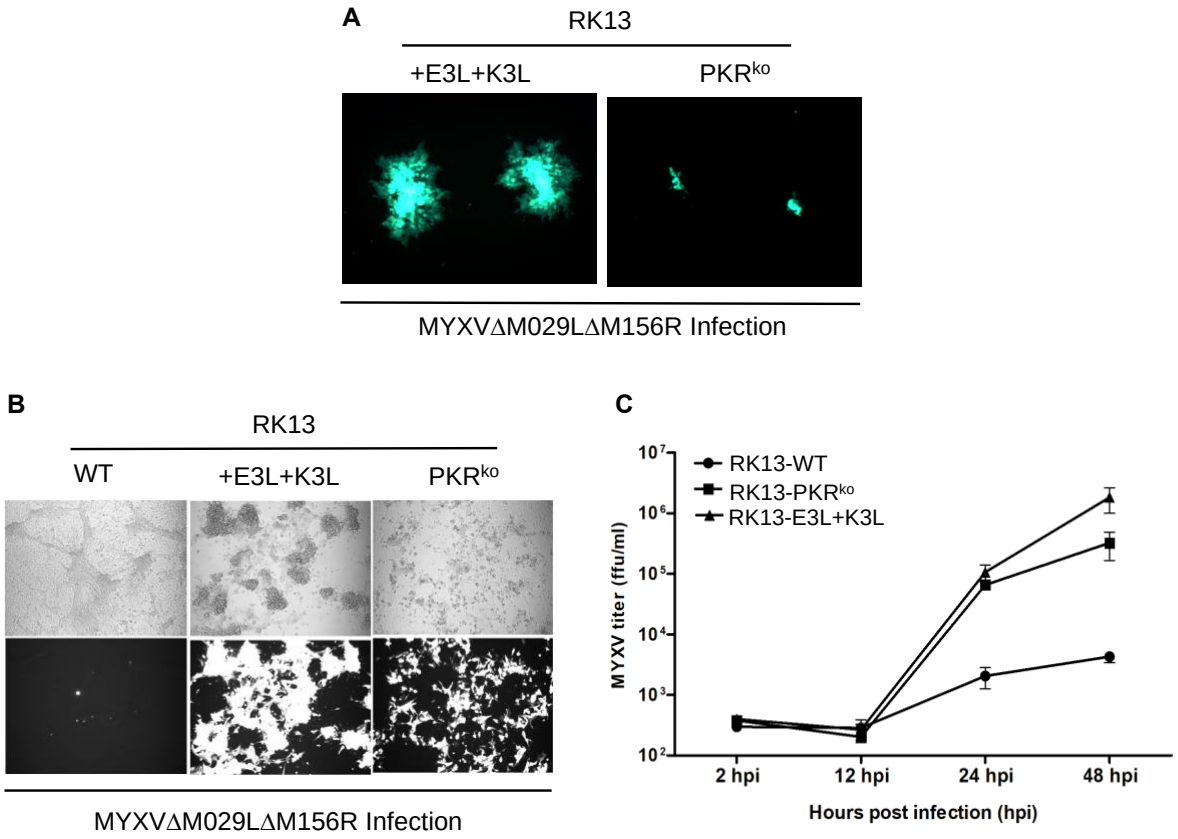

Fig. 3.2 Knock out of rabbit PKR facilitates the replication of MYXVΔM029LΔM156R

(A) RK13 expressing E3 and K3 and RK13-PKR^{ko} cells were infected with MYXVΔM029LΔM156R for 72 h. (B) RK13-WT, RK13 expressing E3 and K3 and RK13-PKR^{ko} cells were infected with MYXVΔM029LΔM156R at an MOI of 1 for 48 h. (C) Viral replication curve. RK13-WT, RK13-PKR^{ko}, and RK13 expressing E3 and K3 cells (RK13+E3L+K3L) were infected with MYXVΔM029LΔM156R at an MOI of 0.1 for 48 h. At the indicated time points, the collected viruses were titrated on RK13+E3L+K3L cells to determine viral titers.

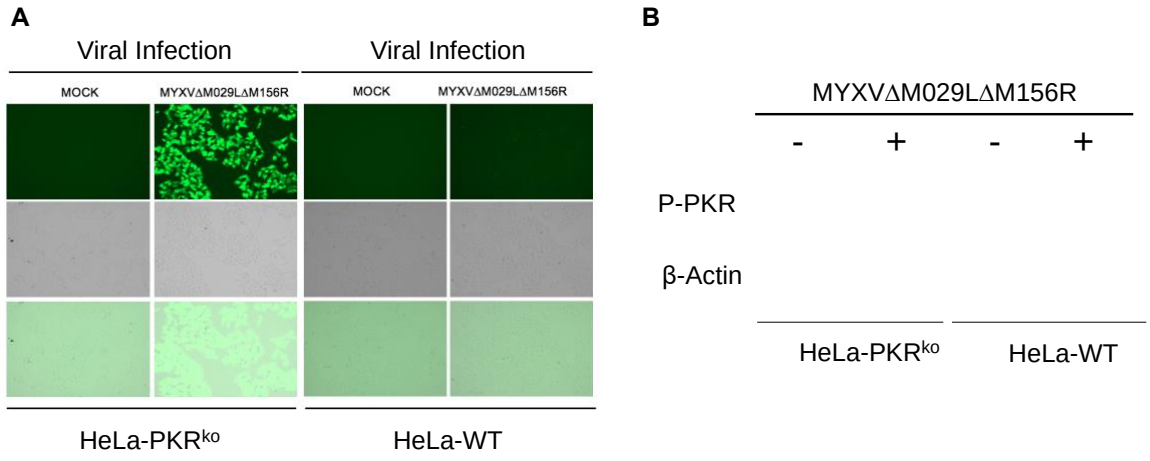

Fig. 3.3 Knock out of PKR in in HeLa cells facilitates the replication of MYXV lacking PKR inhibitors

(A) HeLa-WT and HeLa-PKR^{ko} cells were infected with MYXVΔM029LΔM156R at an MOI of 3 for 24 h. Virus replication was monitored at 24 hpi by fluorescence imaging. (B) HeLa-WT and HeLa-PKR^{ko} cells were infected with MYXVΔM029LΔM156R at an MOI of 3 (+) or mock (-). At 12 hours post infection, the cells were collected and lysed. Cells lysates were separated, and phosphorylation of PKR was assayed by immunoblot analysis using phospho-specific antibodies against threonine 446 PKR (P-PKR).

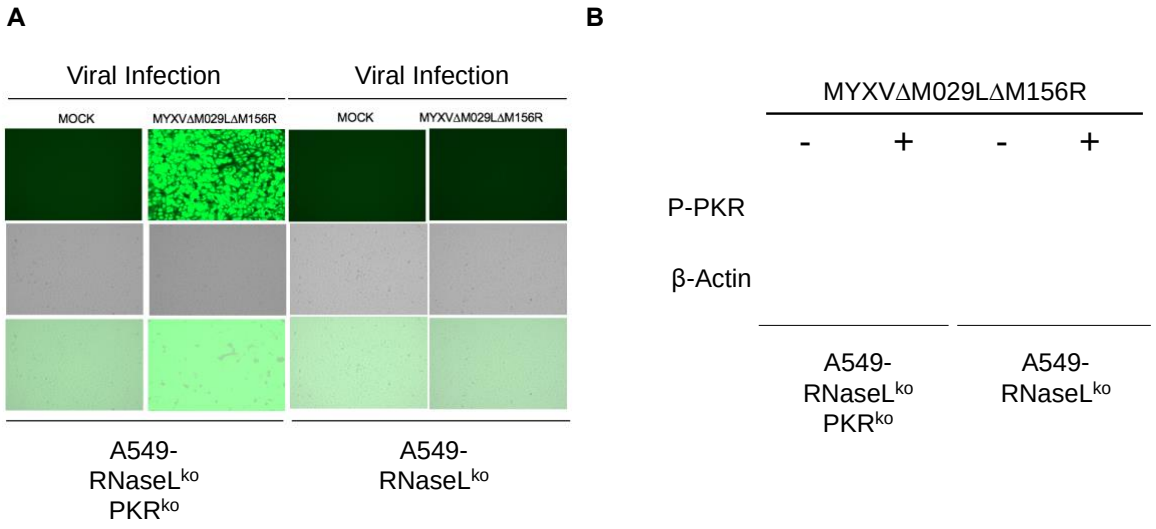

Fig. 3.4 Knock out PKR facilitates the replication of MYXV lacking PKR inhibitors in A549 cells

(A) A549-RNaseL^{ko} and A549-RNaseL^{ko} PKR^{ko} cells were infected with MYXVΔM029LΔM156R at an MOI of 3 for 24 h. Virus replication was monitored at 24 hpi by fluorescence imaging. (B) A549-RNaseL^{ko} and A549-RNaseL^{ko}PKR^{ko} cells were infected with MYXVΔM029LΔM156R at an MOI of 3 (+) or mock (-). At 12 hours post infection, the cells were collected and lysed. Cells lysates were separated, and phosphorylation of PKR was assayed by immunoblot analysis using phospho-specific antibodies against Threonine 446 PKR (P-PKR).

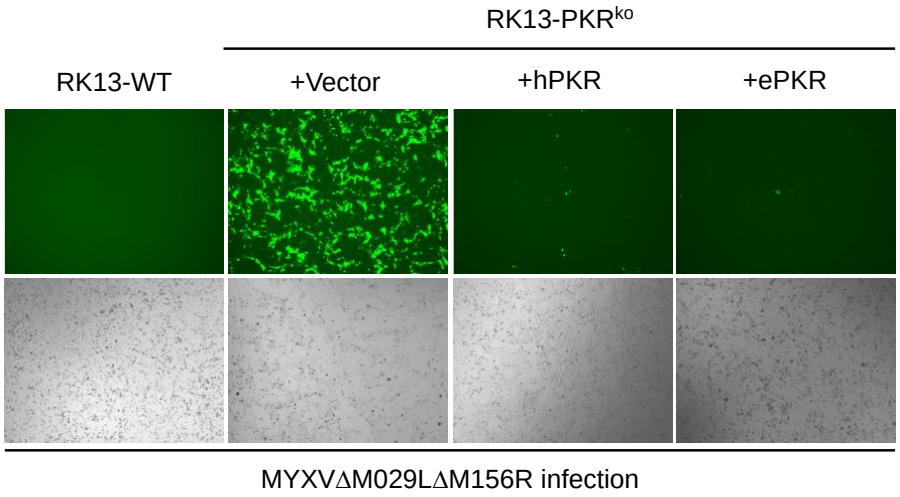

Fig. 3.5 Complementation of human and European rabbit PKRs inhibit the replication of MYXVΔM029LΔM156R

(A) RK13 wild type or RK13-PKR^{ko} cells expressing either empty vector, human PKR and rabbit PKR were infected with MYXVΔM029LΔM156R at an MOI of 1. Virus replication is indicated by EGFP expression. Fluorescent images were taken at 36 hpi.

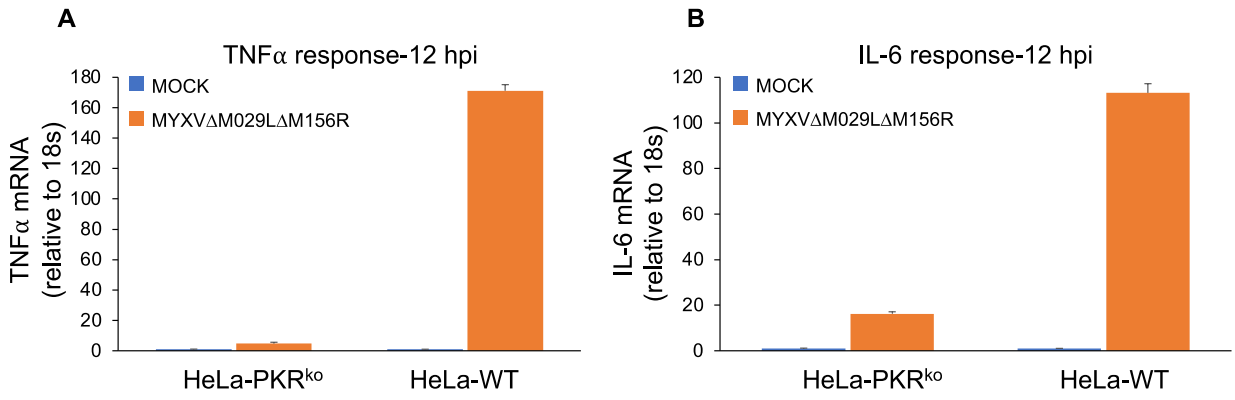

Fig. 3.6 PKR-dependent induction of pro-inflammatory cytokines during MYXV Infection

(A) HeLa-WT and HeLa-PKR^{ko} cells were infected with MYXV-M029L^{ko}M156R^{ko} at an MOI of 3. At 12 hours post infection, total RNA was isolated from the infected cells and subjected to qRT-PCR analysis of TNFα and IL-6 transcripts.

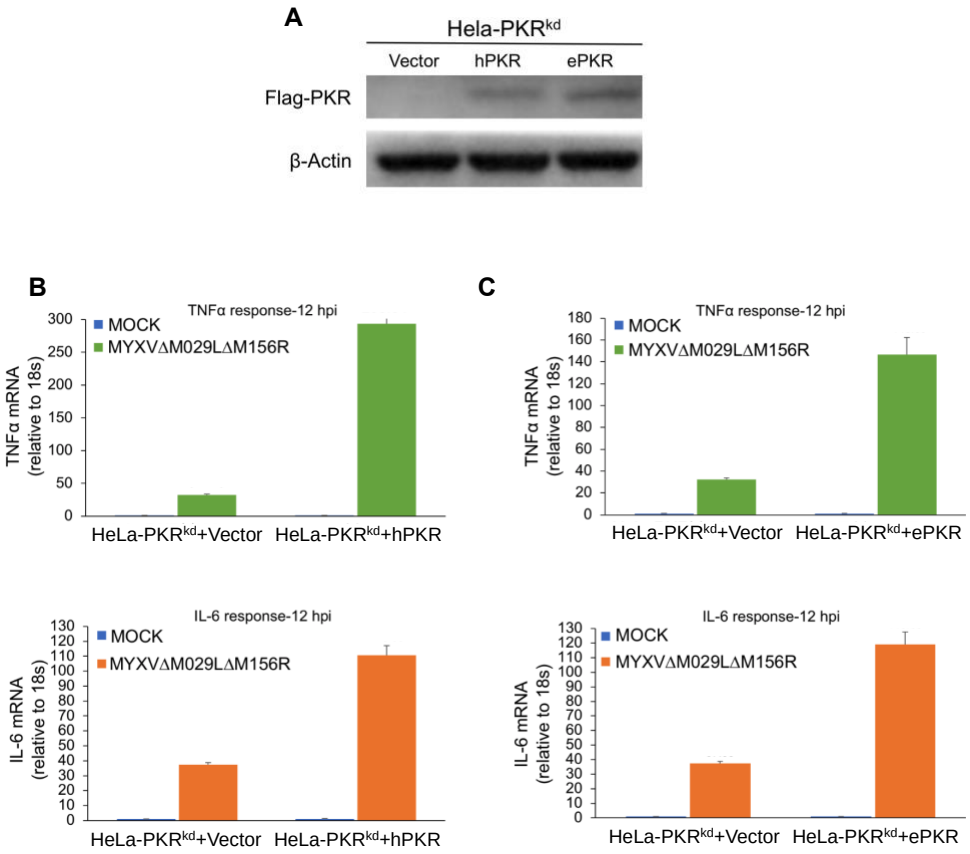

Fig. 3.7 Complementation of human and European rabbit PKRs leads to induction of inflammatory responses during MYXV Infection

(A) HeLa-PKR^{kd} cells were stably transfected with empty vector (Vector), human PKR (hPKR) or European rabbit PKR (ePKR) under the control of the human PKR promoter. Flag tagged PKRs and β-actin were detected by immunoblotting using anti-Flag and anti-β-actin antibody respectively. (B, C) HeLa-PKR^{kd} cells stably transfected with empty vector (Vector), human PKR or European rabbit PKR were infected with MYXVΔM029LΔM156R at an MOI of 3. At 12 hpi, total RNA was isolated from the infected cells and subjected to qRT-PCR analysis of TNFα and IL-6 transcripts.

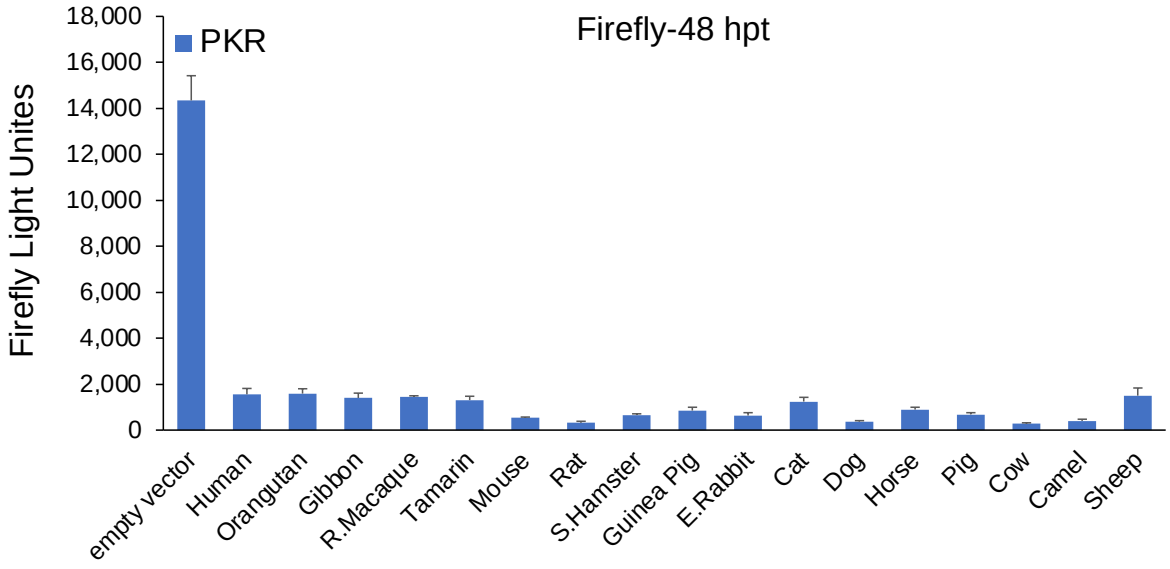

Fig. 3.8 Reduction of luciferase expression by PKRs from different species

PKR from the indicated species (0.2 μg) or empty vector pSG5 (0.2 μg) were co-transfected with firefly luciferase reporter (0.05 μg) into HeLa-PKR^{ko} cells for 48 hours and luciferase activity was measured. Experiments were performed in triplicate and the results are representative of three independent experiments. Error bars indicate standard deviations. Abbreviations used: R. = Rhesus; S. = Syrian; E. = European.

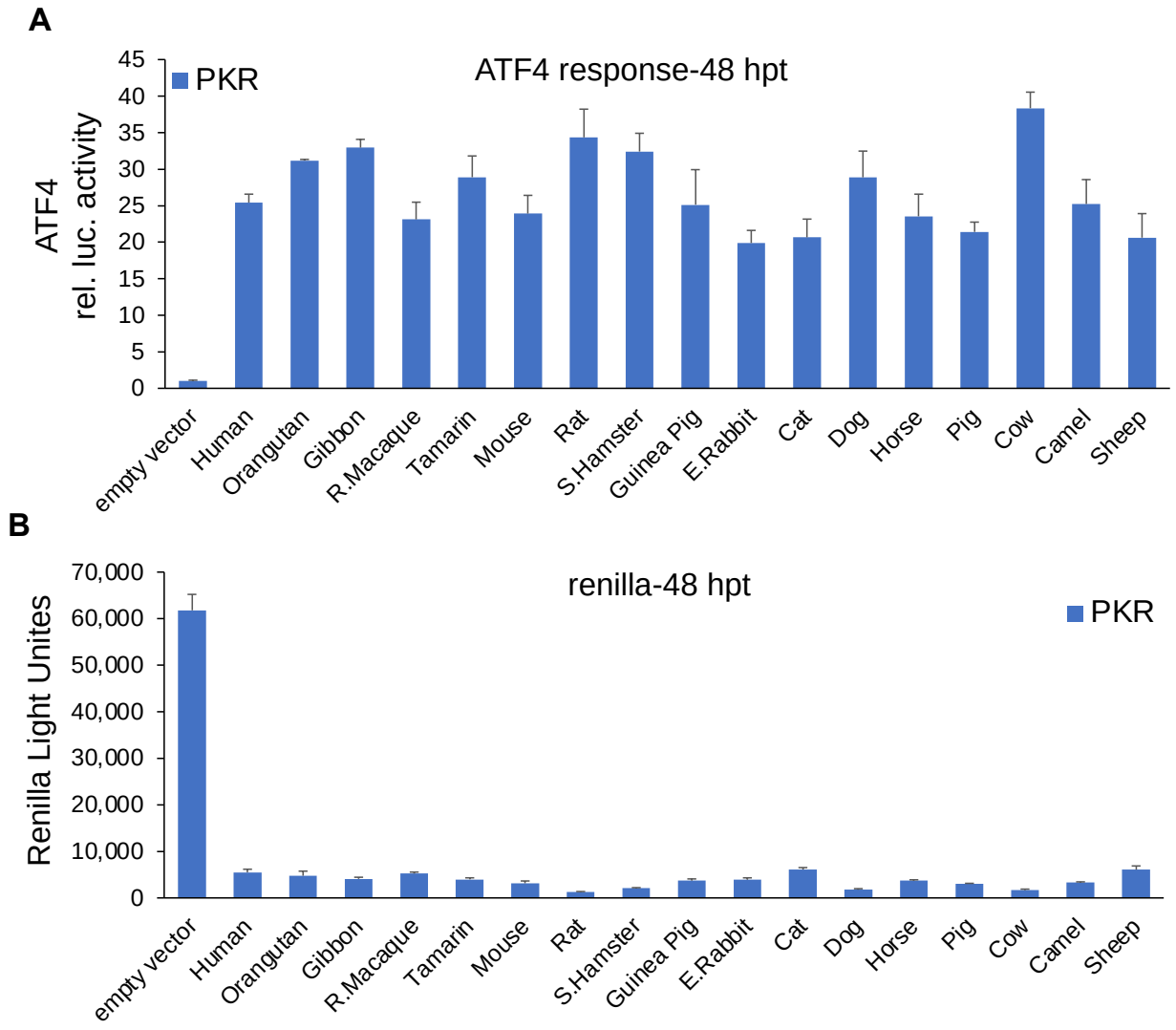

Fig. 3.9 Inverse correlation of luciferase activity driven by an ATF4-reporter with translational repression in PKR-transfected HeLa cells

HeLa-PKR^{ko} cells were transfected with ATF4-firefly luciferase reporter (0.05 μg) which contains the mouse ATF4 mRNA-5'UTR sequence, TK-renilla luciferase reporter (0.05 μg) driven by the TK promoter, empty vector (0.2 μg) along with PKRs (0.2 μg) or empty vector (0.2 μg). At 48 hours post transfection, luciferase activities were measured. The luciferase values were internally controlled by normalizing light units produced by firefly luciferase to that

produced by renilla luciferase. Values obtained were then further normalized to empty vector-only transfected cells to calculate relative luciferase activity. Error bars indicate standard deviation.

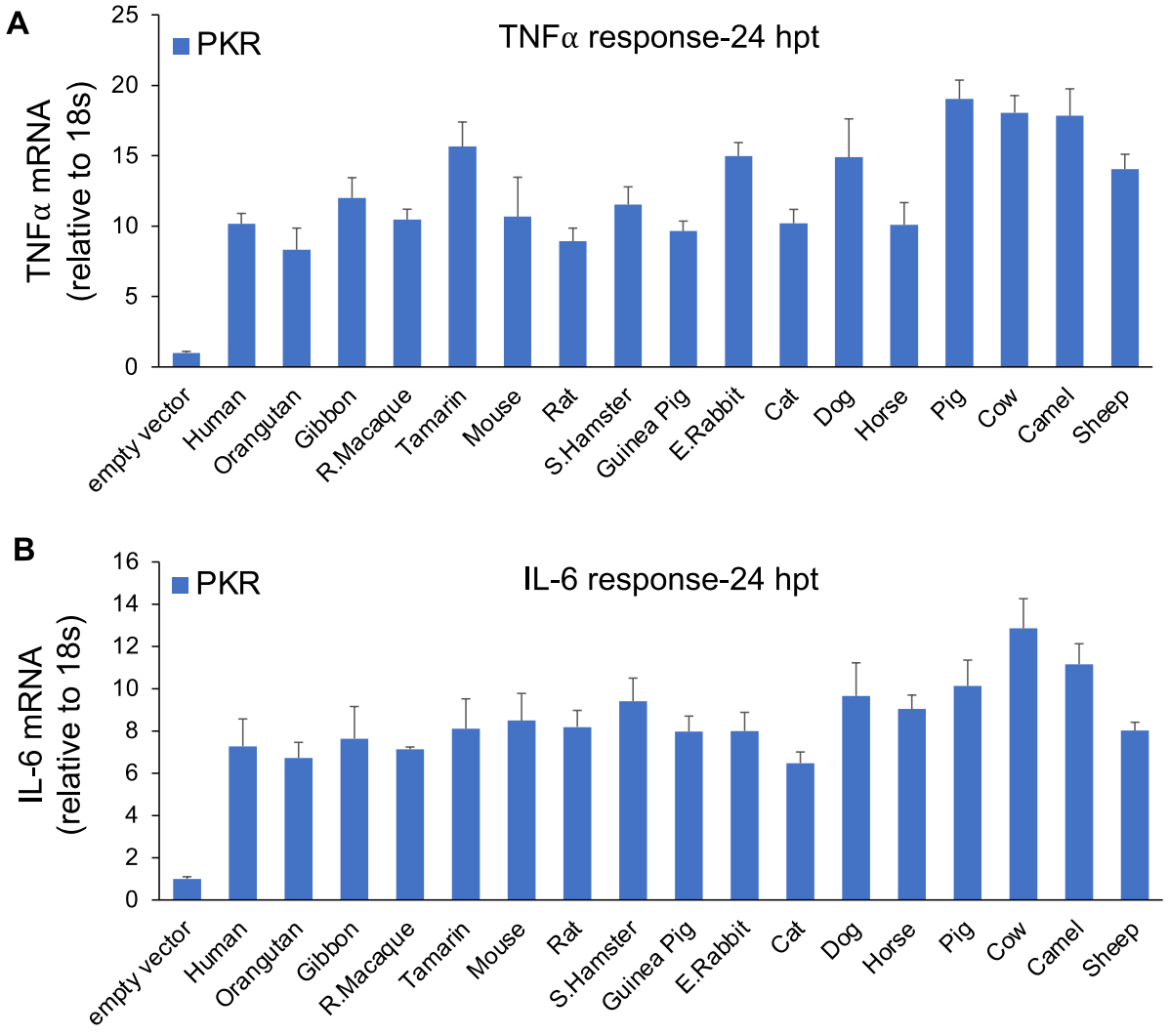

Fig. 3.10 PKRs from various species activate NF-κB dependent inflammatory responses at transcriptional level

PKRs from different species (0.75 μg) or empty vector (0.75 μg) were co-transfected with additional empty vector (0.75 μg) into HeLa-PKR^{ko} cells. 24 hours post transfection (hpt), total RNA was isolated from the cells and subjected to qRT-PCR. The transcriptional levels of endogenous TNFα and IL-6 genes were tested. Values obtained were normalized to empty

vector-only transfected cells to calculate relative mRNA level. Error bars indicate standard deviation.

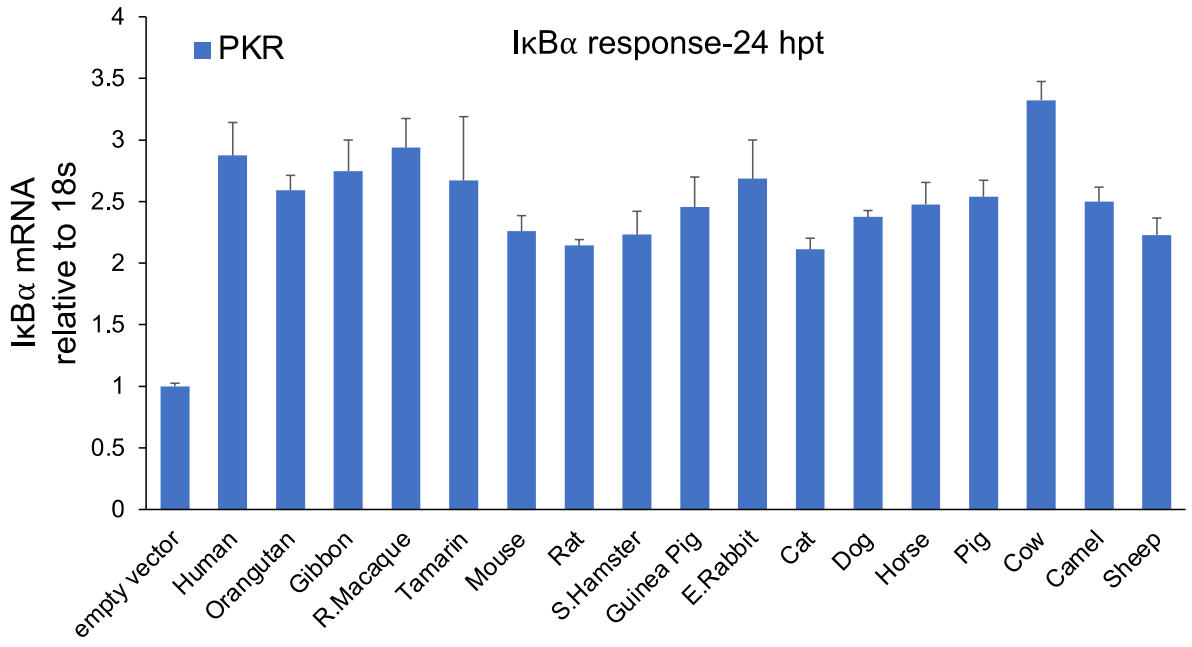

Fig. 3.11 PKRs upregulate the transcription of NF-κB dependent IκBα at the mRNA level

PKRs from the indicated species (0.75 μg) or empty vector (0.75 μg) were co-transfected with additional empty vector (0.75 μg) into HeLa-PKR^{ko} cells. 24 hours post transfection (hpt), total RNA was isolated from the cells and subjected to qRT-PCR analysis. The transcriptional level of endogenous IκBα gene was tested. Values obtained were normalized to empty vector-only transfected cells to calculate relative mRNA level. Error bars indicate standard deviation.

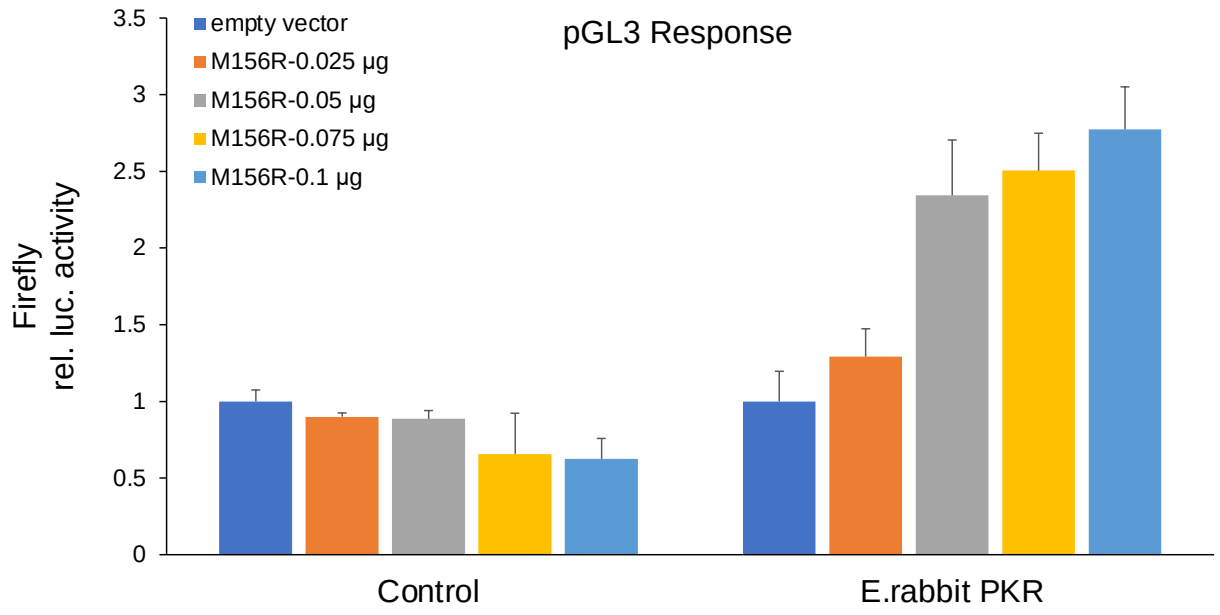

Fig. 3.12 Dose dependent inhibition of rabbit PKR by M156 in relevant rabbit cells

Constant amounts of European rabbit PKR (0.1 µg) were co-transfected with increasing amounts of M156R, along with luciferase reporter (0.05 µg) into the RK13-PKR^{ko} cells. After 48 h, luciferase light units were measured and normalized to PKR-only transfected cells to obtain relative luciferase activities. Relative luciferase activities are shown.

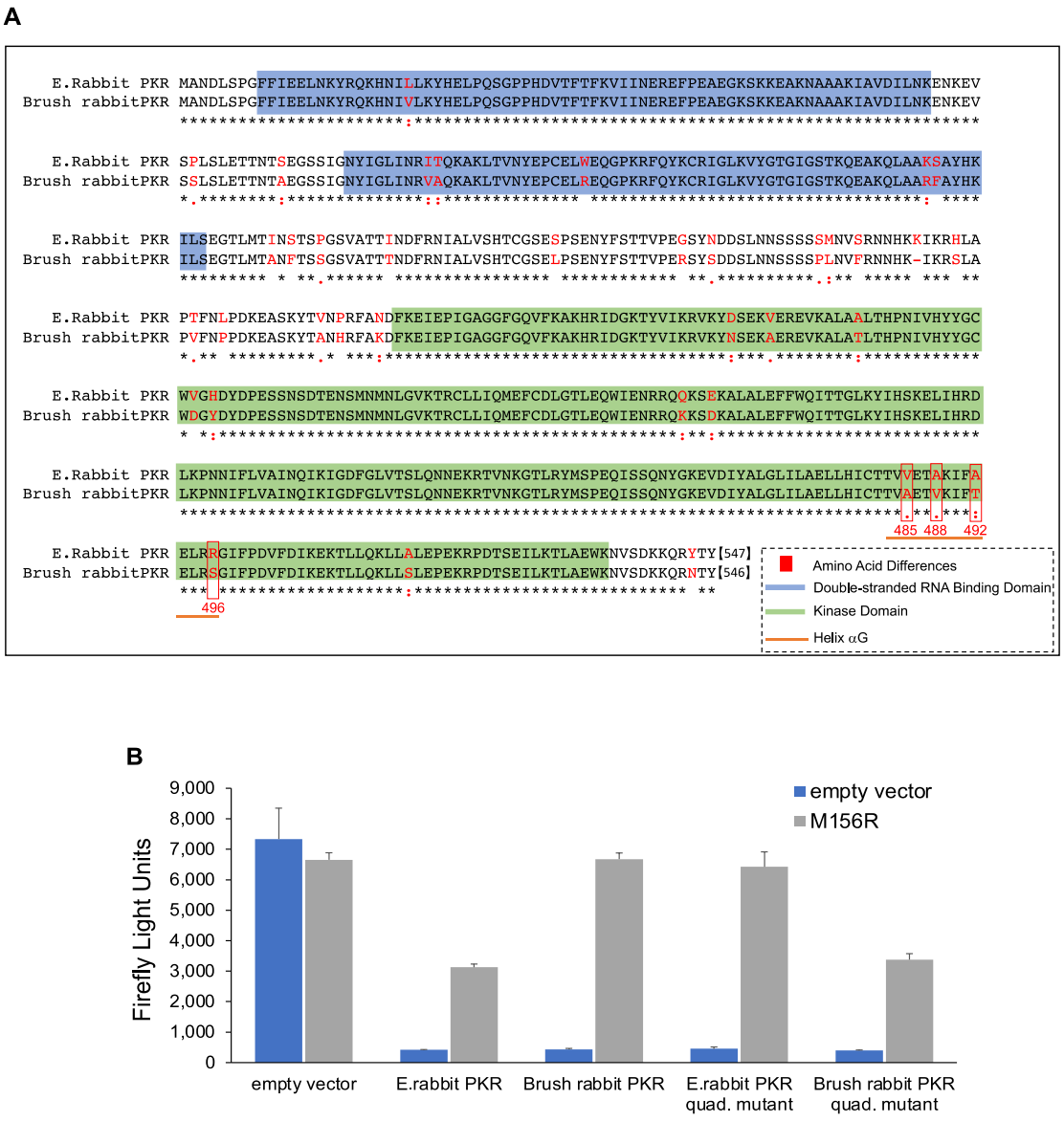

Fig. 3.13 Quadruple mutations in the helix αG region of rabbit PKRs reverse sensitivities to M156 inhibition

(A) Sequence alignment of PKR from European rabbit and brush rabbit. Differences between the two PKRs are found throughout the protein sequence including the dsRNA binding domains, linker region and the kinase domain. (B) M156-mediated differential PKR inhibition. HeLa-PKR^{ko} cells were transfected with expression vectors for luciferase (0.05 μg), M156R (0.4 μg),

and PKR (0.2 μg) from the indicated species. Luciferase value were measured 48 hours post-transfection.

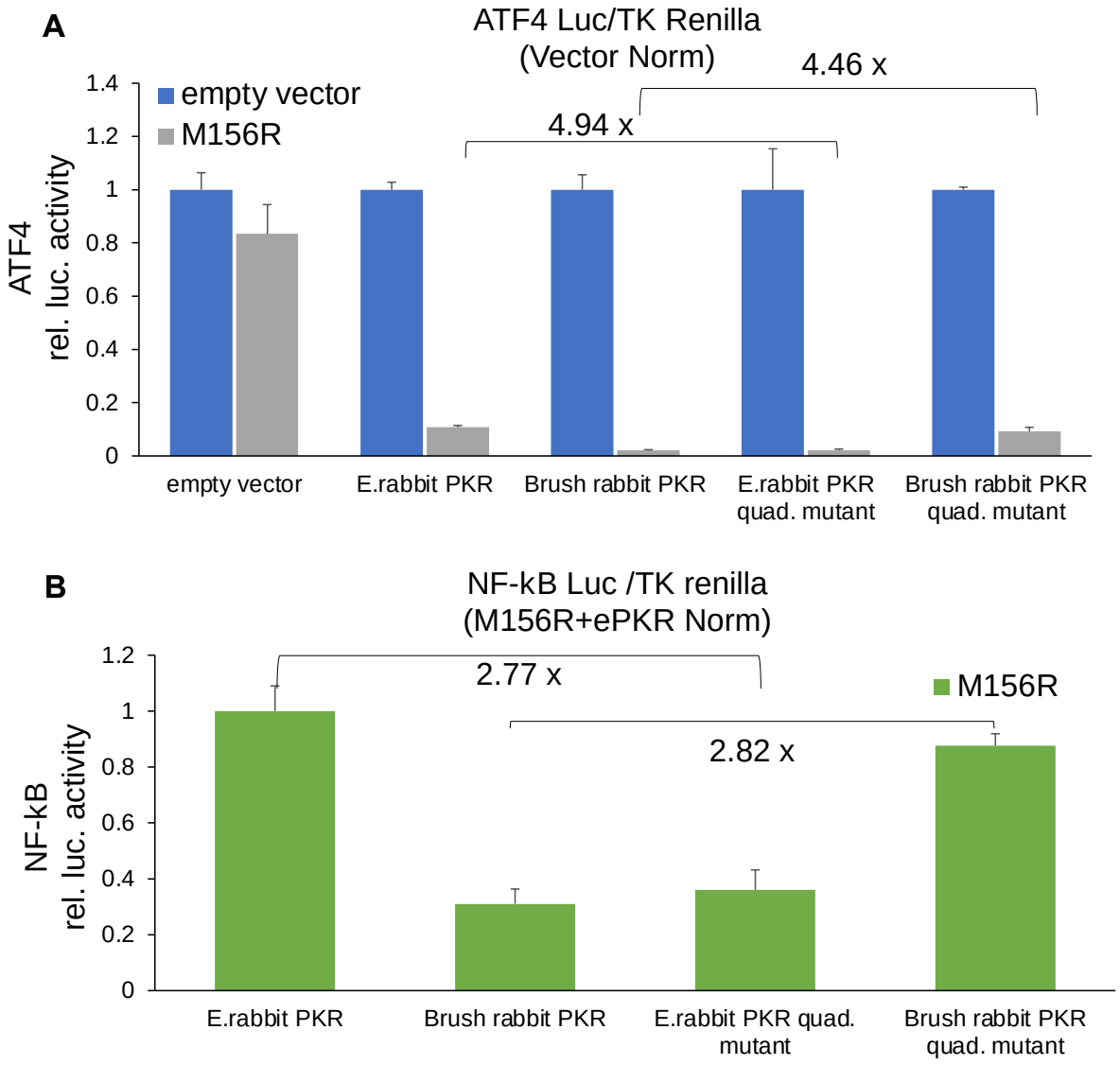

Fig. 3.14 The levels of PKR inhibition by M156 affect ATF4 and NF-κB activities

HeLa-PKR^{ko} cells were co-transfected with (A) a ATF4-firefly luciferase reporter (0.05 μg), which contains the mouse ATF4 mRNA-5'UTR sequence or (B) a NF-κB luciferase reporter (0.05 μg) and a renilla luciferase reporter (0.05 μg), expression plasmids of indicated PKRs and mutants (0.2 μg), and M156R (0.4 μg) into HeLa-PKR^{ko} cells. Luciferase activities were measured 48 hours post-transfection. Firefly luciferase activity was normalized to renilla luciferase activity (A, B). Obtained values were then normalized to PKR-only transfected cells to

obtain relative luciferase activities (A, B). For B, values were further normalized to European rabbit PKR and M156R co-transfected cells to obtain relative luciferase activities. Experiments were performed in triplicate and the results are representative of three independent experiments. Error bars indicate SD.

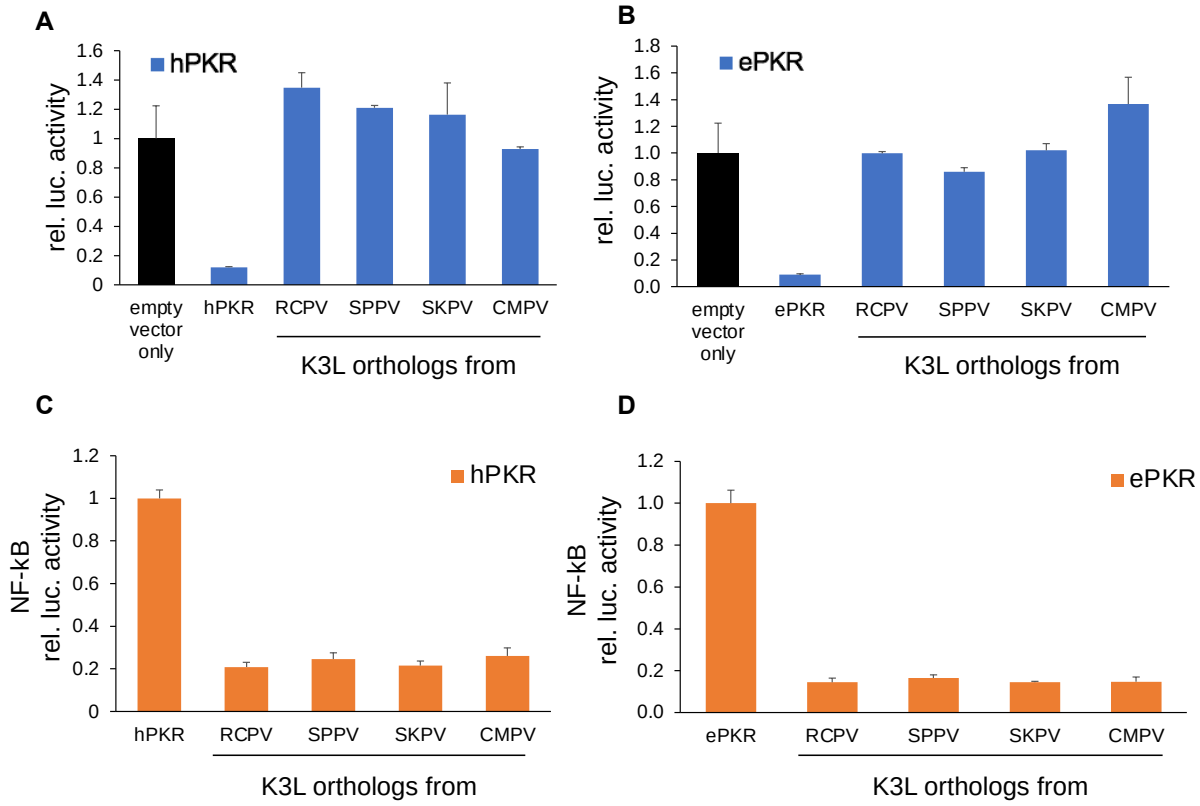

Fig. 3.15 Four other tested K3 orthologs from poxviruses significantly inhibit NF-κB activity through high inhibition on PKRs

(A, B) Human (A) or E. rabbit PKR (B) (0.2 μg) were co-transfected with firefly luciferase reporter (0.05 μg), along with K3L orthologs (0.4 μg) from indicated poxviruses into HeLa-PKR^{ko} cells for 48 hours. Luciferase activities were measured and normalized to empty vector transfection only cells to obtain relative luciferase activities. (C, D) K3L orthologs (0.2 μg) from indicated poxviruses were co-transfected with human (A) or E. rabbit PKR (B) (0.2 μg), NF-κB reporter (0.05 μg) and renilla luciferase reporter (0.05 μg). At 48 hpt, NF-κB firefly luciferases activities were measured and normalized to renilla luciferase activities. Obtained values were then further normalized to vector-only to calculate relative luciferase activities (B, D).

Experiments were performed in triplicate and the results are representative of three independent experiments. Error bars indicate SD.

Reference

1. Meurs, E.; Chong, K.; Galabru, J.; Thomas, N.S.; Kerr, I.M.; Williams, B.R.; Hovanessian, A.G. Molecular cloning and characterization of the human double-stranded RNA-activated protein kinase induced by interferon. Cell 1990, 62, 379–390, doi:10.1016/0092-8674(90)90374-n.
2. Weber, F.; Wagner, V.; Rasmussen, S.B.; Hartmann, R.; Paludan, S.R. Double-stranded RNA is produced by positive-strand RNA viruses and DNA viruses but not in detectable amounts by negative-strand RNA viruses. J. Virol. 2006, 80, 5059–5064, doi:10.1128/JVI.80.10.5059-5064.2006.
3. Li, S.; Peters, G.A.; Ding, K.; Zhang, X.; Qin, J.; Sen, G.C. Molecular basis for PKR activation by PACT or dsRNA. Proc. Natl. Acad. Sci. U. S. A. 2006, 103, 10005–10010, doi:10.1073/pnas.0602317103.
4. Dey, M.; Cao, C.; Dar, A.C.; Tamura, T.; Ozato, K.; Sicheri, F.; Dever, T.E. Mechanistic link between PKR dimerization, autophosphorylation, and eIF2alpha substrate recognition. Cell 2005, 122, 901–913, doi:10.1016/j.cell.2005.06.041.
5. Jiang, H.-Y.; Wek, S.A.; McGrath, B.C.; Scheuner, D.; Kaufman, R.J.; Cavener, D.R.; Wek, R.C. Phosphorylation of the Subunit of Eukaryotic Initiation Factor 2 Is Required for Activation of NF- B in Response to Diverse Cellular Stresses. Mol. Cell. Biol. 2003, 23, 5651–5663, doi:10.1128/mcb.23.16.5651-5663.2003.
6. Deng, J.; Lu, P.D.; Zhang, Y.; Scheuner, D.; Kaufman, R.J.; Sonenberg, N.; Harding, H.P.; Ron, D. Translational Repression Mediates Activation of Nuclear Factor Kappa B by Phosphorylated Translation Initiation Factor 2. Mol. Cell. Biol. 2004, 24, 10161–10168, doi:10.1128/mcb.24.23.10161-10168.2004.

7. Jiang, H.-Y.; Wek, R.C. GCN2 phosphorylation of eIF2alpha activates NF-kappaB in response to UV irradiation. Biochem. J. 2005, 385, 371–380, doi:10.1042/BJ20041164.
8. Vattem, K.M.; Wek, R.C. Reinitiation involving upstream ORFs regulates ATF4 mRNA translation in mammalian cells. Proc. Natl. Acad. Sci. U. S. A. 2004, 101, 11269 LP – 11274, doi:10.1073/pnas.0400541101.
9. Harding, H.P.; Novoa, I.; Zhang, Y.; Zeng, H.; Wek, R.; Schapira, M.; Ron, D. Regulated translation initiation controls stress-induced gene expression in mammalian cells. Mol. Cell 2000, 6, 1099–1108, doi:10.1016/S1097-2765(00)00108-8.
10. Liu, Y.; Wang, M.; Cheng, A.; Yang, Q.; Wu, Y.; Jia, R.; Liu, M.; Zhu, D.; Chen, S.; Zhang, S.; et al. The role of host eIF2α in viral infection. Virol. J. 2020, 17, 112, doi:10.1186/s12985-020-01362-6.
11. Gil, J.; Rullas, J.; García, M.A.; Alcamí, J.; Esteban, M. The catalytic activity of dsRNA-dependent protein kinase, PKR, is required for NF-kappaB activation. Oncogene 2001, 20, 385–394, doi:10.1038/sj.onc.1204109.
12. Bonnet, M.C.; Weil, R.; Dam, E.; Hovanessian, A.G.; Meurs, E.F. PKR stimulates NF-kappaB irrespective of its kinase function by interacting with the IkappaB kinase complex. Mol. Cell. Biol. 2000, 20, 4532–4542, doi:10.1128/mcb.20.13.4532-4542.2000.
13. Hayden, M.S.; West, A.P.; Ghosh, S. NF-κB and the immune response. Oncogene 2006, 25, 6758–6780, doi:10.1038/sj.onc.1209943.
14. Liu, T.; Zhang, L.; Joo, D.; Sun, S.-C. NF-κB signaling in inflammation. Signal Transduct. Target. Ther. 2017, 2, 17023-, doi:10.1038/sigtrans.2017.23.
15. Zandi, E.; Rothwarf, D.M.; Delhase, M.; Hayakawa, M.; Karin, M. The IkappaB kinase complex (IKK) contains two kinase subunits, IKKalpha and IKKbeta, necessary for

IkappaB phosphorylation and NF-kappaB activation. Cell 1997, 91, 243–252, doi:10.1016/s0092-8674(00)80406-7.

16. Pahl, H.L. Activators and target genes of Rel/NF-kappaB transcription factors. Oncogene 1999, 18, 6853–6866, doi:10.1038/sj.onc.1203239.

17. Hoffmann, A.; Levchenko, A.; Scott, M.L.; Baltimore, D. The IkappaB-NF-kappaB signaling module: temporal control and selective gene activation. Science 2002, 298, 1241–1245, doi:10.1126/science.1071914.

18. Shih, V.F.-S.; Kearns, J.D.; Basak, S.; Savinova, O. V; Ghosh, G.; Hoffmann, A. Kinetic control of negative feedback regulators of NF-kappaB/RelA determines their pathogen- and cytokine-receptor signaling specificity. Proc. Natl. Acad. Sci. U. S. A. 2009, 106, 9619–9624, doi:10.1073/pnas.0812367106.

19. Rahman, M.M.; Liu, J.; Chan, W.M.; Rothenburg, S.; McFadden, G. Myxoma virus protein M029 is a dual function immunomodulator that inhibits PKR and also conscripts RHA/DHX9 to promote expanded host tropism and viral replication. PLoS Pathog. 2013, 9, e1003465, doi:10.1371/journal.ppat.1003465.

20. Peng, C.; Haller, S.L.; Rahman, M.M.; McFadden, G.; Rothenburg, S. Myxoma virus M156 is a specific inhibitor of rabbit PKR but contains a loss-of-function mutation in Australian virus isolates. Proc. Natl. Acad. Sci. U. S. A. 2016, 113, 3855–3860, doi:10.1073/pnas.1515613113.

21. Romano, P.R.; Zhang, F.; Tan, S.-L.; Garcia-Barrio, M.T.; Katze, M.G.; Dever, T.E.; Hinnebusch, A.G. Inhibition of Double-Stranded RNA-Dependent Protein Kinase PKR by Vaccinia Virus E3: Role of Complex Formation and the E3 N-Terminal Domain. Mol. Cell. Biol. 1998, 18, 7304–7316, doi:10.1128/mcb.18.12.7304.

22. Kawagishi-Kobayashi, M.; Silverman, J.B.; Ung, T.L.; Dever, T.E. Regulation of the protein kinase PKR by the vaccinia virus pseudosubstrate inhibitor K3L is dependent on residues conserved between the K3L protein and the PKR substrate eIF2alpha. Mol. Cell. Biol. 1997, 17, 4146–4158, doi:10.1128/MCB.17.7.4146.

23. Ramelot, T.A.; Cort, J.R.; Yee, A.A.; Liu, F.; Goshe, M.B.; Edwards, A.M.; Smith, R.D.; Arrowsmith, C.H.; Dever, T.E.; Kennedy, M.A. Myxoma virus immunomodulatory protein M156R is a structural mimic of eukaryotic translation initiation factor eIF2alpha. J. Mol. Biol. 2002, 322, 943–954, doi:10.1016/s0022-2836(02)00858-6.

24. Cao, J.; Varga, J.; Deschambault, Y. Poxvirus encoded eIF2α homolog, K3 family proteins, is a key determinant of poxvirus host species specificity. Virology 2020, 541, 101–112, doi:10.1016/j.virol.2019.12.008.

25. Makarova, K.S.; Aravind, L.; Wolf, Y.I.; Koonin, E. V Unification of Cas protein families and a simple scenario for the origin and evolution of CRISPR-Cas systems. Biol. Direct 2011, 6, 38, doi:10.1186/1745-6150-6-38.

26. Barrangou, R.; Marraffini, L.A. CRISPR-Cas systems: Prokaryotes upgrade to adaptive immunity. Mol. Cell 2014, 54, 234–244, doi:10.1016/j.molcel.2014.03.011.

27. Hsu, P.D.; Lander, E.S.; Zhang, F. Development and applications of CRISPR-Cas9 for genome engineering. Cell 2014, 157, 1262–1278, doi:10.1016/j.cell.2014.05.010.

28. Brunner, E.; Yagi, R.; Debrunner, M.; Beck-Schneider, D.; Burger, A.; Escher, E.; Mosimann, C.; Hausmann, G.; Basler, K. CRISPR-induced double-strand breaks trigger recombination between homologous chromosome arms. Life Sci. alliance 2019, 2, doi:10.26508/lsa.201800267.

29. Jinek, M.; Chylinski, K.; Fonfara, I.; Hauer, M.; Doudna, J.A.; Charpentier, E. A

programmable dual-RNA-guided DNA endonuclease in adaptive bacterial immunity. Science 2012, 337, 816–821, doi:10.1126/science.1225829.

30. Moynahan, M.E.; Jasin, M. Mitotic homologous recombination maintains genomic stability and suppresses tumorigenesis. Nat. Rev. Mol. Cell Biol. 2010, 11, 196–207, doi:10.1038/nrm2851.

31. Park, C.; Peng, C.; Rahman, M.J.; Haller, S.L.; Tazi, L.; Brennan, G.; Rothenburg, S. Orthopoxvirus K3 orthologs show virus- and host-specific inhibition of the antiviral protein kinase PKR. PLoS Pathog. 2021, 17, e1009183, doi:10.1371/journal.ppat.1009183.

32. Carpentier, K.S.; Esparo, N.M.; Child, S.J.; Geballe, A.P. A Single Amino Acid Dictates Protein Kinase R Susceptibility to Unrelated Viral Antagonists. PLoS Pathog. 2016, 12, e1005966, doi:10.1371/journal.ppat.1005966.

33. Liu, R.; Moss, B. Opposing Roles of Double-Stranded RNA Effector Pathways and Viral Defense Proteins Revealed with CRISPR-Cas9 Knockout Cell Lines and Vaccinia Virus Mutants. J. Virol. 2016, 90, 7864–7879, doi:10.1128/JVI.00869-16.

34. McAllister, C.S.; Taghavi, N.; Samuel, C.E. Protein kinase PKR amplification of interferon β induction occurs through initiation factor eIF-2α-mediated translational control. J. Biol. Chem. 2012, 287, 36384–36392, doi:10.1074/jbc.M112.390039.

35. Pham, A.M.; Santa Maria, F.G.; Lahiri, T.; Friedman, E.; Marié, I.J.; Levy, D.E. PKR Transduces MDA5-Dependent Signals for Type I IFN Induction. PLoS Pathog. 2016, 12, e1005489, doi:10.1371/journal.ppat.1005489.

36. Taddeo, B.; Luo, T.R.; Zhang, W.; Roizman, B. Activation of NF-kappaB in cells productively infected with HSV-1 depends on activated protein kinase R and plays no

apparent role in blocking apoptosis. Proc. Natl. Acad. Sci. U. S. A. 2003, 100, 12408–12413, doi:10.1073/pnas.2034952100.

37. Dey, S.; Baird, T.D.; Zhou, D.; Palam, L.R.; Spandau, D.F.; Wek, R.C. Both transcriptional regulation and translational control of ATF4 are central to the integrated stress response. J. Biol. Chem. 2010, 285, 33165–33174, doi:10.1074/jbc.M110.167213.

38. Blais, J.D.; Filipenko, V.; Bi, M.; Harding, H.P.; Ron, D.; Koumenis, C.; Wouters, B.G.; Bell, J.C. Activating transcription factor 4 is translationally regulated by hypoxic stress. Mol. Cell. Biol. 2004, 24, 7469–7482, doi:10.1128/MCB.24.17.7469-7482.2004.

39. Park, C.; Peng, C.; Brennan, G.; Rothenburg, S. Species-specific inhibition of antiviral protein kinase R by capripoxviruses and vaccinia virus. Ann. N. Y. Acad. Sci. 2019, 1438, 18–29, doi:10.1111/nyas.14000.

40. Dar, A.C.; Dever, T.E.; Sicheri, F. Higher-order substrate recognition of eIF2alpha by the RNA-dependent protein kinase PKR. Cell 2005, 122, 887–900, doi:10.1016/j.cell.2005.06.044.

41. Dar, A.C.; Sicheri, F. X-ray crystal structure and functional analysis of vaccinia virus K3L reveals molecular determinants for PKR subversion and substrate recognition. Mol. Cell 2002, 10, 295–305, doi:10.1016/S1097-2765(02)00590-7.

42. Elde, N.C.; Child, S.J.; Geballe, A.P.; Malik, H.S. Protein kinase R reveals an evolutionary model for defeating viral mimicry. Nature 2009, 457, 485–489, doi:10.1038/nature07529.

43. Rothenburg, S.; Seo, E.J.; Gibbs, J.S.; Dever, T.E.; Dittmar, K. Rapid evolution of protein kinase PKR alters sensitivity to viral inhibitors. Nat. Struct. Mol. Biol. 2009, 16, 63–70, doi:10.1038/nsmb.1529.

44. Lu, B.; Nakamura, T.; Inouye, K.; Li, J.; Tang, Y.; Lundbäck, P.; Valdes-Ferrer, S.I.; Olofsson, P.S.; Kalb, T.; Roth, J.; et al. Novel role of PKR in inflammasome activation and HMGB1 release. Nature 2012, 488, 670–674, doi:10.1038/nature11290.

45. Zhang, P.; McGrath, B.C.; Reinert, J.; Olsen, D.S.; Lei, L.; Gill, S.; Wek, S.A.; Vattem, K.M.; Wek, R.C.; Kimball, S.R.; et al. The GCN2 eIF2alpha kinase is required for adaptation to amino acid deprivation in mice. Mol. Cell. Biol. 2002, 22, 6681–6688, doi:10.1128/MCB.22.19.6681-6688.2002.

46. Chen, J.-J. Translational control by heme-regulated eIF2α kinase during erythropoiesis. Curr. Opin. Hematol. 2014, 21, 172–178, doi:10.1097/MOH.0000000000000030.

47. Harding, H.P.; Zhang, Y.; Ron, D. Protein translation and folding are coupled by an endoplasmic-reticulum-resident kinase. Nature 1999, 397, 271–274, doi:10.1038/16729.

48. Donnelly, N.; Gorman, A.M.; Gupta, S.; Samali, A. The eIF2α kinases: their structures and functions. Cell. Mol. Life Sci. 2013, 70, 3493–3511, doi:10.1007/s00018-012-1252-6.

49. Costa-Mattioli, M.; Walter, P. The integrated stress response: From mechanism to disease. Science 2020, 368, doi:10.1126/science.aat5314.

50. B'chir, W.; Maurin, A.-C.; Carraro, V.; Averous, J.; Jousse, C.; Muranishi, Y.; Parry, L.; Stepien, G.; Fafournoux, P.; Bruhat, A. The eIF2α/ATF4 pathway is essential for stress-induced autophagy gene expression. Nucleic Acids Res. 2013, 41, 7683–7699, doi:10.1093/nar/gkt563.

51. Saito, A.; Ochiai, K.; Kondo, S.; Tsumagari, K.; Murakami, T.; Cavener, D.R.; Imaizumi, K. Endoplasmic reticulum stress response mediated by the PERK-eIF2(alpha)-ATF4 pathway is involved in osteoblast differentiation induced by BMP2. J. Biol. Chem. 2011, 286, 4809–4818, doi:10.1074/jbc.M110.152900.

52. Clavarino, G.; Cláudio, N.; Couderc, T.; Dalet, A.; Judith, D.; Camosseto, V.; Schmidt, E.K.; Wenger, T.; Lecuit, M.; Gatti, E.; et al. Induction of GADD34 is necessary for dsRNA-dependent interferon-β production and participates in the control of Chikungunya virus infection. PLoS Pathog. 2012, 8, e1002708, doi:10.1371/journal.ppat.1002708.

53. Suragani, R.N.V.S.; Zachariah, R.S.; Velazquez, J.G.; Liu, S.; Sun, C.-W.; Townes, T.M.; Chen, J.-J. Heme-regulated eIF2α kinase activated Atf4 signaling pathway in oxidative stress and erythropoiesis. Blood 2012, 119, 5276–5284, doi:10.1182/blood-2011-10-388132.

54. Huang, P.; Peslak, S.A.; Lan, X.; Khandros, E.; Yano, J.A.; Sharma, M.; Keller, C.A.; Giardine, B.; Qin, K.; Abdulmalik, O.; et al. The HRI-regulated transcription factor ATF4 activates BCL11A transcription to silence fetal hemoglobin expression. Blood 2020, 135, 2121–2132, doi:10.1182/blood.2020005301.

55. Wu, S.; Tan, M.; Hu, Y.; Wang, J.-L.; Scheuner, D.; Kaufman, R.J. Ultraviolet light activates NFkappaB through translational inhibition of IkappaBalpha synthesis. J. Biol. Chem. 2004, 279, 34898–34902, doi:10.1074/jbc.M405616200.

56. Bender, K.; Göttlicher, M.; Whiteside, S.; Rahmsdorf, H.J.; Herrlich, P. Sequential DNA damage-independent and -dependent activation of NF-kappaB by UV. EMBO J. 1998, 17, 5170–5181, doi:10.1093/emboj/17.17.5170.

57. Li, N.; Karin, M. Ionizing radiation and short wavelength UV activate NF-kappaB through two distinct mechanisms. Proc. Natl. Acad. Sci. U. S. A. 1998, 95, 13012–13017, doi:10.1073/pnas.95.22.13012.

58. Willis, K.L.; Langland, J.O.; Shisler, J.L. Viral double-stranded RNAs from vaccinia virus early or intermediate gene transcripts possess PKR activating function, resulting in NF-κB

activation, when the K1 protein is absent or mutated. J. Biol. Chem. 2011, 286, 7765–7778, doi:10.1074/jbc.M110.194704.

59. Hu, Y.; Conway, T.W. 2-Aminopurine inhibits the double-stranded RNA-dependent protein kinase both in vitro and in vivo. J. Interferon Res. 1993, 13, 323–328, doi:10.1089/jir.1993.13.323.

60. Cheung, B.K.W.; Lee, D.C.W.; Li, J.C.B.; Lau, Y.-L.; Lau, A.S.Y. A role for double-stranded RNA-activated protein kinase PKR in Mycobacterium-induced cytokine expression. J. Immunol. 2005, 175, 7218–7225, doi:10.4049/jimmunol.175.11.7218.

61. Cheshire, J.L.; Williams, B.R.; Baldwin, A.S.J. Involvement of double-stranded RNA-activated protein kinase in the synergistic activation of nuclear factor-kappaB by tumor necrosis factor-alpha and gamma-interferon in preneuronal cells. J. Biol. Chem. 1999, 274, 4801–4806, doi:10.1074/jbc.274.8.4801.

62. Werner, S.L.; Kearns, J.D.; Zadorozhnaya, V.; Lynch, C.; O'Dea, E.; Boldin, M.P.; Ma, A.; Baltimore, D.; Hoffmann, A. Encoding NF-kappaB temporal control in response to TNF: distinct roles for the negative regulators IkappaBalpha and A20. Genes Dev. 2008, 22, 2093–2101, doi:10.1101/gad.1680708.

63. Haskill, S.; Beg, A.A.; Tompkins, S.M.; Morris, J.S.; Yurochko, A.D.; Sampson-Johannes, A.; Mondal, K.; Ralph, P.; Baldwin, A.S.J. Characterization of an immediate-early gene induced in adherent monocytes that encodes I kappa B-like activity. Cell 1991, 65, 1281–1289, doi:10.1016/0092-8674(91)90022-q.

64. Sun, S.C.; Ganchi, P.A.; Ballard, D.W.; Greene, W.C. NF-kappa B controls expression of inhibitor I kappa B alpha: evidence for an inducible autoregulatory pathway. Science 1993, 259, 1912–1915, doi:10.1126/science.8096091.

65. Sharif, O.; Bolshakov, V.N.; Raines, S.; Newham, P.; Perkins, N.D. Transcriptional profiling of the LPS induced NF-kappaB response in macrophages. BMC Immunol. 2007, 8, 1, doi:10.1186/1471-2172-8-1.

66. Seo, E.J.; Liu, F.; Kawagishi-Kobayashi, M.; Ung, T.L.; Cao, C.; Dar, A.C.; Sicheri, F.; Dever, T.E. Protein kinase PKR mutants resistant to the poxvirus pseudosubstrate K3L protein. Proc. Natl. Acad. Sci. U. S. A. 2008, 105, 16894–16899, doi:10.1073/pnas.0805524105.

67. Zhang, P.; Samuel, C.E. Protein kinase PKR plays a stimulus- and virus-dependent role in apoptotic death and virus multiplication in human cells. J. Virol. 2007, 81, 8192–8200, doi:10.1128/JVI.00426-07.

68. Krüll, M.; Klucken, A.C.; Wuppermann, F.N.; Fuhrmann, O.; Magerl, C.; Seybold, J.; Hippenstiel, S.; Hegemann, J.H.; Jantos, C.A.; Suttorp, N. Signal transduction pathways activated in endothelial cells following infection with Chlamydia pneumoniae. J. Immunol. 1999, 162, 4834–4841.

69. Vipat, S.; Brennan, G.; Park, C.; Haller, S.L.; Rothenburg, S. Rapid, Seamless Generation of Recombinant Poxviruses using Host Range and Visual Selection. J. Vis. Exp. 2020, doi:10.3791/61049.

Chapter 4-Conclusion

Both viral infection and host innate immune responses shape and contribute to the progression of induced diseases. Nuclear Factor Kappa B (NF-κB) is a rapid response transcription factor and plays a key role in regulating the inflammatory, innate and adaptive immune responses in mammals [1,2]. Appropriate inflammatory response and sufficient cytokine production are important to eliminate of the pathogens. However, hyperinflammation and detrimental cytokine storm can occur as a result of continuous NF-κB activation and failure to return to homeostasis. Exaggerated inflammatory responses have been found in various infections. Early up-regulation of inflammatory related genes has been suggested as the contribution for lethal disease in 1918 Influenza virus-infected macaques [3,4]. The detrimental cytokine storms also happened in severe cases of SARS-CoV-2, SARS-CoV and MERS-CoV infections, along with dramatic increase of pro-inflammatory cytokines (Interferon-alpha (IFNα), IL-1β, IL-6, TNFα, etc.) and chemokines (CCL5, CXCL-1, CXCL8 etc.) in serum [5,6]. Symptoms of acute myxomatosis in MYXV infected European rabbit include swollen head, eyelids and base of ears, ano-genital oedema, mucopurulent conjunctivitis, rhinitis and nasal discharge, indicating the abnormal hyperinflammatory responses and cytokine storm syndromes [7]. The molecular mechanism underlying this unnormal inflammatory responses remains poorly investigated. A variety of pathways are functionally interconnected with NF-κB signaling to mediate selectivity and diversity of NF-κB functions [8,9]. The research presented in this dissertation reveals the involvement of PKR in regulation of pro-inflammatory NF-κB activities and their underlying molecular mechanism during poxvirus infection. We also found that K3 orthologs, including M156, regulates differential NF-κB dependent proinflammatory immune response through targeting PKR activation, which may contribute to different disease courses.

We have previously shown that the MYXV protein M156 inhibited the host antiviral protein kinase R (PKR) derived from European rabbits (ePKR), but it did not inhibit PKR from 7 other tested mammalian species. We further cloned brush rabbit PKR (bPKR) to test the sensitivity of PKR from a natural MYXV host. Interestingly, we revealed that M156 inhibited brush rabbit PKR more strongly than European rabbit PKR, which is consistent with the hypothesis that M156 evolved to inhibit PKR from its natural host and that European rabbit PKR is suboptimally inhibited by M156. We identified four residues in helix αG of PKR that are responsible for the differential sensitivities. In order to investigate whether M156 inhibition of European rabbit PKR could be improved, we screened for hyper-active M156 in a yeast assay using random mutagenesis. We identified several M156 mutants that showed better inhibition of European rabbit PKR, without altering the ability to inhibit brush rabbit PKR. Although the lower sensitivity of European rabbit PKR to M156 inhibition does not correlate with the higher virulence of MYXV infection in European rabbits, we hypothesized that the intermediate inhibition of European rabbit PKR by M156 might only incompletely suppress the signal transduction pathways modulated by PKR, such as the pro-inflammatory NF-κB pathway. The NF-κB inhibitor IκB has a short-half life and is therefore disproportionately depleted after translational inhibition, which results in NF-κB activation. Using reporter assays, we found that co-transfection of M156 with European rabbit PKR but not brush rabbit PKR led to NF-κB activation. Co-transfection of either hyperactive or hypoactive M156 with European rabbit PKR resulted in no NF-κB activation. Those findings demonstrate that partial inhibition of PKR can lead to altered signaling pathways.

By employing molecular and biochemical approaches, we further revealed the molecular mechanism underlying crosstalk between PKR-eIF2α phosphorylation pathway and pro-

inflammatory responses. We showed that PKR-eIF2α phosphorylation mediated translational repression led to reduction of IκBα protein while inversely increased IκBα transcripts (Chapter 2). Other tested PKRs from diverse mammalian species all upregulated the transcription of NF-κB dependent pro-inflammatory cytokines, including TNFα and IL-6. During MYXV infection, the upregulation of TNFα and IL-6 transcripts depended on the existence of endogenous PKR in wild type HeLa and A549 cells, knock out PKR impaired PKR associated NF-κB transcriptional activities. We also found that inhibition of dsRNA generation consequently diminished pro-inflammatory responses during viral infection. In addition to the established antiviral function and regulatory role in NF-κB dependent pro-inflammatory responses, PKR activation resulted in increased ATF4 response. Using generated stable cell lines expressing European rabbit PKR and brush rabbit PKR, we demonstrated that M156R led to higher TNFα and IL-6 responses in European rabbit PKR expressing cells than that in brush rabbit PKR expressing cells during MYXV infection, suggesting the high inhibition of PKR by M156 inhibit the NF-κB activation. Additionally, high inhibition of human or rabbit PKR by other four tested K3L orthologs from different poxviruses also resulted in substantial reduction of the level of NF-κB activation. Those findings suggested that the interactions between PKR and K3 orthologs influence the outcomes of pro-inflammatory responses.

As showed here, the differentially induced host immunes responses by MYXV infection in two sub-rabbit species provides us with unique views to investigate host-virus protein interactions and potential contribution of immune responses to disease progression. Overall, we reveal how K3 orthologs differentially inhibit PKR-eIF2α phosphorylation pathway and regulate the scale of NF-κB activities. We further found that moderate inhibition of PKR by K3 ortholog showed high

NF-κB activation than high PKR inhibition by K3 ortholog. These findings provide us clues that the incompletely inhibited inflammatory responses may result in cytokine storm and potentially contribute to progression of MYXV induced lethal myxomatosis. K3L orthologs, as poxvirus immunomodulator, could mitigate severity of inflammatory response through high inhibition of PKR-eIF2α activation.

References

1. Hayden, M.S.; West, A.P.; Ghosh, S. NF-κB and the immune response. Oncogene 2006, 25, 6758–6780, doi:10.1038/sj.onc.1209943.

2. Liu, T.; Zhang, L.; Joo, D.; Sun, S.-C. NF-κB signaling in inflammation. Signal Transduct. Target. Ther. 2017, 2, 17023-, doi:10.1038/sigtrans.2017.23.

3. Kobasa, D.; Jones, S.M.; Shinya, K.; Kash, J.C.; Copps, J.; Ebihara, H.; Hatta, Y.; Kim, J.H.; Halfmann, P.; Hatta, M.; et al. Aberrant innate immune response in lethal infection of macaques with the 1918 influenza virus. Nature 2007, 445, 319–323, doi:10.1038/nature05495.

4. Cillóniz, C.; Shinya, K.; Peng, X.; Korth, M.J.; Proll, S.C.; Aicher, L.D.; Carter, V.S.; Chang, J.H.; Kobasa, D.; Feldmann, F.; et al. Lethal influenza virus infection in macaques is associated with early dysregulation of inflammatory related genes. PLoS Pathog. 2009, 5, e1000604, doi:10.1371/journal.ppat.1000604.

5. Xu, Z.; Shi, L.; Wang, Y.; Zhang, J.; Huang, L.; Zhang, C.; Liu, S.; Zhao, P.; Liu, H.; Zhu, L.; et al. Pathological findings of COVID-19 associated with acute respiratory distress syndrome. Lancet. Respir. Med. 2020, 8, 420–422.

6. Yang, L.; Liu, S.; Liu, J.; Zhang, Z.; Wan, X.; Huang, B.; Chen, Y.; Zhang, Y. COVID-19: immunopathogenesis and Immunotherapeutics. Signal Transduct. Target. Ther. 2020, 5, 128, doi:10.1038/s41392-020-00243-2.

7. Kerr, P.J. Myxomatosis in Australia and Europe: a model for emerging infectious diseases. Antiviral Res. 2012, 93, 387–415, doi:10.1016/j.antiviral.2012.01.009.

8. Oeckinghaus, A.; Hayden, M.S.; Ghosh, S. Crosstalk in NF-κB signaling pathways. Nat. Immunol. 2011, 12, 695–708, doi:10.1038/ni.2065.

9. Smale, S.T. Hierarchies of NF-κB target-gene regulation. Nat. Immunol. 2011, 12, 689–694, doi:10.1038/ni.2070.